THESIS FOR THE DEGREE OF DOCTOR OF PHILOSOPHY (Ph.D.)

Cellular adaptation to hypoxia in classic Hodgkin lymphoma

Orsolya Matolay, M.D.

Supervisor: Gábor Méhes, M.D., Ph.D., D.Sc.

University of DEBRECEN

DOCTORAL SCHOOL OF CLINICAL MEDICINE

Debrecen, 2022

THESIS FOR THE DEGREE OF DOCTOR OF PHILOSOPHY (Ph.D.)

Cellular adaptation to hypoxia in classic Hodgkin lymphoma

Orsolya Matolay, M.D.

Supervisor: Gábor Méhes, M.D., Ph.D., D.Sc.

University of DEBRECEN

DOCTORAL SCHOOL OF CLINICAL MEDICINE

Debrecen, 2022

Table of content

1. ABBREVIATIONS

AA	Acetazolamide
ABVD	Doxorubicin, bleomycin, vinblastine, dacarbazine
AID	Activation-induced cytidine deaminase
ASCT	autologous stem cell transplantation
BCR	B-cell receptor
BEACOPP	bleomycin, etoposide, doxorubicin, cyclophosphamide, vincristine, procarbazine, and prednisone
CAIX	carbonic anhydrase IX
CAXII	carbonic anhydrase XII
cHL	Classic Hodgkin's lymphoma
CHOP	Cyclophosphamide, doxorubicin, vincristine, prednisone
COX	cyclooxygenase
CSR	Class switch recombination
CT	Computer tomography
DAB	diaminobenzidine
DHAP	Dexamethasone/high-dose cytarabine/cisplatine
DLBCL	Diffuse large B-cell lymphoma
DSMZ	Deutsche Sammlung von Mikroorganismen und Zellkulturen GmbH/German Collection of Microorganisms and Cell Cultures
EBV	Epstein-Bar virus
EGF	Epidermal growth factor
EGFR	Epidermal growth factor receptor
FDG-PET	^{18}F-fluorodeoxyglucose -PET
GC	Germinal center
GLUT	Glucose transporter
GLUT1	Glucose transporter 1
HDCT	high dose chemotherapy
HE	Hematoxylin-eosin
HIF	Hypoxia-inducible transcriptional factor
HIF1α	Hypoxia-Inducible transcriptional factor 1α
HIV	Human Immunodeficiency Virus
HL	Hodgkin's lymphoma
HRE	Hypoxia response element
HRS cells	Hodgkin-Reed-Sternberg cells
H-score	Histoscore
IARC	International Agency for Research on Cancer
ICE	Ifosfamide/carboplatin/etoposide
IFRT	involved-field radiation therapy
IGEV	Ifosfamide/gemcitabine/vinorelbine
IHC	Immunohistochemistry
L&H cells	Lymphocytic and histiocytic cells
LD	Lymphocyte depleted
LMP1	Latent Membrane Protein 1
LP cells	Lymphocyte predominant cells
LR	Lymphocyte rich
MAPK	Mitogen-activated protein kinase
MC	Mixed cellularity

MDR	Multi-drug resistance
NF-κB	Nuclear factor-kappa B
NHL	Non-Hodgkin lymphoma
NLPHL	Nodular lymphocyte-predominant Hodgkin lymphoma
NPV	Negative predictive value
NS	Nodular sclerosis
NSCLC	Non-small cell lung carcinoma
OS	Overall survival
PAS	Periodic acid-Schiff
PDGFRα	Platelet-derived growth factor receptor α
PD-L1	Programmed death-ligand 1
PFS	Progression-free survival
PG-domain	Proteoglycan domain
PHD	Prolyl-hydroxylase
pHi	Intracellular pH
PI	Propidium-iodide
PPV	Positive predictive value
RT-qPCR	Real-Time Quantitative polymerase chain reaction
SUV	Standardized uptake value
T-ALL/LL	T-cell acute lymphoblastic leukemia/lymphoma
TCR	T-cell receptor
TGF-β3	Transforming growth factor-beta 3
VEGF	Vascular endothelial growth factor
vHL	Von Hippel-Lindau
WHO	World Health Organisation
WSD	Whole slide digital analysis
XAF1	XIAP-associated factor 1

2. INTRODUCTION

Low oxygen level (hypoxia), high metabolic activity, and mitotic rate are characteristic features of rapidly growing tumors. Hypoxia is often the result of insufficient blood supply and nutrient level, which can cause irreversible cell damage, and thus, tissue injury presents itself in form of necrosis. To survive, neoplastic cells must undergo metabolic adaptation and fine-tune the expression of a whole series of proteins, such as carbonic anhydrase IX (CAIX). While there is growing evidence that hypoxia-related upregulation of CAIX is associated with unfavorable prognosis and outcomes in several malignancies, little data is focusing on lymphatic neoplasia and especially regarding classic Hodgkin's lymphoma (cHL). Thus, it appeared reasonable to perform some pioneering work to evaluate the relation of hypoxia with cHL these results shape the main body of this Ph.D. thesis.

To introduce the topic, we first discuss the general clinical presentation of classic Hodgkin's lymphoma. Next, we review broader aspects of hypoxia-associated cellular changes in cancer, including cancer-related carbonic anhydrase (CA) isoenzymes, such as CAIX and CAXII, which appear to be important in the adaptation to hypoxia and the possible pharmacological intervention strategies.

3. HODGKIN'S LYMPHOMA

Lymphomas are a group of malignancies that arise from components of the immune system, usually affecting the T- and B-cells. In 1832 Thomas Hodgkin reported the first lymphoma cases, using the term lymphogranulomatosis. Later Sir Samuel Wilks rediscovered the malady and considered Hodgkin's report, added additional cases, and named the disease as "Hodgkin's lymphoma" (HL) [1,2], coining the term.

HL represents approximately 10% of all lymphomas, thus it is one of the rare monoclonal hematopoietic malignancies with B-cell origin. HL continues to elude researchers and clinicians concerning the etiology, mechanism of malignant transformation. HL differs from non-Hodgkin lymphomas (NHL) not only in clinical behavior but also histologically [1,3].

The classification of HL is based on the pathogenesis, morphology, cellular infiltration, immunophenotype, and clinical behavior.

As a whole, HL is characterized by the following:

1. usually arises from a single lymphatic region and then continuously spreads to other (neighboring) regions or extra lymphatic tissue,
2. the disease typically presents in young adults,

3. the neoplastic cells account for less than 1% of the whole tumor mass,
4. The tumor mass is usually comprised of a rich cellular background of inflammatory/reactive cells of lymphatic, myeloid, or stromal origin, such as lymphocytes, plasma cells, histiocytes, mast cells, neutrophils, eosinophils, and fibroblasts [1,4].

According to the 2008 WHO Classification and revision in 2016, HL is to be divided into two main groups: nodular lymphocyte-predominant Hodgkin's lymphoma (NLPHL) and classic Hodgkin's lymphoma (cHL) [5–7].

Morphologically HL has a unique histopathological appearance. Multinucleated (Reed- Sternberg-cells) and mononucleated (Hodgkin-cells) giant cells, which together are also known as the Hodgkin-Reed-Sternberg cells (HRS-cells), are surrounded by a reactive background. The inflammatory background consists of T- and B-cells, histiocytes, plasma cells, mast cells, neutrophils, and eosinophils. The pathognomonic cells of NPLHL are the lymphocytic and histiocytic cells (L&H-cells), also known as popcorn cells [1,4,8].

3.1 Nodular lymphocyte-predominant Hodgkin lymphoma (NLPHL)

NLPHL accounts for approximately 5-10% of all HL cases, which has its peak incidence in the 4th decade with male preponderance. Most of the patients are presented with isolated lymphadenomegaly without systemic symptoms in the early stages of the disease. NLPHL may not only affect peripheral lymph nodes only, but it also tends to spread into the mediastinum and axial lymph nodes. Interestingly, this is the only type of subtype in which mesenteric lymph node involvement may be observed. On the other hand, the advance stage NLPHL has an aggressive clinical behavior and has a poor response to the conventional cHL regimen [9–11]. The neoplastic cells are the "lymphocyte predominant (LP)" cells – previously termed as L&H cells – that have a characteristic, polylobated nuclear contour, also known as "popcorn cells". Typically, LP cells are CD45 and pan-B cell markers (e.g., BCL6, PAX5) positive. Histological appearance of NLPHL is generally follicular or nodular, but diffuse infiltration areas can be observed with a small lymphocyte rich background – typically with $CD4^+$ T cells - without inflammatory cells. Usually, NLPHL is CD30, CD15 negative and EBV-positivity can be observed only in rare cases [8–11].

3.2 Classic Hodgkin's lymphoma

cHL accounts for approximately 85% of all HL. cHL can be further subdivided into four histological subtypes (Figure 1):

- nodular sclerosis (NS)
- mixed cellularity (MC),
- lymphocyte rich (LR),
- and lymphocyte depleted (LD) subtype.

The determination of the subtype is based on clinical and histopathological features, in particular the tissue growth pattern, presence or absence of fibrosis, the composition of cellular background. Further, the characteristic neoplastic cells are determined by special aberrant immunophenotype [1,4,5,7,12]. It seems that socioeconomic status and exposure to common infections influence the incidence of cHL subtypes, as suggested by epidemiologic studies [9,12].

Epstein-Bar virus (EBV) is a herpes virus with linear, double-stranded DNA. It was shown that EBV can transform resting B-cells *in vitro*, thus EBV has been linked to the development of hematologic malignancies such a cHL, diffuse Large B-Cell Lymphoma (DLBCL), and NK/T-cell lymphoma. Viral genome was found in infected HRS-cells and it was suggested that EBV could provide an important growth advantage to HRS-cells. A surrogate marker of EBV is the Latent Membrane Protein 1 (LMP1), the expression of which can be confirmed by immunohistochemistry (IHC). LMP1 is a membrane protein and can induce proliferation, survival, migration, and immune evasion through the activation of NF-κB, JAK/STAT, AP-1, and PI3K/AKT or mitogen-activated protein kinase (MAPK) signaling pathways [13–16]. Alternatively, the EBER sequences of the viral genome can be demonstrated by *in situ* hybridization.

3.2.1 Nodular sclerosis (NS) variant

NS is the most frequent type of cHL, accounting for approximately 70% of the cases in developed countries. NS usually affects young adults (ages between 15 and 34 years old) and a female preponderance is unique in this subtype in comparison to other subtypes of HL. According to epidemiologic studies, NS was associated with higher socioeconomic status which is thought to be related to the delayed exposure to common infections [9,17].

The WHO classification defined NS as a subtype of cHL, which has lacunar-type HRS cells, mixed with inflammatory background and at least one nodule surrounded by collagen bands. Abundant, clear, organelle poor cytoplasm characterizes lacunar HRS-cells. Due to formalin-fixation the cytoplasm

shrinks and retracts, leaving HRS cells in a clear space (thus the lacunar appearance). Next to the above-mentioned histological appearance, necrosis and histiocytic reaction can be often observed with the cellular aggregation of HRS-cells [1,9,17].

3.2.2 Mixed cellularity (MC) subtype

MC is the second frequent type of cHL, accounting for approximately 20-25% of all cHL cases and according to epidemiologic studies, it is more frequent in men and in developing countries. MC and LD variants represent a biological continuum since they overlap in many epidemiological, clinical, and biologic features. MC exhibits a bimodal age distribution with one peak in childhood and a second peak in the elderly. MC is often associated with viral infections, such as EBV and Human Immunodeficiency Virus (HIV) infection. Patients with MC experience B-symptoms (unintentional weight loss, night sweats, fever) frequently [9,10,17].

Morphologically, MC cases may show a diffuse or interfollicular pattern with or without hyperplastic reactive lymphoid follicles. In this subtype, the cellular background is diffuse or vaguely nodular without fibrosis. The rich inflammatory background is comprised of T-cells, eosinophils, neutrophils, histiocytes, and plasma cells [9,17].

3.2.3 Lymphocyte rich (LR) subtype

LR accounts for approximately 3-5% of all cHL cases, frequently diagnosed in older patients. The most common clinical presentation of the LR variant is peripheral lymphadenopathy with mediastinal involvement (15%). LR has a better prognosis than other subtypes of cHL and is often diagnosed in the early stages of the disease. Patients with LR may not experience B-symptoms. LR has a nodular growth pattern with small, inactive germinal centers in many of the nodules with typical CD30 positive HRS-cells. Neoplastic cells could be observed around reactive lymphoid follicles with rare or no eosinophils or neutrophils. Similar to the NLPHL, in the LR subtype the cellular background is also dominated by small B-lymphocytes forming nodules frequently with peripheral regressed germinal centers. In the differential diagnosis, it is important to distinguish it from NPLHL, as both of them have a similar histological picture, however, in LR the presence of HRS-cells is the foundation of the diagnosis [1,9,17].

3.2.4 Lymphocyte depleted (LD) subtype

1% of all cHL cases in the Western countries, thus it is the rarest variant and often associated with aggressive clinical behavior. As mentioned before, LD represents a biological continuum with the MC variant. Like the MC subtype, LD is more frequent in the developing countries, often associated with different infections (EBV, HIV), LMP-EBV is relatively frequent in this subtype. LD is more frequent in the elderly. In contrast to the MC and NS subtypes, LD is more common in men and B-symptoms are also frequent [9,10,17].

LD has two forms (according to Lukes-Butler): the reticular/sarcomatous type characterized by sheets of HRS-cells with sparse lymphocytes and other reactive cells; and the diffuse fibrotic type presenting with scattered HRS cells (paucicellular) in a thick eosinophilic, periodic acid-Schiff (PAS)-positive stroma. The differential diagnosis should separate this variant from the EBV-positive large-cell lymphoma and the anaplastic large T-cell lymphoma [1,10,17,18].

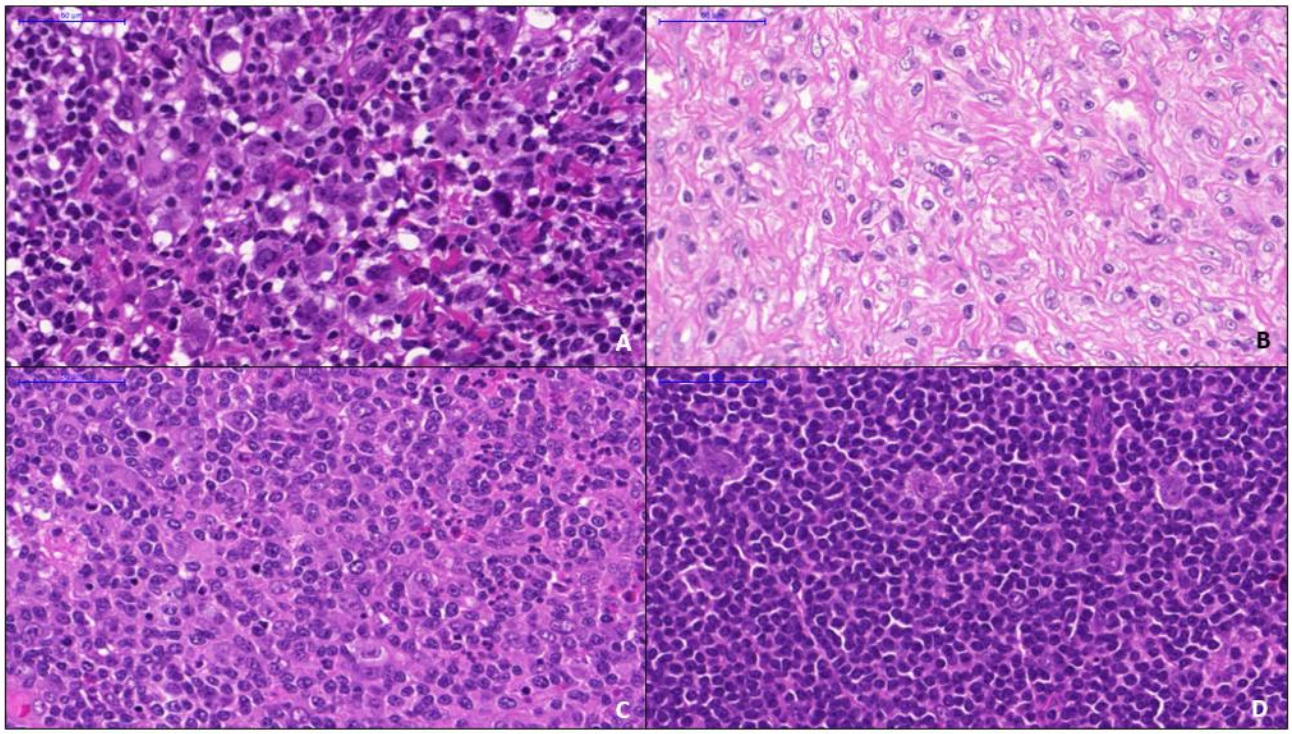

Figure 1 Morphologic features of the different cHL subtypes. A: nodular sclerosis, B: lymphocyte depleted, C: mixed cellularity, D: lymphocyte rich (Magnification : 20x). Pictures are from the archive of the Pathology Department, University of Debrecen.

3.3 Clinical features

The general clinical representation of cHL is painless lymphadenomegaly, commonly in the cervical or supraclavicular region. Common clinical symptoms include B-symptoms (fever, drenching night sweats, unexplained weight loss >10% over 6 months) and the whisky sign – alcohol-induced lymphadenopathy - and general pruritus. In cases affecting the mediastinal or axillary region, lymphadenomegaly rarely cause vena cava superior syndrome. Extranodal involvement generally arises from hematogenous dissemination, and the most frequently involved organs are the lungs, liver, and bone/bone marrow [4,9,12,19]. Staging is carried out according to the Ann Arbor Staging system (Figure 2.), which is based on the anatomical location of the malignant process and systemic symptoms (mentioned above).

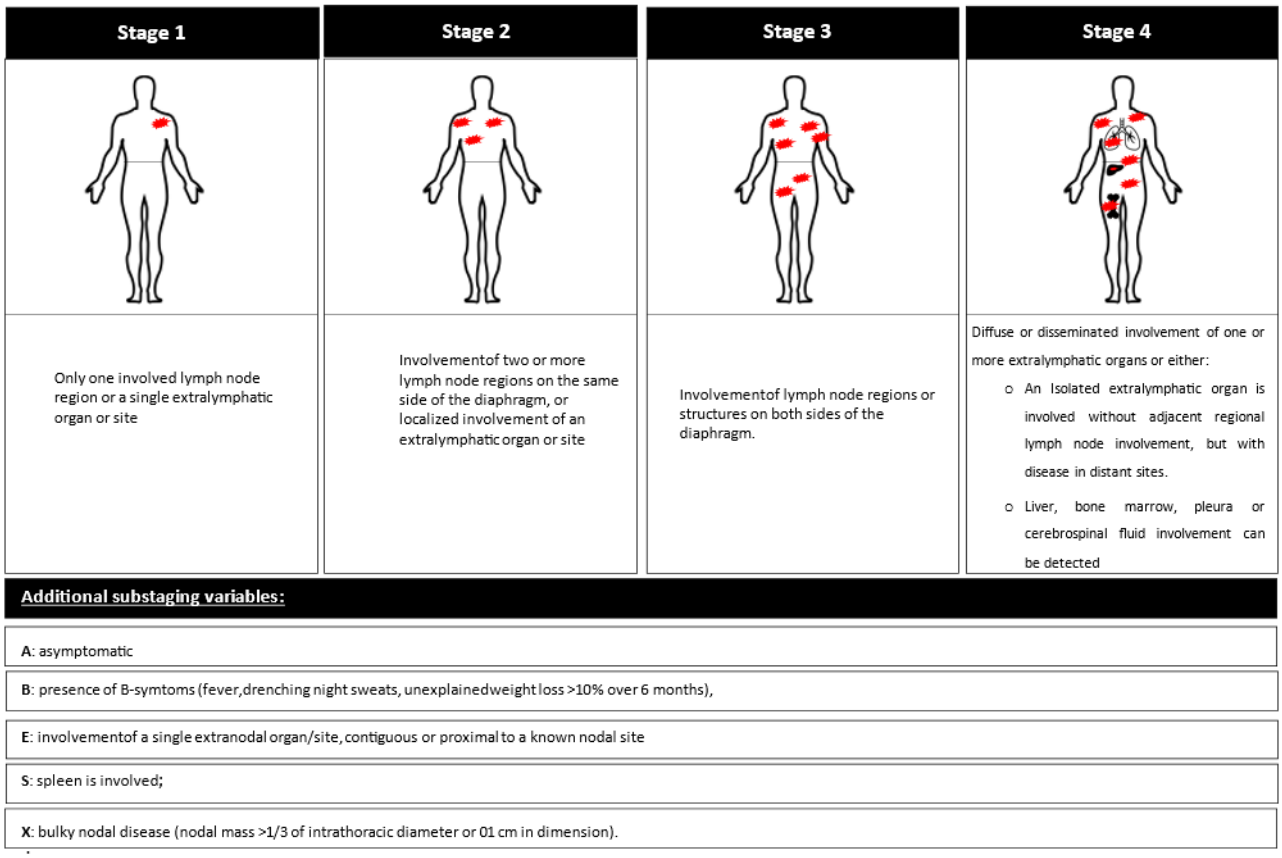

Figure 2. cHL staging according to the Ann Arbor Classification. Most commonly used four-stage classification system, which gives prognostic information about the disease and also provides guidance for therapeutic decisions.

Following several updates and modifications the Ann Arbor Classification is still the basis of the clinical staging and risk-stratification procedure (e.g., Lugano classification, Cotswold-modified Ann Arbor Classification).

3.4 Clinical management of cHL

Commonly cHL is diagnosed by tissue biopsy. Fine-needle aspiration or core needle biopsies are of limited use as they do not provide enough information about the architecture of the lymph node. The diagnosis of cHL is confirmed by histological examination and defined in terms of its microscopic appearance and the immunophenotype of the neoplastic cells.

^{18}F-fluorodeoxyglucose (^{18}F-FDG)-PET and computer tomography (CT) is a recently widely used potent tool for staging, end-of-treatment and interim assessments, and follow-up surveillance.

In the early stages (stage I-IIA) of HL, the commonly accepted treatment is a combination chemotherapy of the four components doxorubicin, bleomycin, vinblastine and dacarbazine (ABVD) with involved-field radiation therapy (IFRT) restricted to the involved lymph nodes. In advanced stages of HL, other combined chemotherapy regimens, such as the BEACOPP (bleomycin, etoposide, doxorubicin, cyclophosphamide, vincristine, procarbazine, and prednisone) or CHOP (Cyclophosphamide, doxorubicin, vincristine, prednisone) can be used in the lack of response to ABVD. In relapsed cases, autologous stem cell transplantation and high-dose chemotherapy and other salvage treatment protocols (e.g., dexamethasone/high-dose cytarabine/cisplatin (DHAP), ifosfamide/gemcitabine/vinorelbine (IGEV) or ifosfamide/carboplatin/etoposide (ICE)) should be considered [19,20]. Patients with poor prognosis can also receive high dose chemotherapy (HDCT) followed by autologous stem cell transplantation (ASCT)[12,19,19,21,22].

The ABVD treatment is consisted of [12,19,20,23]:

- Doxorubicin/Adriamycin(A): an anthracycline antibiotic, which intercalates between base pairs in the DNA helix, thus inhibiting DNA replication and protein synthesis. It also inhibits topoisomerase II, which leads to double-strand breaks. Doxorubicin also forms oxygen-free radicals, which contribute to its cytotoxicity [24].
- Bleomycin (B): is a glycopeptide antineoplastic antibiotic. Bleomycin forms a complex with iron and produces reactive species that lead to DNA strand breaks. Additionally, bleomycin can cause lipid peroxidation, carbohydrate oxidation, and altered prostaglandin synthesis and degradation [25].
- Vinblastine (V): is an alkaloid, which can disrupt microtubule formation, thus interfering with mitosis and influencing glutamic acid metabolism [26].

- and Dacarbazine (D): is a triazene derivate, which can alkylate and cross-link DNA in all phases of the cell cycle, generating DNA function disruption, cell cycle arrest, and apoptosis [27].

3.5 Epidemiology and risk factors

cHL is a rare type of malignancy. The last report by the International Agency for Research on Cancer (IARC) on global cancer incidence, estimated approximately 83 087 new cases in 2020, which is 0.5% of all new cancers [28], compared to other kinds of cancers like breast or colon tumors.

Risk factors for the adult HL are age - below the age of 40 and over the age of 65 years-, male gender, EBV infection, family history of HL [12,28].

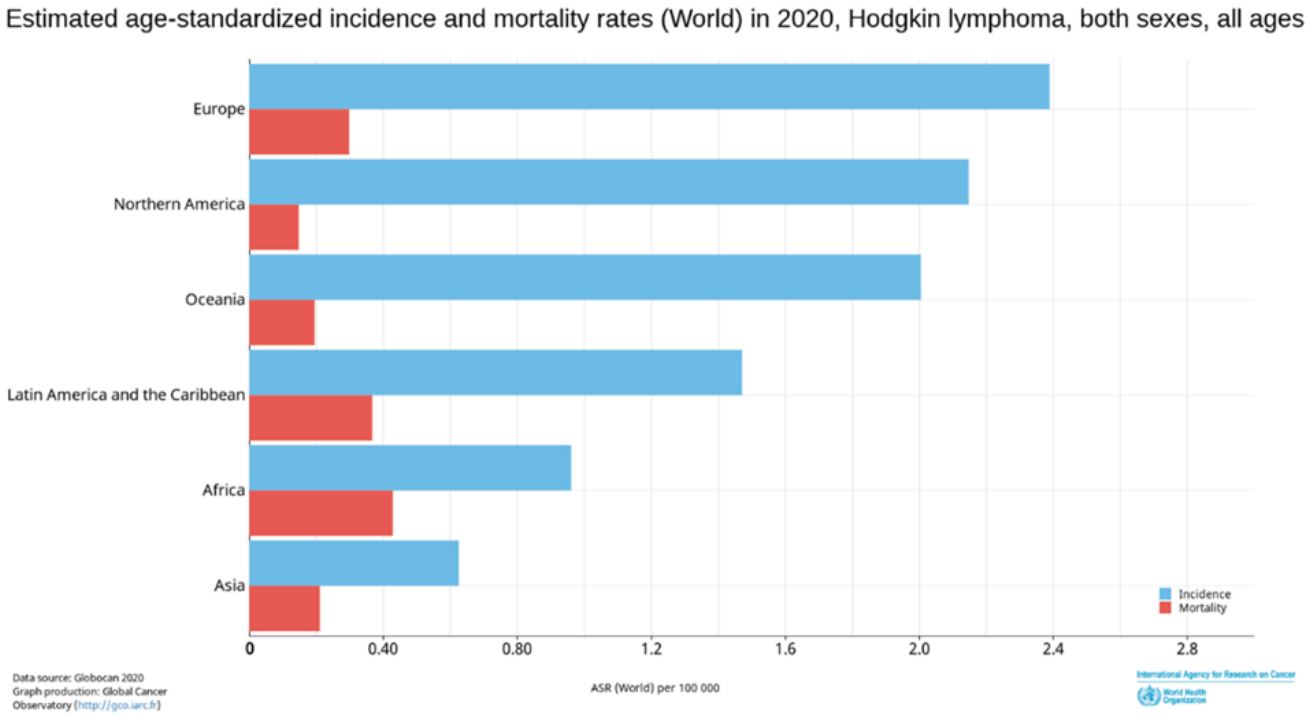

Figure 3 Hodgkin's lymphoma statistics in 2020. Bar chart pf the age-adjusted HL incidence and mortality (per 100000 people) in 2020 in both sexes within all ages, worldwide according to the Global Cancer Observatory (https://gco.iarc.fr/today/home).

The occurrence of cHL shows a geographical and an economical distribution. Rates of HL are generally higher in developed countries compared to the developing regions of the world (Figure 3.). The incidence of HL shows male preponderance compared to females.

Noteworthy is the fact that the HL incidence shows a bimodal age distribution, meaning that the age of most patients at the time of diagnosis is in the early 20s followed by a steady decline, and after the age of 55 and above. This type of age distribution can be seen in both sexes and has a male predominance mainly in the adult years [12].

3.6 Differential diagnosis

Other conditions may have a similar cellular appearance as cHL, hence mimicking cHL. To avoid diagnostic pitfalls, the clinicopathological, and perhaps more importantly, the histopathological evaluation should be carried out carefully. Histological evaluation is based on tissue and cell morphology as well as specific cellular markers, which can be determined by immunohistochemistry.

Commonly used immunohistochemical markers are listed in Table 1.

Table 1 Immunophenotypic markers for the differential diagnosis of Hodgkin's lymphoma. The table is based on [9].

Immunohistochemical staining	NLPHL	cHL	Grey zone lymphoma	EBV+DLBCL	Anaplastic large cell lymphoma
CD15	Negative (positive in rare cases)	Positive (membrane and/or Golgi pattern)	Positive	Frequently positive	Positive (membrane and Golgi pattern)
CD20	Positive	Usually negative	Often positive	Positive	Negative
CD30	Negative	Positive	Positive	Positive	Positive
CD45	Positive	Negative	Variable	Positive	Positive
PAX5	Positive	Weak positive	Positive	Positive	Negative
BCL-6	Positive	Negative	Usually negative	Variable	Negative
EBV	Negative	MC and LD variant are usually positive	Usually negative	Positive	Negative

The following lymphoma types may cause misdiagnosis during the evaluation procedure [9,29]:

- Grey zone lymphoma, which may resemble the mixture of NS variant of cHL and primary mediastinal large B-cell lymphoma [9,29,30].
- EBV-positive DLBCL, which may be HRS-like cells too with polymorphic reactive components [9,29].
- Other EBV-associated B-cell proliferations (e.g. polymorphic B-cell lymphoproliferative disorders) [9,29].
- Peripheral T-cell lymphomas with "HRS-like cells", such as angioimmunoblastic T-cell lymphoma [9,29].
- Anaplastic large cell lymphoma, which is a T-cell lymphoma, and interestingly, it shows strong CD30 positivity. The characteristic highly atypical neoplastic cells usually have horseshoe-shaped nuclei [9,29,31].

Figures 4. and 5. show the immunohistochemical profile of cHL.

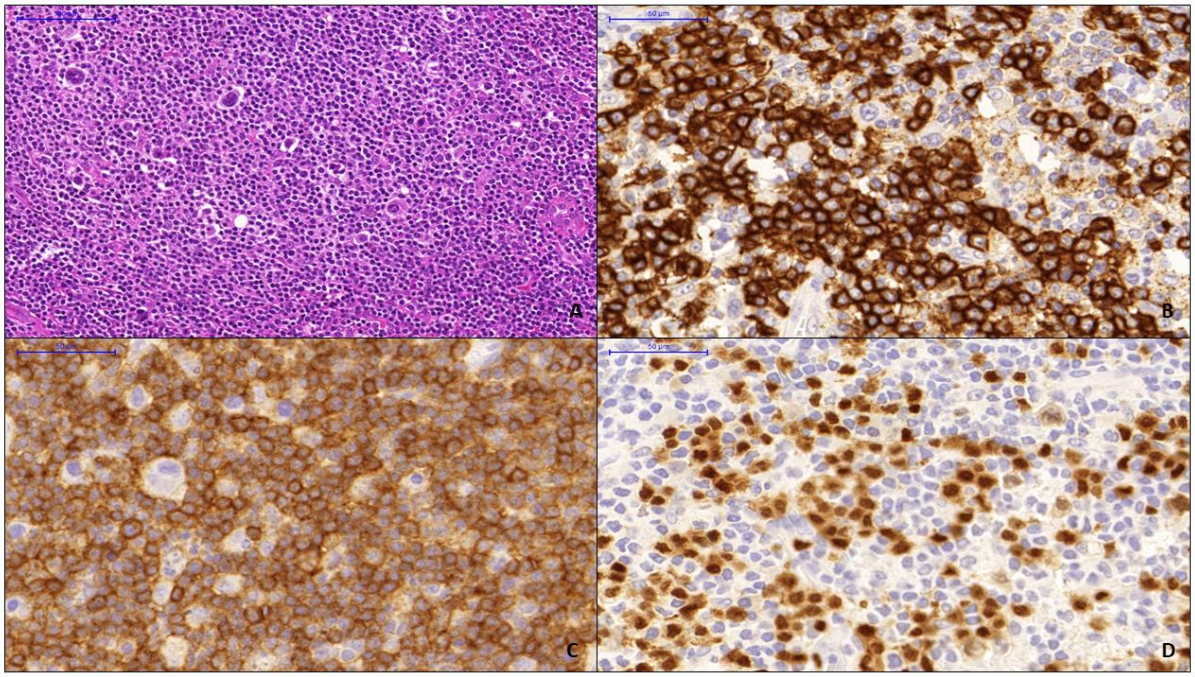

Figure 4 Immunohistochemical profile of cHL. A: H&E staining, B: CD20, C: LCA and D: PAX5 staining. (Magnification :20x). Pictures are from the archive of the Pathology Department, University of Debrecen.

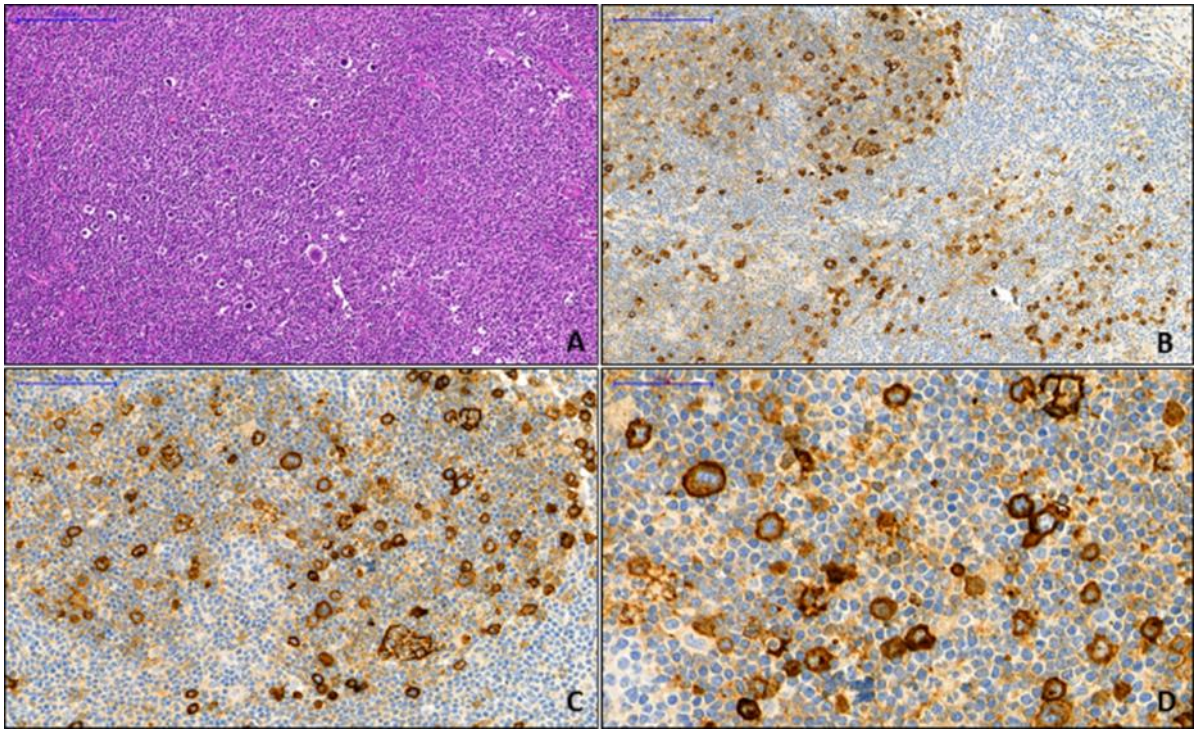

Figure 5 Morphologic and immunohistochemical features in cHL. Panel A: Hematoxylin-eosin staining. Panel B-C-D: CD30 immunohistochemical staining (magnification 10x-20x-40x). Typical HRS cells can be observed with strong CD30 positivity. Pictures are from the archive of the Pathology Department, University of Debrecen.

3.7 Cellular origin of HRS-cells

Neoplastic cells typically keep key features of the normal cellular compartment from which they originate, but the origin of cells presenting with the HRS morphology – the neoplastic cells in cHL- remains obscure since they show a rather unusual phenotype. HRS cells coexpress several hemopoietic lineages markers (B-cell marker – BCR, T-cell marker - TCR), and they also consistently express CD30 and CD40 (Figure 6.) [8,32,33].

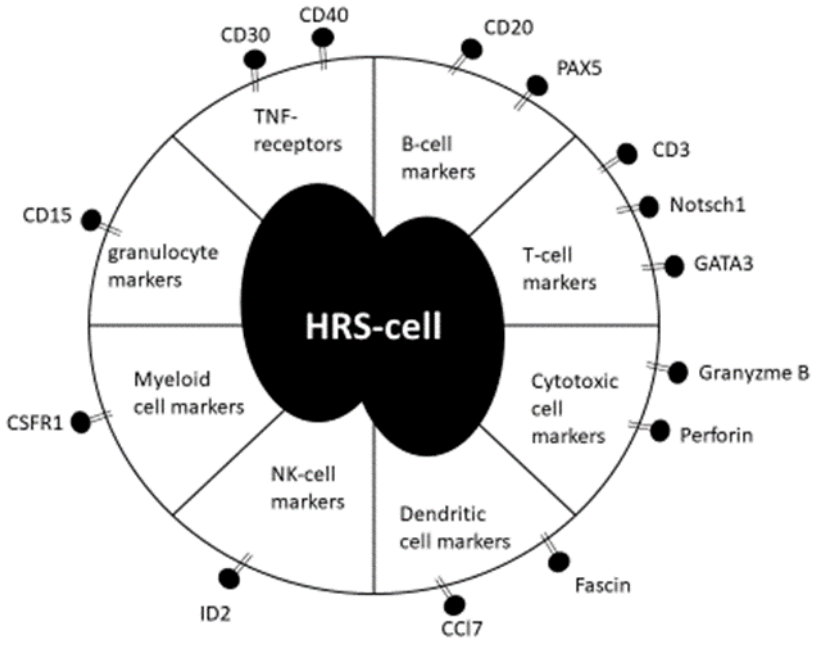

Figure 6 The aberrant immunophenotype of HRS cells is reflected by the expression of major antigens with a broad but virtually unrelated cellular functionality

As already discussed, cHL is characterized by a rare, malignant cell type known as the HRS cell. The large mononucleated Hodgkin cell and the even larger multinucleated Reed- Sternberg (RS) cells coexist with a non-neoplastic cell population [32,34].

HRS-cells used to be frequent subjects of phenotype and genetic studies and were suspected to derive from the B-cell lineage. Lymphatic germinal center (GC) origin was revealed by the single-cell polymerase chain reaction technique. Molecular studies also stated a clonal immunoglobulin heavy and light chain gene rearrangement and somatic hypermutation of the Ig genes. Normally, when a mutation in Ig genes corrupts Ig functions the B-cell would undergo a negative selection, resulting in apoptosis. Thus, HRS-cells most likely derive from B-cells that have been arrested at the GC or post-GC stages of B-cell differentiation. However, these "crippled" HRS-precursor cells have gained the capacity to overcome apoptosis signals [32]. After the acquisition of „crippling" mutations in the Ig V genes these cells lack functional surface BCRs, and instead of undergoing apoptosis, they rescue, suggesting that the HRS cells are derived from pre-apoptotic GC B-cells [32,34,35]. "Despite its GC B-cell origin, HRS cells show a global loss of B-cell phenotype. B-cell specific transcription factors, such as PU.1, Oct-2, BOB.1, EBF1 and TCF3 are not detectable in HRS cells" [32]. Downregulation of different B-cell specific genes by various mechanisms reflects the unique genetic and epigenetic profile of HRS-cells [16,36]. Besides these genetic changes, aberrant expression of master regulators of other hemopoietic cell lineages – such as T-cell factor Notch1 and NK-cell factor ID214- is also characteristic

for HRS-cells [33]. HRS-cells can also harbor T-cell markers; thus, studies were carried out for a potential T-cell derivation of HRS-cells. Müschen et al. [37] concluded that „HRS cells may harbor clonal TCR-β VDJ and a clonal DJ gene rearrangement but no clonal Ig gene rearrangement. Given that the presence of a TCR-β VDJ gene rearrangement defines a T-cell, it was proven that HRS cells could derive from T-cells in a rare subpopulation of the disease (1-2%)".

RS cells may be differentiated end-state tumor cells, since they have no proliferative or clonal growth potential, unlike the progenitor cells of the giant Hodgkin-cell. It is hypothesized that the precursor of Hodgkin-cell is the small mononucleated Hodgkin cells, that show high proliferative potential. However, the exact mechanism of the development of these cells remains to be unknown. It has been already suggested that RS cells develop through endomitosis or acytokinetic mitosis. Nevertheless, a recent study applying continuous single cell tracking of HL cell lines by long-term time-lapse microscopy has found that the re-fusion of daughter cells due to incomplete cytokinesis and the persistence of microtubule bridges connecting the daughter cells is the main route to large RS cells (Figure 7.) [34,38,39]. It was also noted that RS cells have the potential to shape their microenvironment [35]. A recent study [40] showed that hydrogen peroxide induces the differentiation of small cell populations into large H- and RS-like cells and, using microarray analysis, it was confirmed that the small cell population preferentially expresses HIF1α, indicating that these cells are hypoxic.

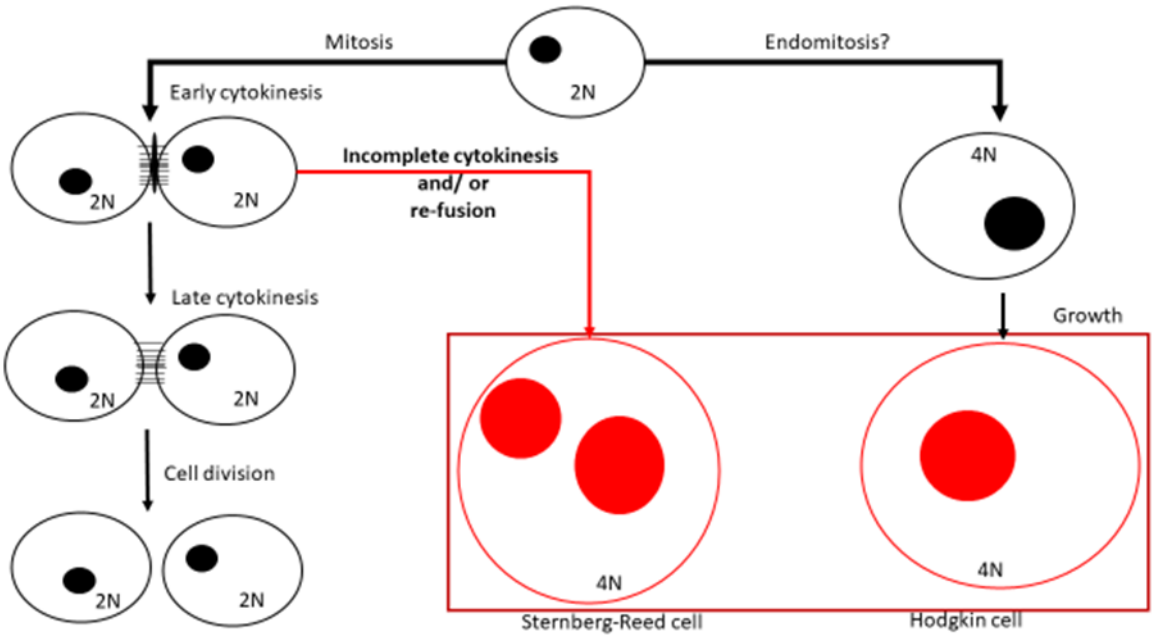

Figure 7 Possible origin of HRS-cells. HRS cells may develop due tore-fusion of daughter cells and/or incomplete cytokinesis and the persistence of microtubule bridges connecting the daughter cells. The figure is based on [38].

4. METABOLIC ADAPTATION TO HYPOXIA

4.1 Tumor Hypoxia

Hypoxia is defined as reduced tissue oxygen partial pressure (pO_2) levels than physiological levels. This can occur due to hypoperfusion or increased cellular demand for molecular oxygen that exceeds vascular supply, leading to a bioenergetic crisis. Hypoxia may develop at an early stage of tumor progression and it has a profound impact on many aspects of tumor biology, inducing signaling pathways in neoplastic cells that allow them to survive under low oxygen tension. It also induces key adaptation mechanisms, such as metabolic reprogramming, immune tolerance, angiogenesis, proliferation, and metastases [41–43]. These adaptive changes act as a strong selection pressure on malignant cells. The regulation of the adaptive mechanisms falls under a key transcriptional factor that is known as the Hypoxia Inducible Factor (HIF) [44–46].

4.1.1 Transcriptional activation of HIF

HIF is a heterodimeric transcriptional factor, composed of oxygen-sensible α and oxygen-stabile β subunits (Figure 8.). Among the various isoforms of HIF α -subunits, HIF1α and HIF2α and HIF3α share similarity in structure and function.

In normoxia, the HIFα subunit is hydroxylated by prolyl-hydroxylases (PHD) targeting it for proteasomal degradation. However, in hypoxia, the hydroxylation of HIF is blunted, allowing the α-subunit to stabilize and translocate from the cytoplasm to the nucleus where it forms a dimer with β subunit (Figure 8.). The freshly formed heterodimer binds to the hypoxia-response elements (HRE), activating the transcription of HIF-dependent genes [44(p1),45(p1),46,47(p1),48]. Under physiological oxygen tension, the process of proteasomal degradation and ubiquitination of HIFα involves von Hippel-Lindau (vHL) protein, a tumor suppressor protein, which mediates the quick degradation process, thus when vHL is mutated or lost, the HIFα-dependent genes are upregulated [43,45,48,49].

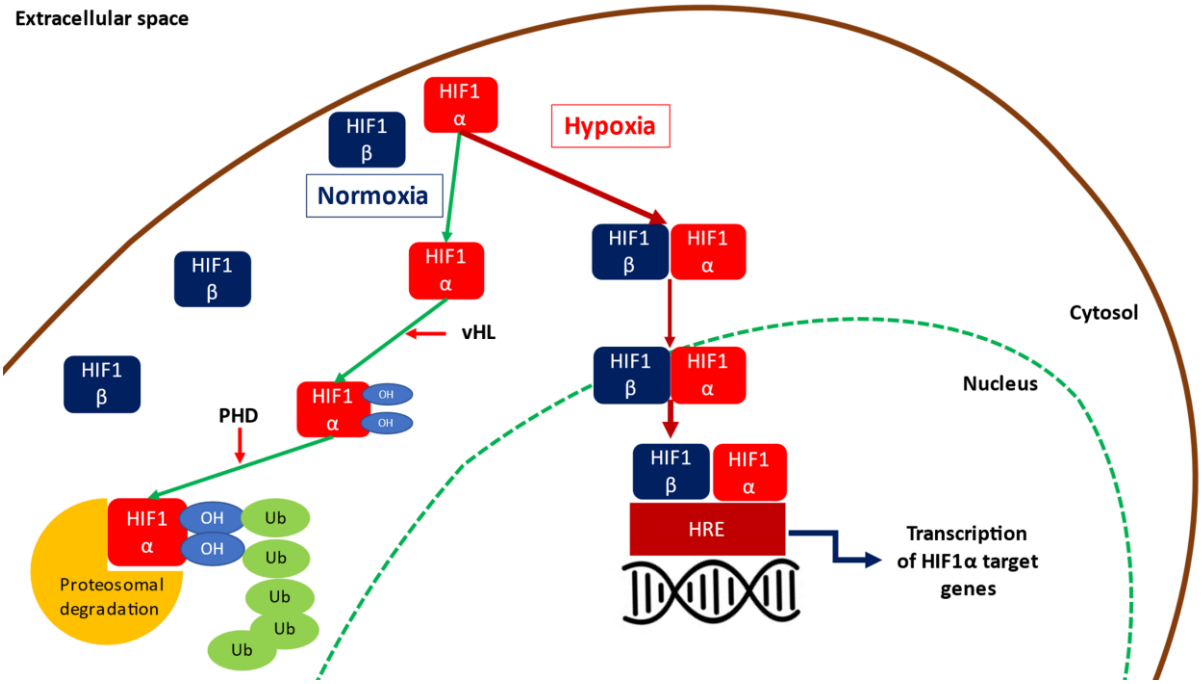

Figure 8 Regulation of HIF1α. In normoxic conditions HIF1α undergoes proteosomal degradation, while in hypoxia the HIF1α and HIF1β dimerizes and translocate into the nucleus, where the freshly formed heterodimer binds to the hypoxia responsive element (HRE) and activates the transcription of HIF1-dependent genes.

HIF1α is responsible for cellular adaptation mechanisms under hypoxic conditions and is associated with neoplastic transformation and the development of therapy resistance [[45,45(p1),47(p1),48]. HIF2α plays role in the adaptation to chronic hypoxia and HIF2α influences the regulation of proinflammatory cytokines during macrophage activation. HIF2α affects vascular remodeling and has a negative influence on prognosis, overall, and disease-free survival in various solid tumors [50,51]. Expression of HIF3α was observed in numerous human organs, and the highest HIF3α expression levels could be measured during fetal organogenesis [48,52(p3),53(p3),54].

HIF1α mediates many aspects of cellular homeostasis. HIF1α transcriptional activation leads to a metabolic shift from oxidative phosphorylation to anaerobic glycolysis. HIF1α also contributes to the expression of glucose transporters (GLUT1, GLUT3) to maintain glucose influx which is essential for the cellular energy supply. The expression of a set of growth factors is also stimulated by the transcriptional activity of HIF1α. These growth factors - vascular endothelial growth factor (VEGF), transforming growth factor beta3 (TGF-β3), epidermal growth factor (EGF) - induce the formation of new blood vessels into the tumor mass that subsequently support tumor growth and distant metastasis formation. Cell proliferation is also induced by HIF1α [45,49], and according to literature, hypoxia can contribute to impaired anti-tumor immunity [55] Additionally, HIF1α is associated with the elevated

expression of several drug resistance genes, such as multi-drug resistance (MDR) and XIAP-associated factor 1 (XAF1) [56].

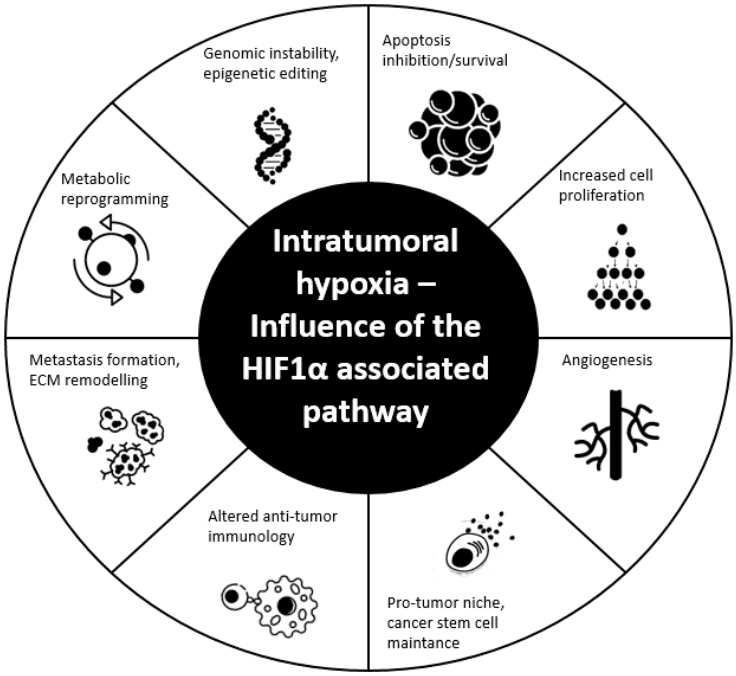

Figure 9 Schematic presentation of basic functions of HIF1α. HIF1α activation contributes to increased cellular proliferation and supports angiogenesis. Altered anti-tumor response, genomic instability, inhibition of apoptosis and metabolic reprogramming of neoplastic cells contributes to a pro-tumor niche, increasing survival and transforming capacity.

Altogether HIF1α orchestrates the adaptation of the tumor cells to hypoxia (Table 2, Figure 9).

Table 2 HIF1α associated genes: nitrogen-monoxide synthetase (NOS), Insulin-like growth factor (IGF-2), C-X-C chemokine receptor type 4 (CXCR-4), matrix metalloproteinase-2 (MMP-2), Epidermal growth factor(EGF), Transforming growth factor-beta 3(TGFβ3) Lactate dehydrogenase (LDH), Glucose transporter 1 (GLUT1), hexokinase 2 (HK2), Glyceraldehyde 3-phosphate dehydrogenase(GAPHD), Carbonic anhydrase IX (CAIX), carbonic anhydrase XII (CAXII), Erythropoietin (EPO), Transforming growth factor-alpha (TGF-α), Vascular endothelial growth factor(VEGF), multi-drug resistance (MDR), XIAP-associated factor 1 (XAF1), Programmed death ligand 1 (PD-L1)

Cellular functions	Genes
Cell proliferation	MYC, NOS, IGF-2
Migration, metastasis forming	CXCR4, MMP2, EGF, TGF-β3
Cell metabolism	LDH, GLUT1, HK2, GAPDH
pH regulation	CAIX, CAXII
Cell survival	EPO, TGF-α, IGF-2
Angiogenesis	VEGF, EPO
Apoptosis	p53 mutation
Therapy resistance	MDR2, XAF1
Tumor immunity	PD-L1

4.2 Hypoxia related tumor acidity

Intraparenchymal tissue hypoxia triggers a metabolic shift: in conditions, with reduced oxygen levels or in the absence of oxygen the cells will switch over to glycolysis to maintain cellular energy levels. Glycolysis does not only generate ATP but also supports other biochemical pathways (e.g., the pentose-phosphate shunt) and through these, glycolysis contributes to the synthesis of biomass (e.g., nucleotides, proteins, fatty acids), which is pivotal to produce new cells during tumor expansion. Neoplastic cells may continue glycolysis even under normoxic conditions, the phenomenon is called the Warburg effect. However, glucose catabolism also results in the accumulation of several metabolic end products, including CO_2, protons, and lactic acid. Prolonged accumulation of these substances may lead to intracellular acidosis that interferes with biosynthetic reactions and signaling because most of the molecules, regulators, and other components of cellular machinery are pH-sensitive. To avoid cytosolic acidification, cells redirect the ion flux and increase the rate of pH-regulating activity. Due to the active upregulation of transmembrane enzymes or channels, the intracellular pH (pHi) returns to near alkaline values that support cell survival and proliferation. The mechanism of enzymes is generally based on the diffusion of CO_2, export of lactate and H^+, and the hydration of CO_2 to produce bicarbonate ions. These mechanisms lead to pericellular acidosis that is a frequent component of the tumor microenvironment, as the metabolic waste cannot be efficiently removed by the insufficient tumor vasculature. This adaptation mechanism may contribute to a selective advantage of neoplastic cells, against surrounding normal cells, which may lead to an acquisition of a more aggressive tumor phenotype. Acidosis is a potent inhibitor of T-cell effector functions, and it also contributes to tumor progression, like angiogenesis, invasion, and metastasis. Altered intracellular pH levels also influence several cellular phenomena, such as aneuploidy, chromatin stability, autophagy, cell migration, survival, and release of exosomes. The shift to acidic pH is associated with resistance of chemo-, radio- and immunotherapies [57–61]. Intracellular acidosis is controlled in both normal and cancer cells through several adaptation mechanisms. One key regulatory system is the expression and activation of carbonic anhydrases.

4.2.1 Carbonic anhydrase IX

4.2.1.1 Regulation of CAIX

Carbonic anhydrase IX (CAIX) is one of the 15 human isoforms of the α carbonic anhydrase family [62–64]. Table 3. summarizes the expression pattern of CAs in non-cancerous cells of the human body. Note, a limited expression of CAIX is typical in physiological conditions.

Table 3 The physiological expression of the CA isoenzyme family in human tissues. The table is based on [65]

Cellular position	Enzymes	Physiological expression
Cytosolic	I	**Red blood cell**
	II	**Kidney**
	III	**Skeletal muscles**
	VII	**Adipose tissue**
	XIII	**Colon**
	VIII, IX, X	**Liver, neuron**
Mitochondrial	VA	**Hepatocyte**
	VB	**Adipocyte, hepatocyte, lymph node, spleen, colon, testis**
Secreted	VI (gustin)	**Tear, Milk, saliva, respiratory tract**
Membrane-bound	IV	**Bone marrow, gastrointestinal tract, liver**
	XIV	**Liver, Gastrointestinal tract, cervix**
	IX	**Hair follicle, Gastrointestinal tract**
	XII	**Gastrointestinal tract, Kidney, Breast, Endometrium**

CAIX is not expressed in most normal cells - the only exception is a gastrointestinal tract – but together with the carbonic anhydrase XII (CAXII), they are the only enzymes that are abundant and strongly expressed on the membrane of tumor cells, contributing to cancer development [64,66–68]. CAIX has an important role in acid-base balance as it contributes to the elimination of the H^+ in order to create a nearly physiological intracellular pH, while extracellular pH becomes acidotic. That would result in the survival of cancer cells, despite the hostile microenvironment and it also facilitates tumor cell invasion. The CAIX-related adaptive response is associated with aggressive tumor phenotype and resistance to chemotherapy [48,62–64,66]. HIF1α has been identified as a master inductor of CAIX by upregulating its expression in hypoxic conditions. However, cases have been reported in which acidosis-induced CAIX overexpression was not HIF1α dependent, but NF-κB mediated. NF-κB also enables the evaluation of intratumoral hypoxia through the expression of CAIX [57,69,70].

4.2.1.2 Structure and function of CAIX

The active form of CAIX is a protein with a unique structure which undergoes dimerization. The glycoprotein consists of a small intracytosolic domain, a transmembrane protein section, an extracellular zinc-containing catalytic domain, and a unique proteoglycan (PG) domain, that could only

be observed in CAIX [57,61]. While the function of the intracytosolic and transmembrane domains is still unclear, it seems that there is a close interplay between the catalytic and the PG-domain. The catalytic domain is responsible for the reversible conversion of H_2O and CO_2 to HCO_3^- and H^+, which is supported by the PG-domain. The PG-domain is proved to be a buffer for protons to promote catalytic enzyme activity [57,60].

The extracellular domain of CAIX undergoes various modifications, which consequently modifies the function of CAIX. The catalytic domain could be N-glycosylated by high mannose sugar chains, while O-glycosylation by heparan or chondroitin sulfate glycosaminoglycan is important for the appropriate biochemical and cellular function of the PG domain. Moreover, the whole ectodomain can be cleaved by matrix metalloproteinases leading to the "ectodomain shedding" phenomenon. The regulated proteolytic cleavage of CAIX is a constitutive process, however, could be enhanced by various stimuli, such as hypoxia, acidosis, or chemotherapeutic drugs [57,61,71]. The role of ectodomain shedding remains to be elucidated, it is tempting to speculate that it may have a potential role in autocrine and/or paracrine signaling. Some observations already suggested that CAIX inhibitors need to block the activity, as well as ectodomain shedding of CAIX for efficient pharmacological effects [57,61,71–73].

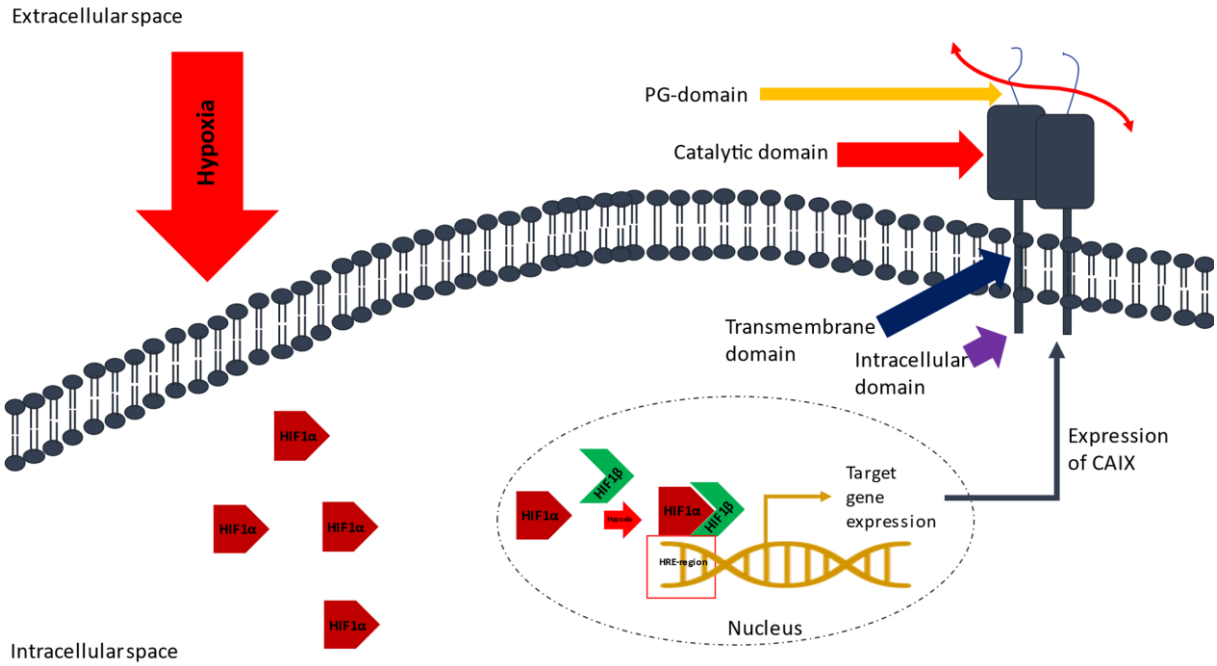

Figure 10 The regulation and expression of CAIX is highly HIF1α-dependent. The transcriptional activation of HIF1α leads to an increased expression of CAIX in support of the restoration of pH. The structure of active CAIX consist of an intracellular, a transmembrane, a catalytic and a unique proteoglycan (PG) – domain.

4.2.1.3 Inhibition of CAIX

The CA activity can be inhibited by various compounds, such as monoclonal antibodies, "dual inhibitors" and small molecule inhibitors [74,75]. Monoclonal antibodies as inhibitors operate in three possible ways: i) antibody-mediated cell cytotoxicity, ii) catalytic domain blockade, or iii) receptor-mediated internalization. Girentuximab® -also known as Rencarex® - is a monoclonal CAIX inhibitor, which is currently used in phase III trials of clear cell carcinoma [75–77]. In recent years, "dual inhibitors" – like celecoxib, polmacoxib - have been used in clinical studies. These compounds can simultaneously inhibit the cyclooxygenase (COX) and CA enzymes. Currently, celecoxib is widely studied in many clinical trials [78,79]. Classical carbonic anhydrase inhibitors belong to the group of sulfonamides, ureidosulfonamides, coumarins, and other small molecule inhibitors [80]. Sulfonamides, like acetazolamide (AA), directly inhibit the zinc-containing catalytic domain of CA, thus disabling the enzyme activity [75,81,82]. Selective inhibition of CAIX can be achieved by new generation sulfonamides [83,84].

Similar to CAIX, CAXII is a membrane-bound enzyme the expression of which is hypoxia and estrogen-receptor dependent. The physiological expression of CAXII could be detected in the gastric mucosa, sweat glands, kidney and ciliary epithelial cells (Table 3.,[65,85]). However, an increased manner of CAXII expression was reported in severaltumor types. Elevated CAXII expression correlated with the histological tumor grade in clear cell carcinomas and oncocytomas. Moreover, the overexpression of CAXII was detected in various central nervous system tumors, including hemangioblastomas, meningiomas and gliomas. Interestingly, in breast cancer, favorable outcome was associated with the degree of CAXII expression and also, it seems that the estrogen-receptor may play an important role in the expression of CAXII [85]. There is only a limited number of studies concerning CAXII and lymphomas. Lounnas et al. [86] examined the expression of CAXII in T-cell acute lymphoblastic leukemia/lymphoma (T-ALL/LL) in vitro and ex vivo. They found that "CA XII is upregulated in T-ALL/LL and that its inhibition decreases cell proliferation and induces cell apoptosis". To our best knowledge, CAXII has never been examined in cHL.

4.3 HIF1α and B-lymphocyte functions

According to *in vivo* experiments, the oxygenation of normal lymphatic tissue is highly variable that can influence immune functions. Abott et al. [87] measured the distance between GC and vascular structures within the murine spleen and found that GCs were generally >40 μm away from the nearest

blood vessel concluding that GCs in the spleen were preferentially located in hypoxic areas. GL-7 - a marker of GC B-cells was also found to be upregulated in these areas in concert with the elevated HIF1α levels, compared to the normoxic lymphatic tissue sites.

In another murine animal model, the bone marrow was examined, and similar results were reported. The distance between perisinusoidal parenchyma and endosteum showed that these structures were also approximately 40 μm from each other and the hypoxic regions had irregular vascularity [88]. Interestingly, both the maturation and activation of the normal lymphatic cells seem to be affected by the actual oxygen level. Hypoxia appears to have an important role in follicular B-cell maturation. *In vitro* results showed that the peak of class switch recombination (CSR) was around 72 h of experimental hypoxia, which was followed by a significant increase in apoptotic caspase 3 activity. Accordingly, follicular GC hypoxia promoted IgM to IgG CSR and also influenced the clonal competition and affinity maturation [87]. Cho et al. [89] investigated the antibody composition in hypoxic GCs and found that PHD/vHL/HIF axis has a fundamental influence on the quality of antibody response. They also reported that levels of activation-induced cytidine deaminase (AID) enzyme could be directly affected by hypoxia consequently, decreased AID enzyme activity could influence the rate of ongoing CSR [89].

The glycolytic pathway – mediated by HIF1α - turned out to be essential for the transition from the pro-B to the pre-B stage and the survival and the differentiation of the B-cells [90]. Deficiency in HIF1α activity was connected to impaired B-cell development in bone marrow, thus an inevitable role of HIF1α in the development and the activation of B-cells was suggested [90,91]. According to the results, the increased glycolytic rate was fundamental for the initial B-cell maturation process [92,93].

HIF1α expression could be detected during the physiological maturation of B-cells and immune activation, while HIF2α was found to be upregulated following malignant transformation, like in diffuse large B cell lymphoma (DLBCL) [94].

4.3.1 Hypoxia associated changes in cHL: what did we learn so far

Examination of hypoxia-related changes in cHL did not gain considerable scientific interest in former times. According to several genetic and epigenetic profiling data, hypoxia-associated pathways were reported not to be generally active in HRS-cells [95–97]. However, Wein et al. suggested that there is a HIF1α induced change, which can result in dynamic B-cell reprogramming and phenotype switch towards HRS-cells, furthermore, NF-kB and MYC can be involved in the process too [98]. Kewitz et. al [56] observed in their *in vitro* study that there is a change in cellular metabolism upon hypoxia mimetic

agent ($CoCl_2$) and they described an altered response to chemotherapeutic compounds under this condition too. In their study, they noted that several hypoxia-associated genes were upregulated e.g., XAF1, GLUT1. GLUT1 is also one of the factors, which expression is HIF1α dependent. The hypoxic tumor cells have a higher demand for glucose to support increased glycolytic activity (the Warburg-effect), thus glucose vehiculation is facilitated via GLUT1. The overexpression of GLUT1 was already associated with poor prognosis in several tumor types, like colon or breast cancer. It was also reported that increased GLUT1 expression has a positive correlation with epidermal growth factor receptor (EGFR) and KRAS oncogenes in non-small cell lung carcinoma (NSCLC) and is also associated with aggressive tumor phenotype [48,99(p1),100(p1),101]. In cHL, GLUT1 was reported to have a prognostic significance in late-stage/advanced cHL cases and the GLUT1 positivity correlated with PD-L1 expression [102(p1)].

In HRS-cells, the expression of the HIF1α dependent VEGF and platelet-derived growth factor receptor α (PDGFRα) were reported. Retrospective studies suggested that angiogenetic adaptation may have a progressive role in the early stages of cHL lymphomagenesis. The results were interpreted as the newly formed vessels can be easily penetrated by the neoplastic cells. A correlation between a micro vessel caliber and the stage of lymphoma could be stated, furthermore, expression of VEGFD correlated with the elevated number of tumor micro vessels in cHL [103–105]. The VEGF ligand on the other hand promoted monocyte chemotaxis and it also hindered the maturation of the antigen-presenting dendritic cells. These results can be interpreted as VEGF inhibiting the anti-tumor immune effector functions [106]. The VEGFC/VEGF3-R signaling pathway was also examined in cHL on cell lines and lymphoma tissue samples and results showed that lymphangiogenesis was inducible through this pathway in HRS-cells. Follow-up clinical data correlated with these findings and indicated that elevated VEGFC expression rates are associated with a higher risk for treatment failure and recurrence [107].

Hypoxia may already develop at an early stage of tumor progression and exerts a pivotal impact on many aspects of cancer biology. In the hypoxic niche, neoplastic cell clusters may undergo metabolic adaption in order to survive. Previous studies have concluded that mature B-cells can turn into cells with key HRS cell characteristics in hypoxic conditions and hypoxia also induces drug resistance. The daily lymphoma histology frequently reflects tissue changes suggesting hypoxic damage in association with other aggressive features [39,40,56,90–94].

Notwithstanding that there is an increasing amount of *in vitro* and clinical data regarding cHL, the exact mechanism of hypoxia-related changes and metabolic adaptation in cHL remains unknown. In our studies, we aimed to examine the significance of HIF1α downstream effectors – CAIX, CAXII, GLUT1 – in classic Hodgkin's lymphoma.

5. OBJECTIVES

5.1 Quantitative analysis of CAIX enzyme expression in cHL patient samples

Our research group reported the aberrant expression of CAIX in HRS-cells of patient's samples for the first time. In this study (Figure 11.), we aimed to examine the biopsy samples from cHL patients to have an insight into the complexity of the hypoxia-related changes, expression of CAIX, and its potential role in the progression of lymphomas.

- We wanted to assess the expression of CAIX in cHL patients' samples using immunohistochemistry.
- Besides light microscopy, we applied digital image analysis for quantitative determination of absolute and relative CAIX expression using the QuantCenter/DensitoQuant module and a new scoring algorithm (3DHistech, Budapest, Hungary).
- We were curious about the potential correlation of CAIX data with patient survival and other clinical parameters (e.g., age, gender, relapse, response to therapy).

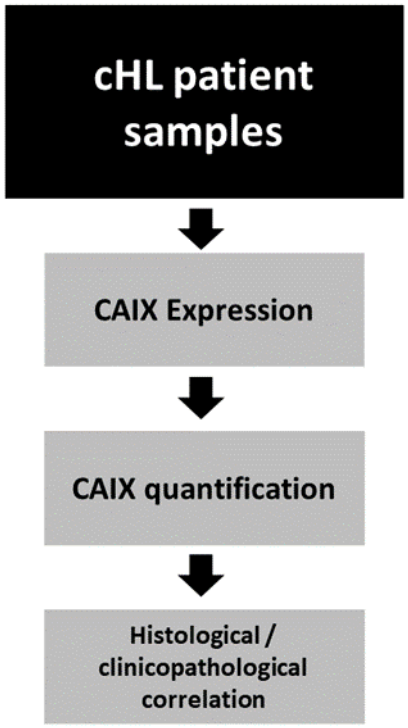

Figure 11 Schematic illustration of the quantitative image analysis approach to evaluate CAIX expression in histological samples (first part of the study).

5.2 Occurrence and dynamics of CAIX in experimental cHL models

We aimed to examine the distinct interplay between hypoxia-associated altered adaptation, expression of cell kinetic factors, markers, and response to therapy in hypoxia in cHL cell cultures (Figure 12.).

For this purpose:

- We validated the human Hodgkin's lymphoma cell lines L1236 and L428 for experimental studies.
- We performed *in vitro* cell culture experiments to determine the effect of hypoxia on the expression of several HIF1α downstream effectors at the mRNA and protein expression levels.
- Further examinations aimed to set up an *in vitro* model to measure the response to common drug combinations in experimental normoxia and hypoxia.

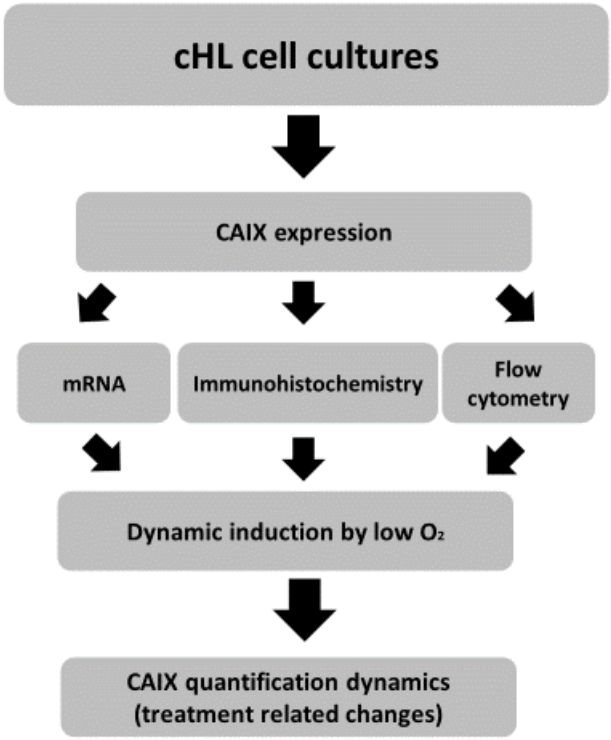

Figure 12 Schematic illustration of the in vitro hypoxia experiments to evaluate CAIX expression in cultivated cHL cells (second part of the study).

6. MATERIALS AND METHODS/PATIENTS AND METHODS

6.1 Sample selection and immunohistochemical analysis

cHL cases were identified from the period between 1999 and 2019, all diagnosed at the Departments of Pathology, Clinical Centre, University of Debrecen, and at the Jósa András Teaching Hospital, Nyíregyháza, Hungary. Histological diagnosis of cHL was reviewed according to the latest WHO classification, cases with larger quantities of pathognomic HRS-cells were identified to enable further analyses. Tissue samples were evaluated by routine pathological staining (hematoxylin-eosin - HE) for tissue characteristics (stroma, necrosis, etc.), and the IHC panel PAX5, CD20, and CD30, and LCA (Table 4.)was regularly done. IHC was done on serial sections using the antibody clone Ber-H2 (Dako-Agilent, Glopsrup, Denmark) for CD30 and rabbit polyclonal antibody clones for CAIX. EnVision Flex horseradish peroxidase/diaminobenzidine (HRP/DAB)$^{+}$ chromogen detection system (Dako-Agilent) was used to show the specific antibody binding, followed by antigen retrieval at pH 9.0. As CAIX negative control reactive lymph node samples were applied, while as CAIX positive control, we used renal cell cancer samples.

Dual immunohistochemical reaction was assessed to examine the expression of MIB1 and CAIX. Firstly, the nuclear MIB1 was specifically labeled and detected by EnVision Flex HRP/DAB^{+}, followed by a second incubation with CAIX antibody. CAIX was visualized with Flex HRP system using violet VIP chromogen (Vector Laboratories, Burlingame, CA, USA). Methyl-green solution (Vector Laboratories) was used to counterstain unlabeled cell nuclei.

CAIX immunohistochemical staining was performed with both poly- and monoclonal antibodies. The immunohistochemical staining was performed according to the manufacturer's protocol and for visualization diaminobenzidine (DAB) chromogen was used.

Table 4 Table of the used antibodies.

Antibody	Company	Cat. Number	Dilution	Expression
CAIX	Novus-Bio	NB100-417	1/2000	cell membrane
CAXII	ThermoFisher Scientific	PA5-52608	1/400	cytoplasmic and membranous
CD3	Agilent Technologies Company	M725401-2	1/100	cytoplasmic
CD20	Agilent Technologies Company	M075501-2	1/1000	cell membrane
CD30	Agilent Technologies Company	M075101-2	1/100	cell membrane
GLUT1	CellPath	CM408B	1/1000	cytoplasmic and membrane
HIF1α	Covalab	pab50130	1/2000	nuclear
LCA/CD45	Agilent Technologies Company	M070101-2	1/100	membrane
MIB1	Agilent Technologies Company	M7240	1/200	nuclear
PAX5	Leica Biosystems	NCL-L-PAX5	1/100	nuclear

As a selection method, we first examined the slides under a light microscope (Leica DM2000) in order to determine their suitability for further analysis. In total 101 cases for CAIX immunohistochemistry were available and this compromised our patient cohort. Patient data (age, gender, stage, response to therapy, relapse) for our cohort was exported from E-Medsol database (T-Systems, Budapest, Hungary).

Local Regional Ethics Board provided the ethical approval for this study (60355-2016/EKU).

6.1.1 Immunocytochemistry

Cell culture-derived cytospin preparations were fixed in 10% formaldehyde, after washing them once in PBS. A droplet of cells was placed on glass slides, followed by 24h fixation time, then they were let to dry (1 h). For immunohistochemistry, the protocol of BenchMark ULTRA was used. The antibodies and the conditions used are summarized in Table 5. Staining was performed in a BenchMark Ultra immunostainer (Roche Diagnostics, Germany). OptiView DAB IHC Detection kit and UltraView Universal DAB Detection kit were used to show specific antibody binding, after antibody retrieval.

The intensity and distribution of CAIX, CAXII, HIF1α, GLUT1, MIB1 expression were assessed by light microscopy (DM2500 microscope, Leica, Wetzlar, Germany) and then digitalized with Pannoramic MIDI Slide Scanner (3D Histech, Budapest, Hungary). For semi-quantitative analysis, we used the

DensitoQuant module of QuantCenter Software 2. (3D Histech, Budapest, Hungary) after the application of manually added annotations. Double staining for Mib1-CAIX was also performed.

Table 5 Antibodies used for immunocytochemistry

Antibody	Company	Cat. Number	Dilution	Expression
CAIX	Cell Marque Tissue Diagnostics, Sigma-Aldrich	08313466001	1/100	Cell membrane
CAXII	ThermoFisher Scientific	PA5-16855	1/400	Cell membrane
CD30	Agilent Technologies Company	M075101-2	1/100	cell membrane
GLUT1	BioCare Medical	CM408B	1/2000	Cell membrane
MIB1	Agilent Technologies Company	M7240	1/200	Nuclear
PAX5	Leica Biosystems	NCL-L-PAX5	1/100	nuclear

6.2 Digital image analysis

Only representative CD30 and CAIX immunostained lymph node samples were used for digital analyses. CD30 and CAIX are membrane-associated proteins, therefore both can be analyzed using the same software. The slides were scanned with Pannoramic Slide Scanner MIDI automatic (3DHistech, Budapest, Hungary). Manual annotations were applied with the use of CaseViewer 2.2. Software (3DHistech). We applied free-hand annotations and we excluded the damaged or color-intensive areas (e.g., artifacts, gum residues, air bubbles, strong background reaction. tissue folds) to avoid false positivity. CD30 and CAIX labelings were quantitatively analyzed by whole slide digital image analysis with the QuantCenter software/DensitoQuant module (3DHistech). This module enabled us to perform stain-intensity-based analyses. The module provided a fast, objective, and semiquantitative analysis by identifying the positive staining through individual positive pixels. In the module, blue and brown tolerance, color intensity, score levels, contrast, and gamma can be set. The software calculated a histoscore (H-score) based on the proportion of positive and negative pixels identified within the digitalized slide. After the analyses, the negative pixels were visually presented with blue color, while the positive pixels were pseudo-colorized according to the intensity score: the less positive was yellow, while the strong positivity was shown in red.

According to our preliminary tests, the nuclear immunohistochemistry for HIF1α was not reliable enough to quantify, thus, HIF1α measurements had to be excluded from the analysis of tissue hypoxia and the consequential adaptive mechanisms.

To exclude non-related staining and analytical events we used slides of NLPHL samples negative for both CD30 and CAIX(n=8).

6.3 Cell culture

Cell lines were obtained from DSMZ (Deutsche Sammlung von Mikroorganismen und Zellkulturen GmbH/German Collection of Microorganisms and Cell Culture, Braunschweig, Germany). The description of the cell lines is listed in Table 6.

Table 6 Description of the cHL cell lines used for the in vitro experiments. Based on[https://www.dsmz.de/collection/catalogue/details/culture/ACC-530, https://www.dsmz.de/collection/catalogue/details/culture/ACC-197].

Cell line	Description
L1236	Human Hodgkin lymphoma cell line, MC variant, stage IV, established from the peripheral blood of a 34-year-old male patient. ()
L428	Human Hodgkin lymphoma cell line, NS variant, stage IV, established from the pleural effusion of a 37-year-old woman.

Both L428 and L1236 grow in suspension. The cells were grown in middle-sized culture flasks (75cm^2) containing 15 mL of medium. The cells were centrifugated at 1200 rpm for 5 minutes and then resuspended in an appropriate volume of fresh medium every 2-3 days. The cells were maintained in RPMI-1640 (Sigma-Aldrich, R5886) medium containing 10% FBS, 1% penicillin/streptomycin, 2 mM L-glutamine, and 1% pyruvate at 37°C with 5% CO_2.

Before analyses, we determined the number of viable cells with the use of trypan blue. 10µl of trypan blue was added to 10 µl of cell suspension. Cell cultures were tested regularly to exclude Mycoplasma infection. Commercially available MycoQuant™ Fast Detection Kit (Avidin Biotechnology, Cat# MQ-250) was used according to the manufacturer's protocol.

The experiments were carried out simultaneously under normoxic and hypoxic conditions. Hypoxic gas mixture contained 1% O_2, 94% N_2, 5% CO_2. The gas tank was purchased by Linde.

From the several commercially available cell lines L1236 and L428 cHL cell lines were selected as *bona fide* Hodgkin lymphoma lines. L1236 was derived from a given patient, while L428 was the first

established cHL cell line [108–110]. According to the Illumina Base Space Database L1236 proved to be positive for CA9, however, L428 lacked the gene (L-1236 Cell Line QuickView - Correlation Engine (illumina.com).

6.4 Chemicals for *in vitro* experiments

Cell cultures were treated with different combinations of drugs in both normoxic and hypoxic conditions. Table 7. summarizes the chemicals used for the *in vitro* experiments. The drugs were diluted with phosphate buffered saline (PBS).

Table 7 Used chemicals.

Chemical	Producer	Concentration
Doxorubicin (A)	TEVA	0,01 µM
Vinblastine (V)	Richter	1 µg/mL
Bleomycin (B)	MERCK	10 µg/mL
Dacarbazine (D)	MERCK	250 µg/mL
Acetazolamide (AA)	Diamox	50 µM

ABVD-treatment was applied for L1236 as follows. 60.000 cells/well were seeded conditioned in hypoxia/normoxia for 24h and then treated with ABVD-mix for 24h in hypoxia/normoxia. Cells were then stained with Propidium iodide (PI) Apoptosis Kit and analyzed by flow cytometry. Further, ABVD+AA treatment was also done in a similar setting. 60.000 cells/well were seeded and after 24h treated with ABVD-mix in normoxic conditions for 2h. After the treatment, the cells were harvested. Cells were stained with Annexin-FITC-PI Apoptosis Kit and analyzed by flow cytometry.

6.5 Detection of cell death – Propidium iodide (PI) uptake

Cells were seeded in a 24-well plate (60.000 cells/well) and they were treated with various concentrations of drugs under normoxic and hypoxic conditions. After the above-mentioned treatment, the cells were stained with 100 µl/mL propidium iodide (PI) for 30 minutes at 37°C. Cells were collected in FACS tubes, cells were washed with PBS and collected in the same FACS tubes (PBS 1:1). Then the number of the dead cells was measured by flow cytometry (FACS Calibur, BD Biosciences) and analyzed using Flowing Software 2.5.1.

6.6 Apoptosis detection using Annexin-V-FITC staining

L1236 and L428 cells were seeded in a 24-well plate (60.000 cells/well) and they were treated with various concentrations of drugs under normoxic and hypoxic conditions. After the above-mentioned treatment, the cells were stained with 100 µl/mL PI and 5 µl FITC Annexin V (Component A) for 1 hour on ice in darkness. Cells were collected in FACS tubes, washed with PBS, and collected in the same FACS tubes (PBS 1:1). Then the number of the dead cells was measured by flow cytometry (FACS Calibur, BD Biosciences) and analyzed using Flowing Software 2.5.1.

6.7 Measuring the hypoxia-related changes

6.7.1 mRNA isolation and RT-qPCR

Total RNA from cells was prepared using TRIzol reagent (Invitrogen, TR118), 2µg RNA was reverse transcribed using High-Capacity cDNA Reverse Transcription kit (Applied Biosystems, Foster City, CA, USA, 4368813) according to the manufacturer's protocol. qPCR BIO SyGreen Lo-ROX Supermix (PCR Biosystems Ltd., London, UK, PB20.11-05) was used for the RT-qPCR reactions, the expression level of the genes was detected with Light-Cycler 480 Detection System (Roche Applied Science). A geometric mean of 36B4 and GAPDH and cyclophilin A was used for normalization. Primers are listed in Table 8. The primers for the relevant coding regions of HIF1α, CAIX, CAXII, GLUT1 were designed with the use of National Center for Biotechnology Center – Nucleotide database, Primer 3 and NCBI-BLAST, while

the normalization genes were provided by the Cell metabolism Research Group (Péter Bay Ph.D., D.Sc.).

Table 8 PCR primers used in the RT-qPCR reactions. All primers refer to human sequences.

Gene Symbol	Human forward primer (5'-3')	Human reverse primer (3'-5')
HIF1α	aatgccaccactaccactgccac	ggacagcctcaccaaacagagca
CAIX	cttggaagaaatcgctgagg	gacttcagccgctacttcca
CAXII	gctctgagcacaccgtca	tgtccattataactcagacctttatcc
GLUT1	ctgtcgtgtcgctgtttgtg	ggaagcacatgcccacaatg
GAPDH	agccacatcgctcagacac	ggatttggtcgtattgggc
36B4	ccattgaaatcctgagtgatgtg	gtcgaacacctgctggatgac
18S	tcgaggccctgtaattggaat	tcccaagatccaactacgagctt
Cyclophillin A	gtctcctttgagctgtttgcagac	cttgccaccagtgccattatg

6.7.2 Flow cytometry

CAIX expression was determined with APC Conjugation Lightning-Link® (ab201807) kit and Mab75 antibody (dilution: 1:1000). Briefly, L1236 and L428 cells were seeded into a T25 flask (10^6 cells) and incubated for 48h under normoxic and hypoxic conditions followed by washing with PBS and centrifugation at 1000 RPM for 5 minutes, room temperature. After the removal of PBS, cells were fixed in 1% formalin. Formalin was washed out from the samples with HEPES and then the APC Conjugation Lightning-Link kit was used according to the manufacturer's protocol. CAIX expression was analyzed by flow cytometry (Novocyte Flow Cytometer, ACEA Biosciences, Inc., San Diego, CA, USA). Data analysis was carried out by NovoExpress® software (1.3.0, ACEA Biosciences, Inc., San Diego, CA, USA, 2018).

6.8 Statistical analysis

Histoscore (H-score) is calculated with the following formula, as previously described in [111]. Briefly,

H-score = ((1 × % weakly stained cells) +(2 × % moderately stained cells) + (3 × % strongly stained cells)).

The range of histoscore is between 0-300. For better visualization, the axes in consideration with H-score were set at 200 or 100.

In our statistical analysis, we used a non-parametric Wilcoxon signed-rank test for the comparison of two groups, unless stated otherwise. Mann-Whitney U-test was applied for group-based comparisons. Non-parametric Spearman correlation and non-parametric Kruskal-Wallis calculations were carried out to analyze the value differences in matched CD30 and CAIX cases. Data are presented as average ± SD unless stated otherwise. Statistical analysis was done using GraphPad Prism 6 software (La Jolla, CA, USA). Figures *, **, *** indicate statistically significant differences between control and treated groups at $p<0.05$, $p<0.01$, $p<0.001$, respectively.

7. RESULTS

7.1 Investigation of CAIX and CAXII expression in cHL

In order to quantify the CD30+, CAIX+, and CAXII+ tumor burden, serial tissue sections were examined for CD30, CAIX, and CAXII immunohistochemical staining. In total 101 diagnostic cHL samples were evaluated under the microscope. In our cohort, the most frequent histological subtype was the NS (70/101, 69.3%), followed by MC (20/101, 19.8%) and LR (7/101, 6.9%), then LD (4/101, 0.39%). The distribution of the subtype was all consistent with the current scientific literature.

As CD30 is the characteristic marker of HRS-cells in cHL, we correlated the expression of CAIX with CD30 positivity. Virtually no other cell type further to HRS-cells proved to be positive for CAIX (Figure 13.), having a strong membrane and/or weak cytoplasmic positivity. 56/101 (55,4%) cases were CAIX positive, the rest of our study cohort was declared as negative. Morphologically obvious necrosis was detected in only 27/101 (26.7%) cases, but 85% (23/27) of the evaluated samples proved to be CAIX positive.

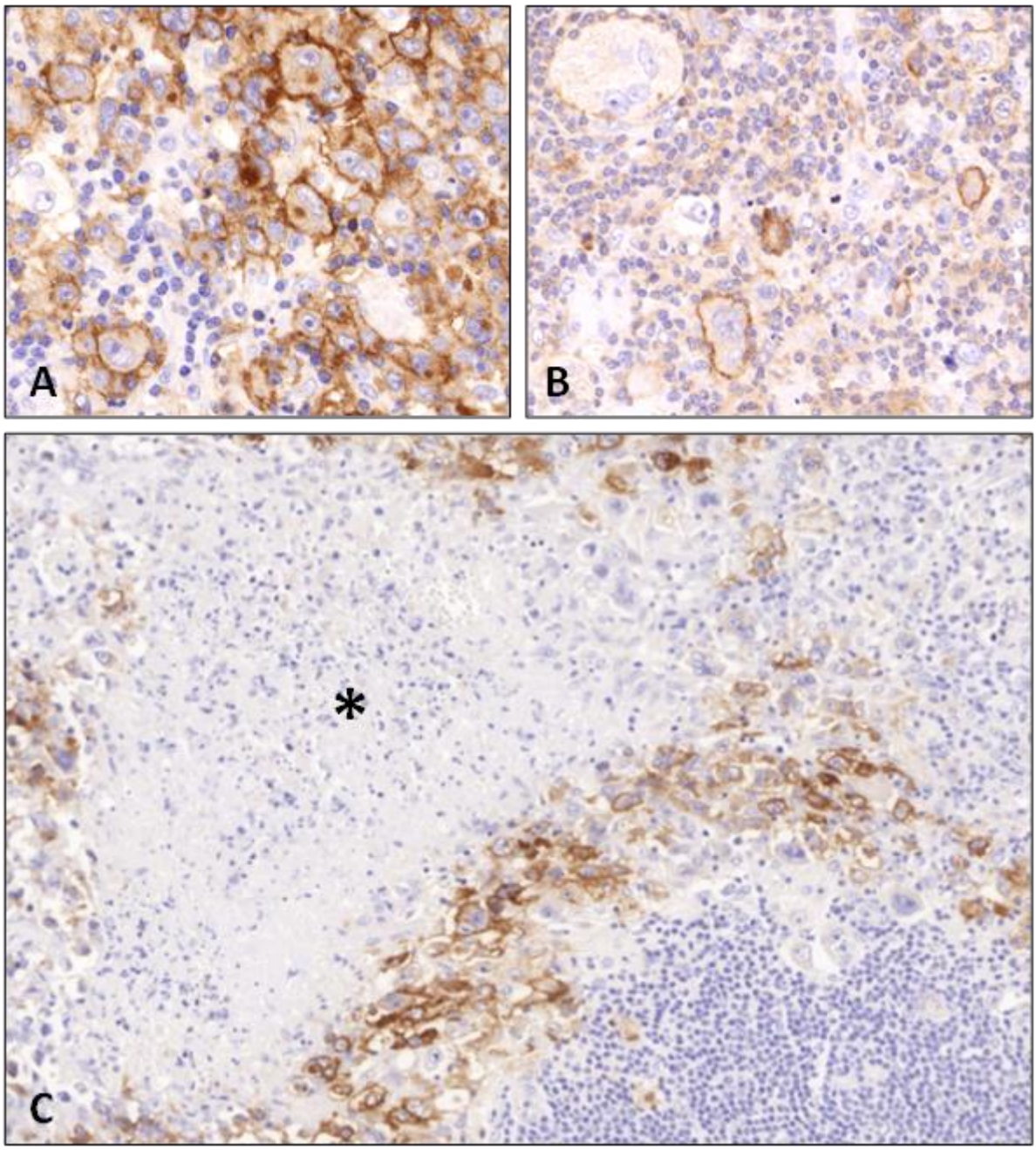

Figure 13 Selective membrane expression of CD30 (A) and CAIX (B) in the mixture of neoplastic and reactive cell masses characteristic for cHL. Selective membrane CAIX expression could be observed in the malignant HRS subfraction, while the non-neoplastic cellular background remained virtually negative. Intense CAIX expression could be observed in samples with necrosis especially in atypical cells of the perinecrotic area (C). Asterisk indicates the necrotic center [106]. Pictures are from the archive of the Pathology Department, University of Debrecen.

Regarding histological subtypes in detail, 20/27 (74.07%) NS, 4/27 (14.81%) MC, and 3/27 (11.11%) LD samples showed some degree of necrosis. Interestingly, in the LR subtype there were no detectable necrotic areas.

Necrotic foci were typically lined by a rim of CAIX positive cells. The observed phenomenon was consistent with the current theory on CAIX expression, representing the adaptation zone surrounding the necrotic core (Figure 13.).

An overall CAIX positivity was seen in 56/101 (55.44%) cHL samples. The majority of the CAIX positive cases was found in the NS subtype (46/70, 65.7%), while in the case of MC, the positive cases were only 20% (4/20) of all MC cases. In LR the positivity was low too (2/7, 28%), on the other hand, the most aggressive clinical variant LD proved to be the highest positivity rate 100% (4/4).

While CAIX positivity (Figure 14.) showed to have specific membrane expression, in case of CAXII there was a prominent stromal reaction.

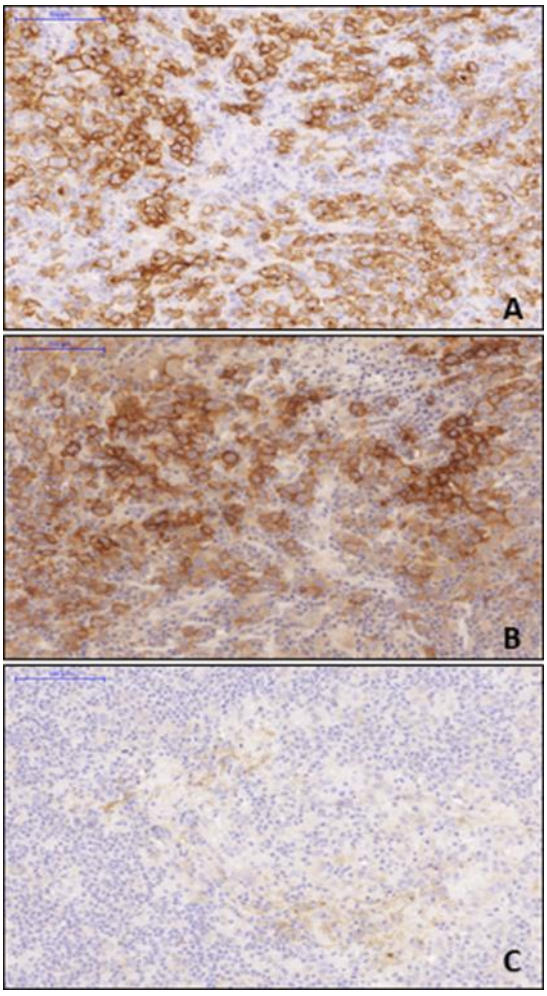

Figure 14 CAIX positive case. CD30 staining (A), CAIX staining (B). Note the strong positivity in the HRS-cells.: CAXII staining (C). Magnification 20x. Pictures are from the archive of the Pathology Department, University of Debrecen.

Figure 15. Shows the immunohistochemical profile of a CAIX negative case.

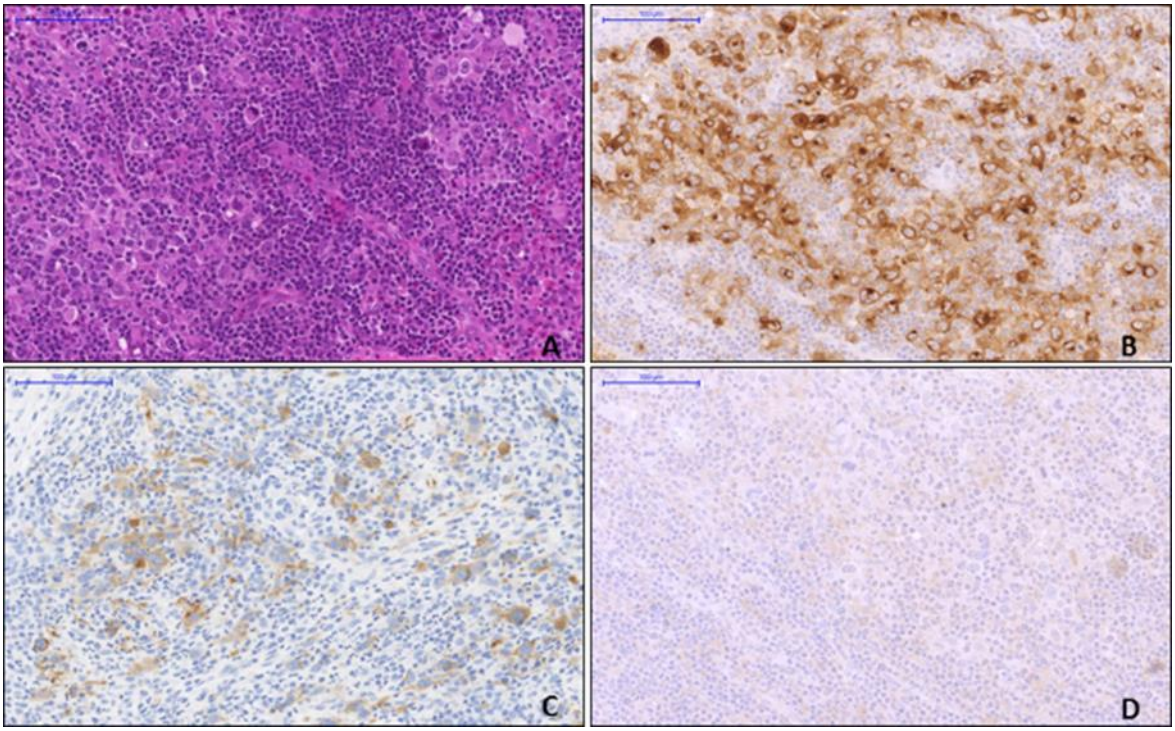

Figure 15 Immunohistochemical profile of a CAIX negative case. A: HE staining, B: CD30 staining, C: GLUT1 staining, D: CAIX negative staining. Magnification 20x. Pictures are from the archive of the Pathology Department, University of Debrecen.

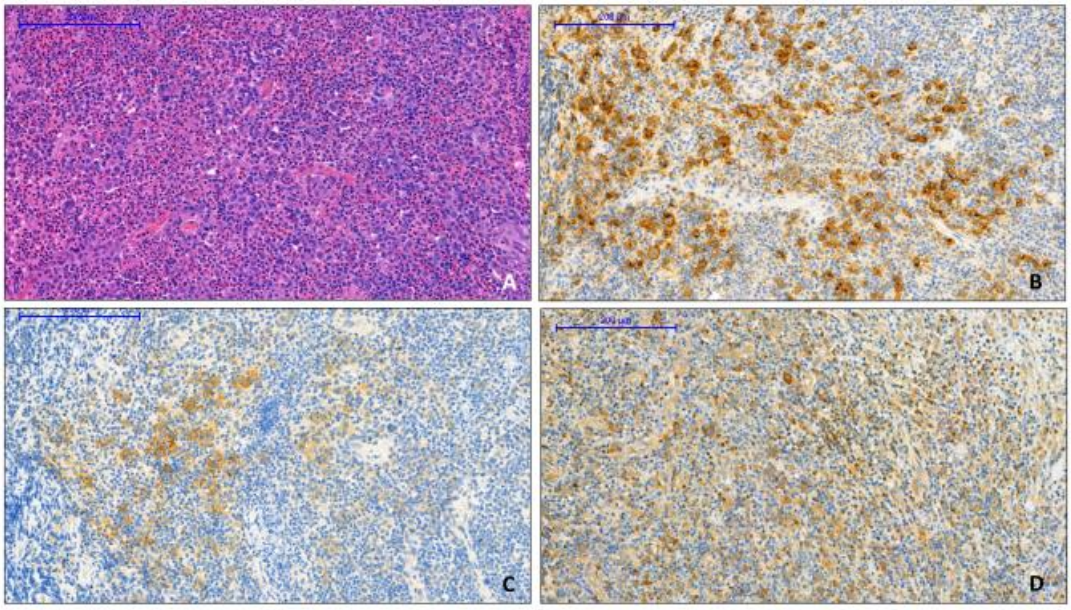

Figure 16 A CAIX and CAXII positive case. A: HE staining, B: CD30 staining, C: CAIX staining, D: CAXII staining. Note, the strong stromal reaction and the indefinite binding to the HRS-cells. Magnification 10x. Pictures are from the archive of the Pathology Department, University of Debrecen

We examined the expression of CAXII in 77 cases, from which 18/77 (23.4%) were CAXII positive and 59/77 (76.6%) remained CAXII negative. CAXII positivity was also observed in the perinecrotic area (9/18, 11.7%). CAXII labelling was demonstrated in the minority of neoplastic cells (23.4%) of the evaluated cases and in other non-neoplastic cell types, like fibroblasts and histiocytes, thus CAXII could not be determined specifically on HRS-cells. In one case, we observed CAIX and CAXII positivity simultaneously (Figure 16.).

GLUT1 immunostaining was generally positive in HRS-cells, not providing information on hypoxic areas. Thus, we conducted a further analysis using digital analysis on CAIX, while CAXII and GLUT1 were dropped as a useful biomarker for this setting (Figure 16.).

Figure 17. displays the expressional difference between CAIX and CAXII in cHL cases. It is noteworthy, that in case of CAXII, not only the HRS-cells, but further cell types were also positive.

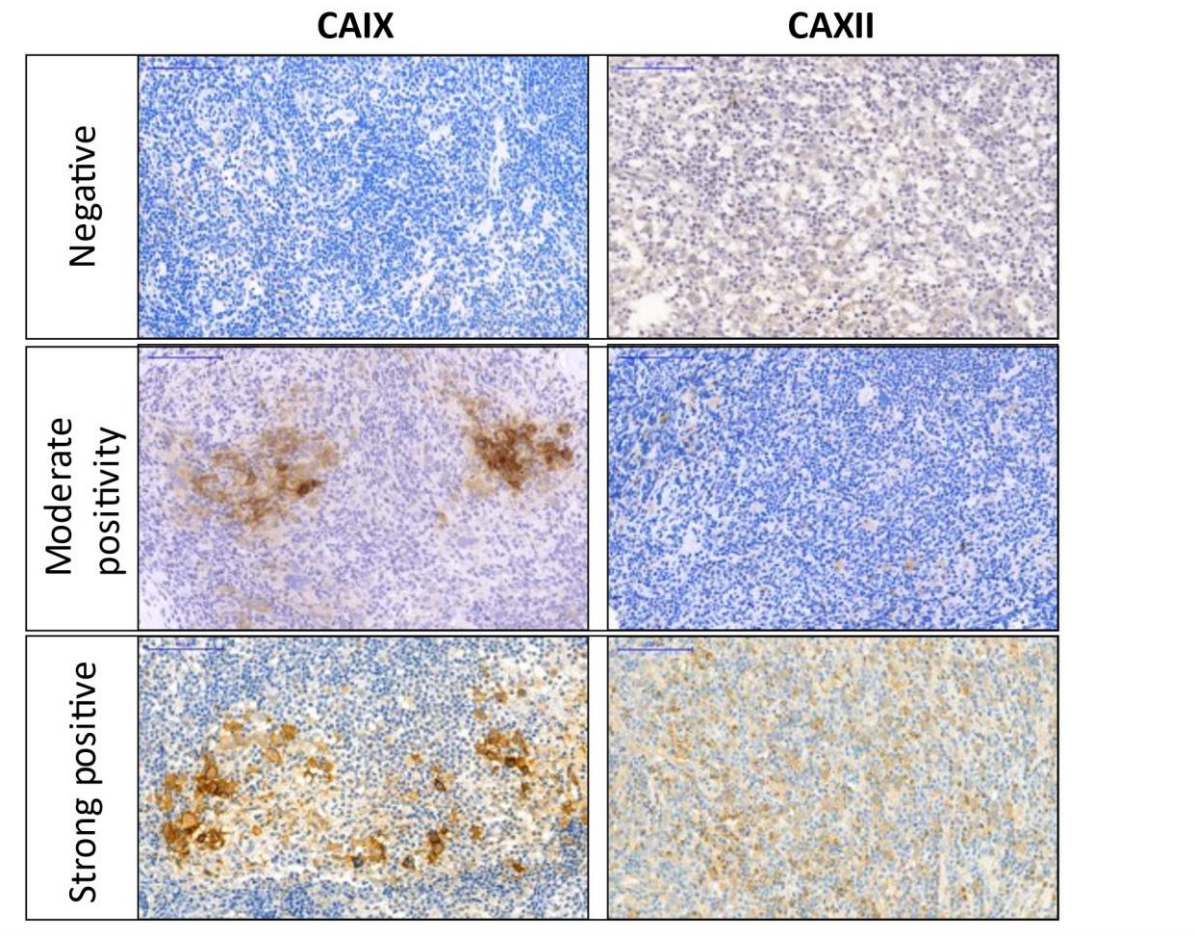

Figure 17 Comparison of CAIX and CAXII immunohistochemical staining patterns in different cHL cases. Magnification 20x. Pictures are from the archive of the Pathology Department, University of Debrecen

To test the cell proliferation capacity of HRS-cells we introduced the MIB1 antibody as an established marker for cells in cell cycle. MIB1 expression could be evaluated individually in CD30 or CAIX labeled cells following dual immunohistochemical staining. This cell proliferation assay could be performed in 26 cases of our cHL cohort (Figure 18, Figure 19).

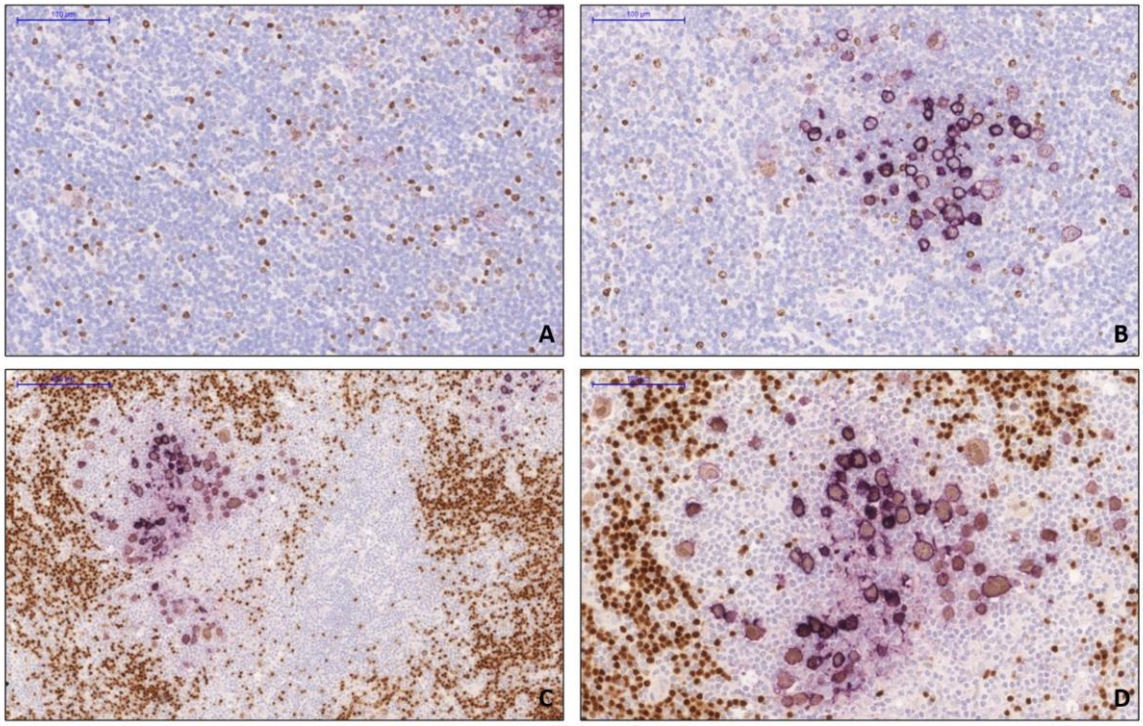

Figure 18 Double immunohistochemical staining. Panel A&B: MIB1 and CAIX staining (magnification 20x). Panel A shows CAIX negative, proliferating cells. Panel B shows CAIX positive but MIB1 negative cells. The majority of the CAIX+ HRS-cells show no Mib-1 staining suggesting cellular quiescence of this cell fraction. Panel C&D: PAX5 and CAIX staining (magnification 10x and 20x). Nuclear PAX-5 positivity highlights both CAIX+ and CAIX- HRS-cells. Pictures are from the archive of the Pathology Department, University of Debrecen.

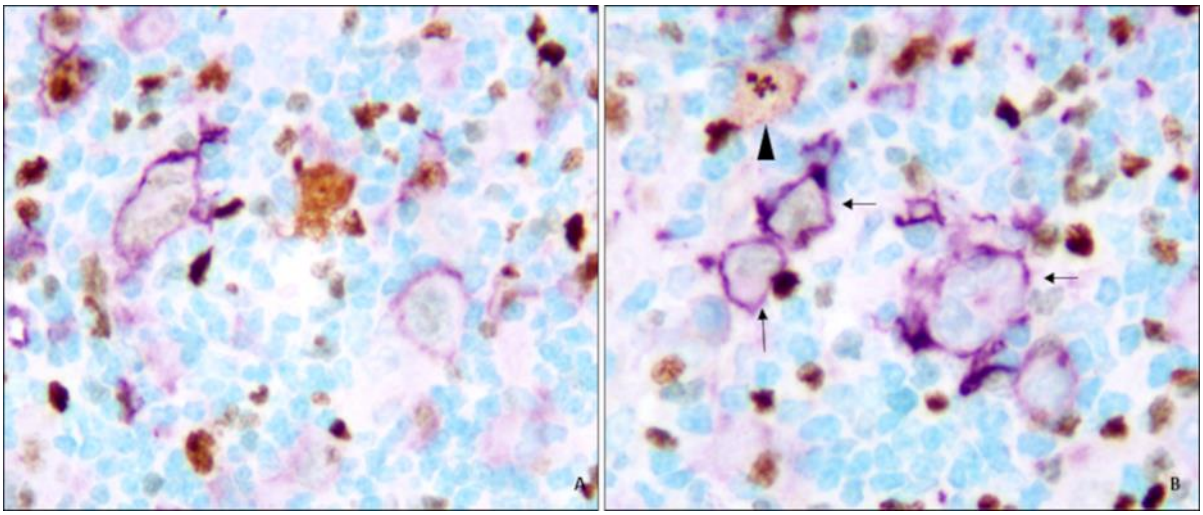

Figure 19 MIB1 and CAIX dual immunohistochemical staining. Nuclear MIB1 [diamonobenzidine (DAB)-brown] and carbonic anhydrase IX (CAIX)-specific staining (VIP-violet). Note the missing nuclear staining in CAIX+ large HRS cells (arrows) compared to the intense MIB1 labeling in some of the surrounding large cells lacking CAIX staining (arrowheads) [106]. Pictures are from the archive of the Pathology Department, University of Debrecen.

According to our results, MIB1 values proved to be significantly lower in the CAIX positive population compared to the CAIX negative population ($p < 0.001$), which may indicate that CAIX positive cases are more frequently cell cycle arrest in agreement with an adaptation-related status (Figure 20.).

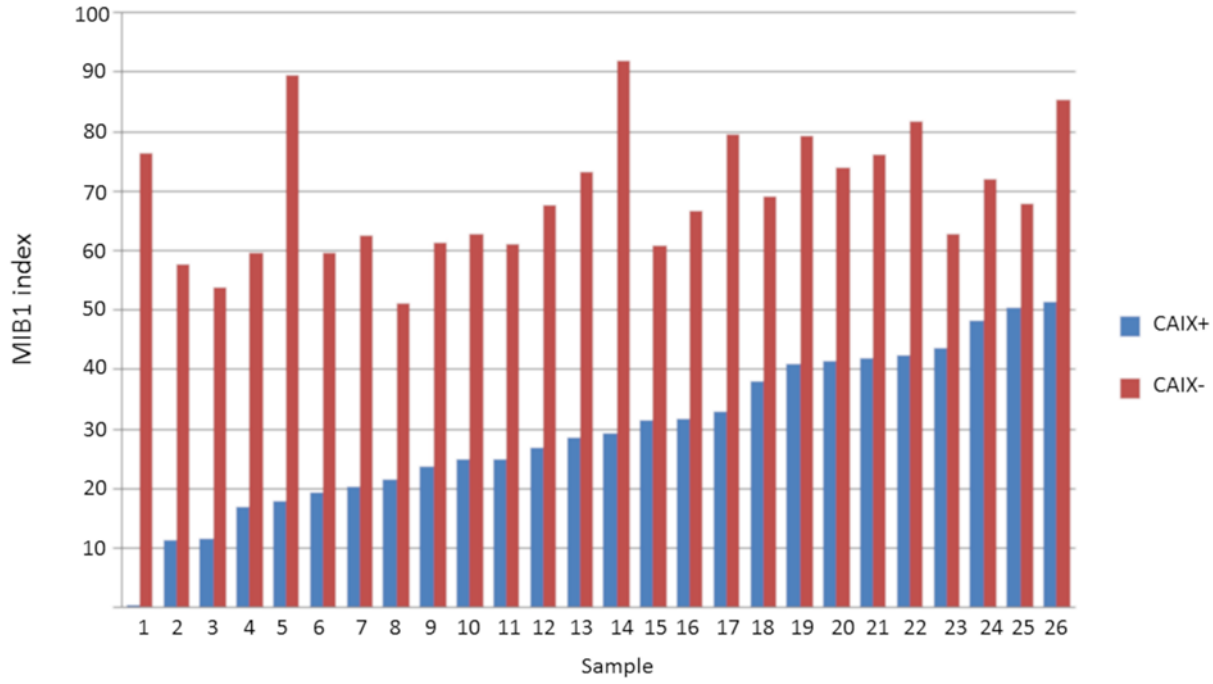

Figure 20 The relation of MIB1 and CAIX expression in altogether 26 cHL samples. Mib-1 positivity was counted in the CAIX-positive and CAIX negative HRS-cell fraction following double IHC staining for CAIX (VIP-blue) and MIB1 (DAB-brown) [106].

7.2 Digital analysis - Quantification of CD30 and CAIX expression in cHL

101 samples were examined with our newly developed digital analysis method. As a first step, manual annotations were applied to each slide in order to avoid the false positivity, caused by artifacts (mentioned before). The samples were analyzed with the DensitoQuant module of the QuantCenter Software (3DHistech, Budapest, Hungary), which can calculate an H-score automatically. The cut-off level was defined at H-score 1. This cut-off level was validated by CD30 or CAIX negative cases and was never reached when specific staining was absent (Figure 21.).

CD30 scores were highly variable depending on the density of the HRS-cells and the expression intensity. In contrast, the CAIX values were generally low. However, within this, samples identified as

CAIX immunopositive by light microscopy presented with significantly higher H-scores compared to negative cases.

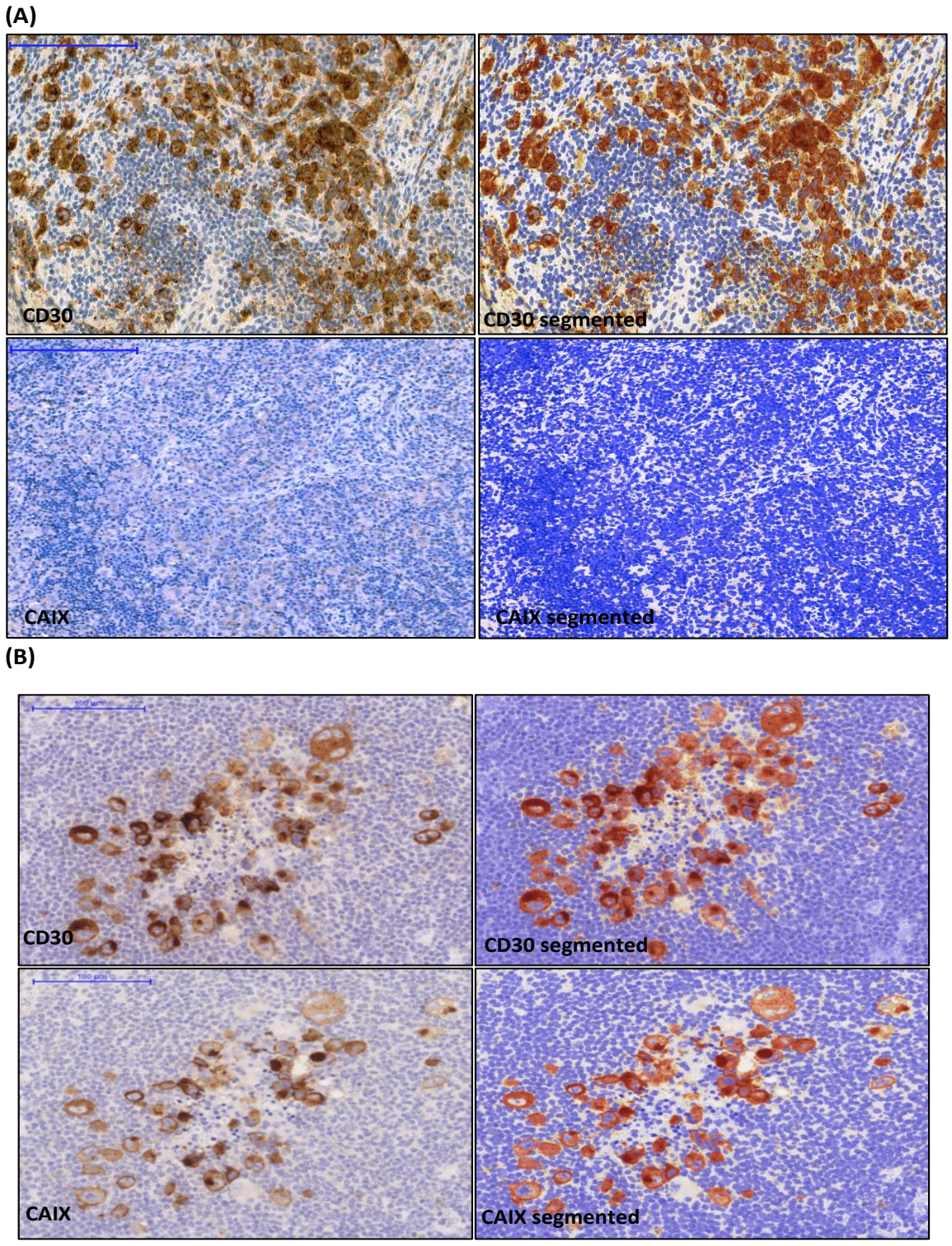

Figure 21 DensitoQuant digital image analysis of CD30 and CAIX-immunolabeling in CAIX negative (A) and positive (B) in cHL. Immunopositivity of HRS-cells (left) is highlighted as red/orange/yellow pseudocolored pixels following digital segmentation (right), while the negative cells are indicated with blue color. The number and intensity of positive pixels were expressed as individual H-score for each sample [107.]. Pictures are from the archive of the Pathology Department, University of Debrecen.

7.3 Relation between CD30 and CAIX

Whole slide digital analysis was performed on paired immunohistochemical stainings with the DensitoQuant module. As previously mentioned, DensitoQuant identifies the positive and negative pixels and, calculates a H-score, based on the proportion of positive and negative pixels. A whole slide digital analysis was carried out to determine the H-score values of the individual slides.

Descriptive analysis was used to determine the minimum and maximum H-score values, mean values, and standard deviation values.

In most of the cases the CD30 positive tumor mass was higher in CAIX+ cases, compared to CAIX- cases. CAIX expression proved to be highly variable, and generally low compared to CD30 expression. It may suggest that the partial upregulation of the enzyme according to the functional diversity of the HRS cell subpopulation, as CAIX overexpression is a feature of the malignant cell compartment, while the accompanying cellular background remained negative.

The minimum score for CD30 was 3.46, and the maximum was 151.33 (mean 52.37 ± 30.74), while for CAIX the minimum was 2.16 and the maximum was 90.4 (mean 18.7 ± 18.8). According to the statistical analysis (Mann-Whitney U-test), the CD30+ signal proved to be significantly higher, which was associated with a higher CAIX+ labeling (p= 0.008) (Figure 22).

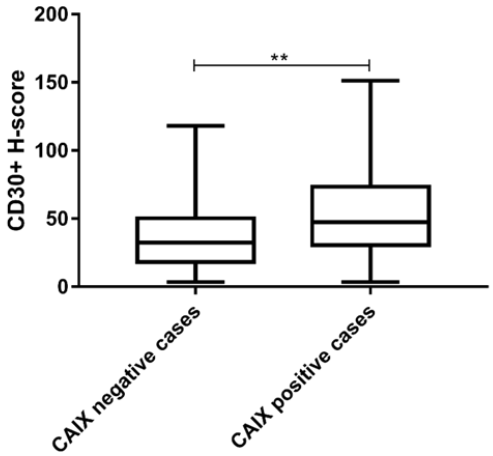

*Figure 22 The CD30 H-scores representing the total HRS-cell burden proved to be higher in CAIX-positive compared to the CAIX-negative samples according to the Mann-Whitney test (p-value 0.008, statistically significant). The increased CD30 staining indicates a higher mass of CD30+ HRS-cells in the CAIX positive group [[112]]. Data are plotted as box-and-whiskers plots. Statistical significance was determined using unpaired Wilcoxon's t-test. ** indicates significant difference at p<0.01.*

Following the pixel-based analysis, cHL subtypes could be evaluated separately. The CD30 expression was the highest in the LD variant (n = 4, range 24.29–109.95, mean 63.1 ± 32.9), which was followed by NS (n= 70, range 2.16–128.3, mean 46.85 ± 27.5), MC (n = 20, range 3.38–151.3, mean 45.65 ± 35.2) and LR subtype, as expected (n = 7, range: 2.518–28.5, mean: 17.5 ± 8.8) (Figure 23.).

The H-score range in CAIX negative cases was 0.01 – 0.99 (mean 0.37 ± 0.29), which did not overlap with the score range of the CAIX-positive samples. The CD30 H-score in CAIX positive cases was between 3.38 and 118.2 (mean: 37.38 ± 25.34).

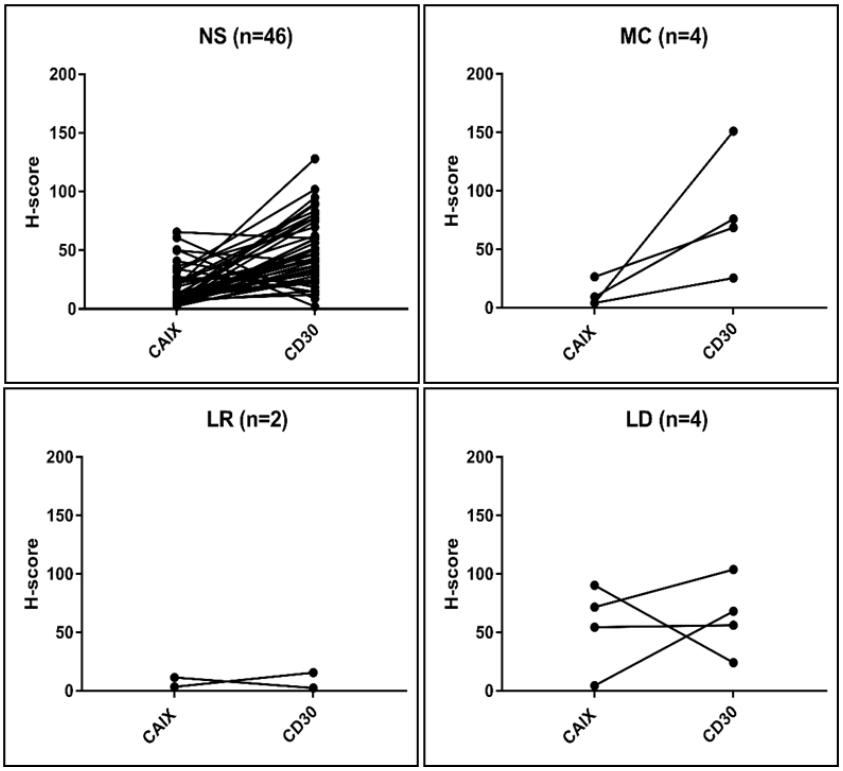

Figure 23 CAIX and CD30 expression were measured in serial sections of CAIX-positive cHL (n=56) samples according to the histological subtypes. H-scores for both reactions were determined with the DensitoQuant analysis.[112]

CAIX expression was limited to the neoplastic HRS-cells, the surrounding inflammatory, and stromal elements remained negative. In line with the literature, CAIX expression was observed in the perinecrotic foci, however only in a small number of cases (CAIX+ cases 27/56, 48.21%). Results suggest that CAIX occurs dynamically, probably as an evolving feature of hypoxia-related adaptive mechanism.

The expression of the enzyme refers to the activation of a protective mechanism in a hostile microenvironment.

CAIX expression proved to be a feature of a subfraction of CD30+ cells suggesting that CAIX expression was not an integral feature of the transformed cells. In the perinecrotic foci, a higher rate of CAIX expression could be observed, supporting the hypothesis that the enzyme has a function in the adaptation to hypoxic conditions.

Figure 24. summarizes the H-score values of CAIX and CD30. It also demonstrates the relation of the two factors to each other. According to the statistical analysis (Figure 24.), the CD30+ mass proved to be significantly higher, which was associated with a higher CAIX+ fraction ($p < 0.0001$). Multiple comparison analyses showed a significant difference between the analyzed subgroups too. The significant difference between the CD30+ tumor burden in CAIX+ and CAIX- cases indicates that CAIX upregulation occurs in progressive forms of cHL, which is tempting to speculate that the HRS-cells gain a survival advantage.

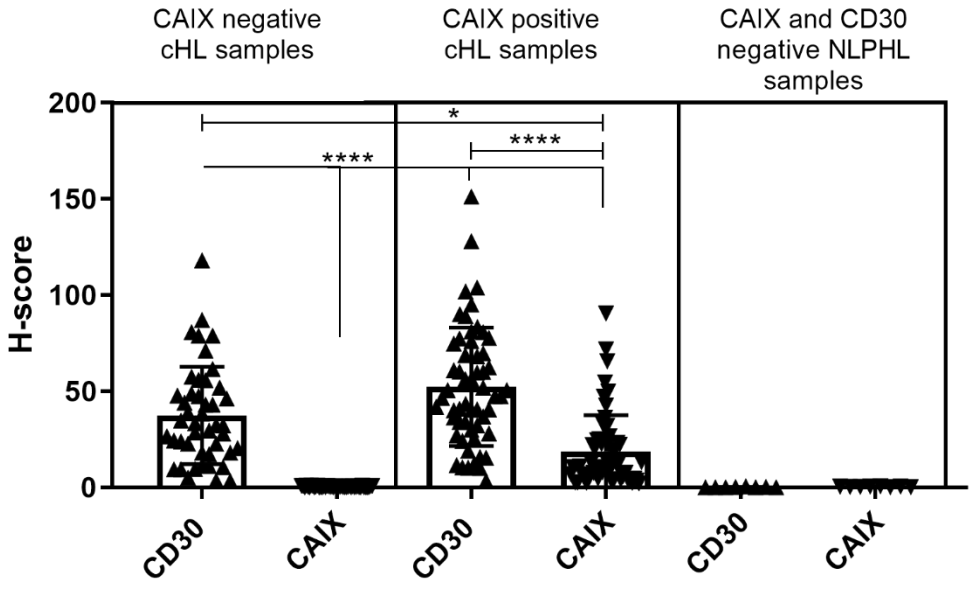

Figure 24 The distribution and mean values of CD30 and CAIX-immunostaining related H-scores determined by the DensitoQuant image analysis application. Samples were grouped as CAIX-negative (n=45) and CAIX-positive (n=56) based on light microscopy. As negative control slides of CD30- and CAIX-double negative NLPHL cases were measured (n=8). Statistical analysis was carried out with Mann-Whitney analysis. Asterisks represent the statistically significant differences between the groups (, p<0.05, ****, p<0.0001) [112].*

However, with the increase of the CD30+ cell mass in the CAIX+ cases no further positive correlation could be stated (p-value = 0.475, Spearman rs: −0.008) (Figure 25.).

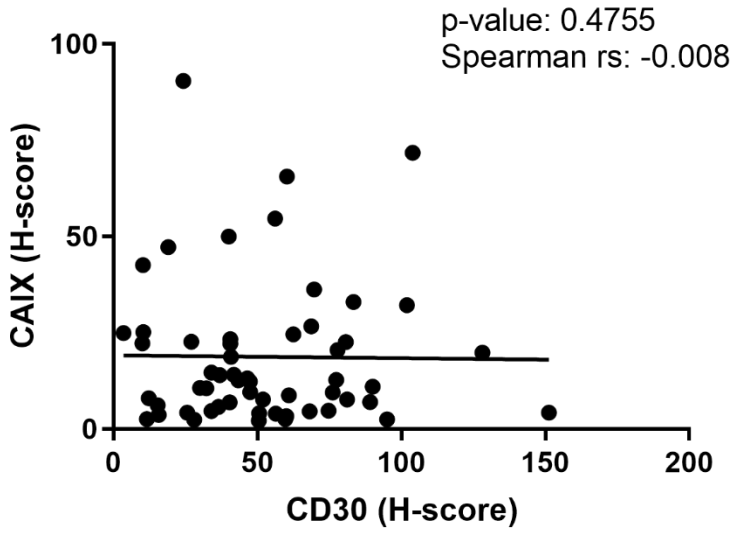

Figure 25 The CD30 related H-score representing the HRS-cell burden did not correlate with the amount of CAIX expression in individual cHL samples presenting with any CAIX positivity. CAIX H-score exceeded CD30 in six samples, that was associated with low CD30 staining intensity The correlation was calculated using the Spearman correlation test. (p-value 0.4755, Spearman rs: -0.008) [107].

It is worth mentioning that in 6/56 cases (10.7%) CAIX H-scores were higher than CD30 values, which could be due to low HRS-cell numbers or with low CD30-staining intensity. In 6 cases, CD30 intensity proved to be weaker than the CAIX expression, weak immunostaining, or the low number of HRS cells could both serve for acceptable explanation.

In order to eliminate the factors of tumor cell density and intratumor variability, a relative positivity rate was calculated for all cHL variants, considering the CAIX+ labeling per unit of CD30+ labeling. The CAIX/CD30 mean ratio was 0.23 ± 0.57 SD for all cases and 0.35 ± 0.61 SD for the CAIX+ cases. CAIX/CD30 ratio was the highest in LD (0.87) subtype, followed by the NS (0.35), the MC (0.13), and the LR variant (0.83). In the LR subtype, the CAIX/CD30 ratio remained to be high, but the low number of cases (n=2) and frequency of positive events within the samples did not allow further statistical analysis. Our exploratory study focused on the digital analysis of CD30 and CAIX expressing HRS-cells in order to quantify the expression of both markers. The results are displayed in Table 9.

*Table 9 Relative expression of CAIX and CD30 based on the digital analysis results (H-score) dependent on the different histological subtypes of cHL (*only two samples and low cell numbers) [112].*

	n	CD30 mean	CAIX mean	CAIX/CD30 ratio
All cHL cases	101/101	45.7±29.3	10.54±16.65	0.23±0.57
CAIX- total	45/101	37.38±25.34	0.37±0.29	0.01±0.01
CAIX+ total	56/101	52.37±30.74	18.70±18.88	0.35±0.61
NS	46/70	49.86±27.49	17.46±15.8	0.35±0.57
MC	4/20	80.46±52.23	11.13±10.62	0.13±0.20
LR*	2/7	9.114±9.325	7.64±5.63	0.83±0.60
LD	4/4	63.16±32.9	55.3±36.8	0.87±1.12

To sum our digital image analysis up: CAIX-positive HRS-cells is a subfraction of CD30 positive cells and indicate a significant functional heterogeneity within the malignant clone, which potentially contribute to an aggressive and resistant tumor cell phenotype.

7.4 Clinical impact of CAIX

The sex ratio of the included patients was balanced (female vs male = 47.5% vs 52.5%), CAIX expression was observed more often in cHL of female patients (62.5% vs 49.0%) 86.13% of our patients were over the age of 60 (87/101), without any difference in CAIX expression according to the age. Patient characteristics was summarized in Table 10.

Table 10 Patient characteristics of the 101 cHL cases evaluated for CAIX and CD30 immunopositivity by both light microscopy and digital image analysis (No.: number) [112].

	No.	%
CAIX positivity in the cHL variants		
Total	**56/101**	**55.44**
NS	46/70	65.7
MC	4/20	20.0
LR	2/7	28.6
LD	4/4	100.0
Necrosis		
CAIX+	23/27	85.0
CAIX-	4/27	14.8
Gender - Female		
CAIX+	30/48	62.5
CAIX-	18/48	37.5
Gender - Male		
CAIX+	26/53	49.0
CAIX-	27/53	50.9
B-symptoms		
CAIX+	29/48	60.4
CAIX-	19/48	39.5
Age		
Mean	36.66	
<60 years	87/101	86.13
>60 years	14/101	13.86

According to previous and our own observation CAIX expression reproducibly appeared in close proximity with necrotic areas but was found to extend to large areas without necrosis. As CAIX expression proved to have a dynamic fashion and appeared more frequently in sub-lethal foci with potential adaptive features, CAIX seems to be a potent biomarker in cHL, induced by hypoxic stress.

cHL patient survival analysis was performed for 72 months (n=81). The overall survival (OS) rate was 0.823 and the progression-free survival (PFS) was 0.504 for the analyzed study population. Kaplan-Meier curves and Mantel-Cox statistical analysis showed that necrosis – absence or presence – did not influence the overall survival (0.812 versus 0.833, p=0.469) however, there was a mild difference between the two groups in PFS (0.19 versus 0.579, p=0.146) (Figure 26.).

In contrast, a significant difference in survival was found in relation to CAIX expression. The OS differed minimally between the CAIX negative and positive cases (0.934 versus 0.699, p=0.097, not significant), but in PFS there was a striking difference between the groups. According to our analysis, there was a statistically significant longer cumulative PFS in the CAIX negative group compared to CAIX positive cases (0.771 vs 0.19, p<0.001).

In case of CAIX positivity, the positive predictive value (PPV) for initial treatment failure proved to be 0.76. The negative predictive value (NPV) for CAIX negativity proved to be 0.66 ($p<0.003$). These results suggest that the expression of CAIX elevates the likelihood of poor response/progression after initial chemotherapy (76.2% and 65.9%, respectively).

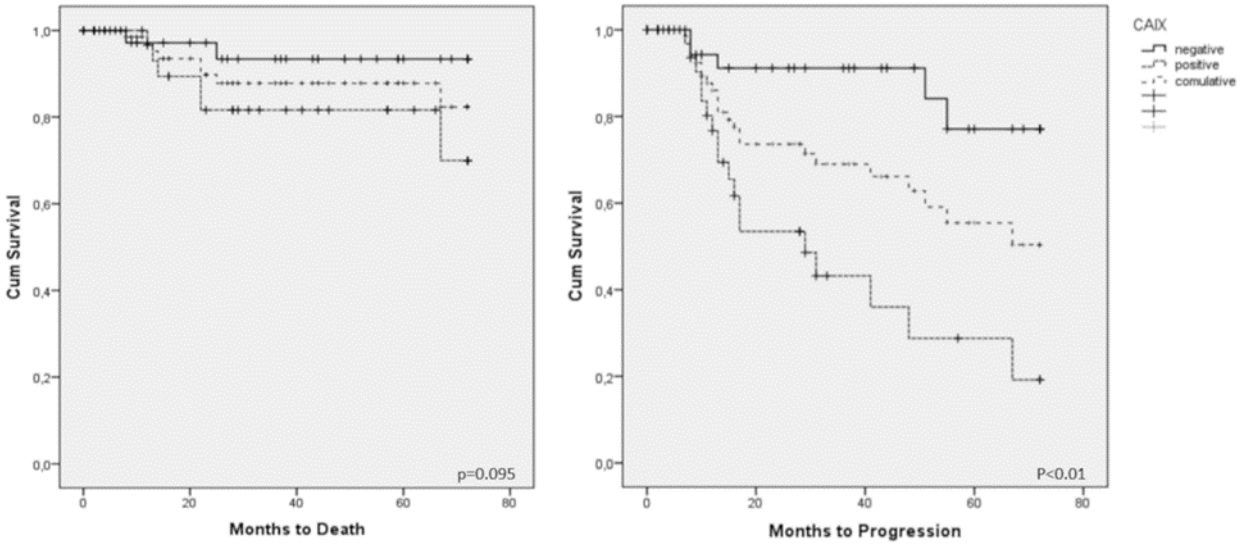

Figure 26 Kaplan- Meier analysis reflects the 72 months overall survival (left) and progression-free survival (right) related to the presence of carbonic anhydrase IX in cHL. A statistically highly significant difference in PFS was calculated in favor of the CAIX negative (0.771) compared to CAIX positive (0.19) groups (p<0,001) [113].

PPV, NPV, OS, and PFS were also calculated in a setting of CAXII. There was no significant difference in OS and PFS (P = 0.301 and P = 0.524, Breslow scores were 1.977 and 0.649, respectively), furthermore, PPV and NPV was generally weak (no statistical difference, no predictive value).

According to these statistical approaches CAXII functionally may possess similar qualities as CAIX, but the practical utility to differentiate prognostic categories of CAXII immunostaining could not be proven within the frame of this study.

7.5 *In vitro* analysis of hypoxia-related changes

7.5.1 Verification of the Hodgkin's lymphoma cell lines

In order to gain a better insight into the hypoxia-related changes, we aimed to create a hypoxia model. Our experiments were carried out with a hypoxia chamber to implement the examination of the global effect of hypoxia.

We determined the expression of PAX5 and CD30 in the L1236 and L428 cell lines to provide evidence for the Hodgkin lineage (Figure 27.). Hematoxylin-eosin staining is also provided. Both cell lines expressed the characteristic markers of cHL.

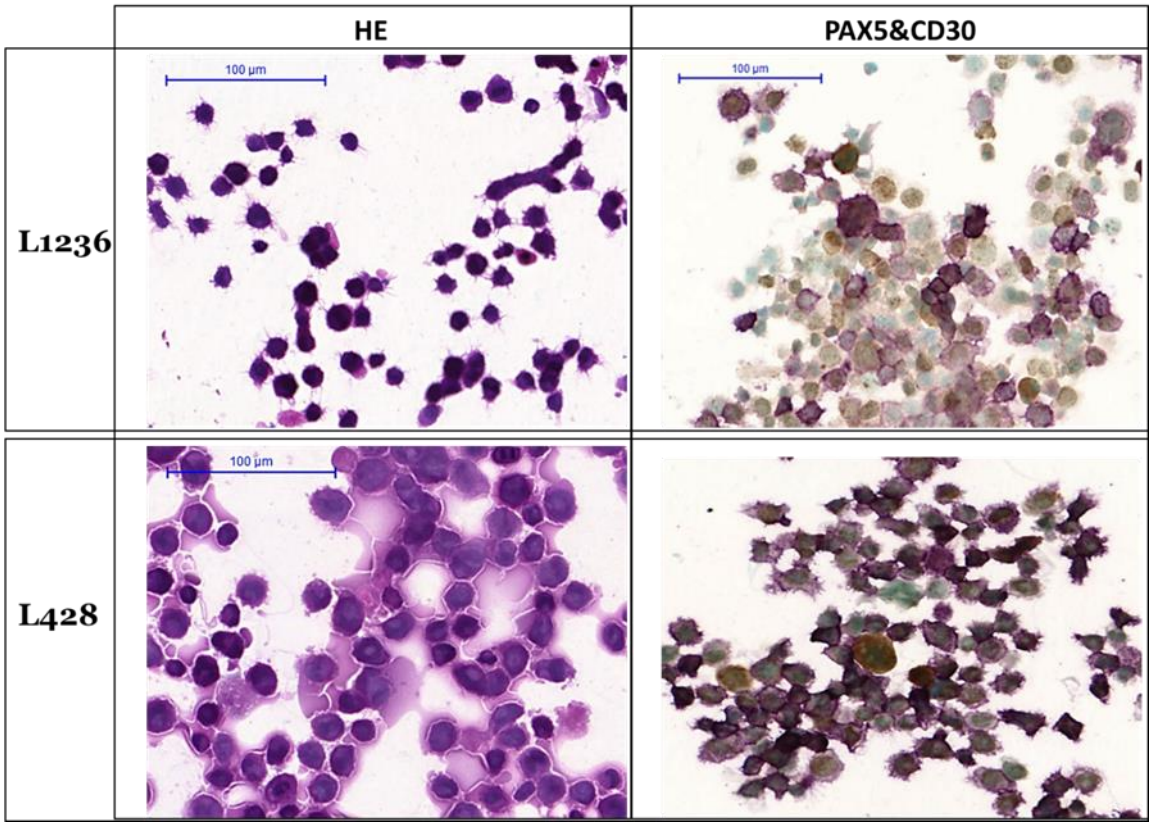

Figure 27 Hematoxylin-eosin, PAX5, and CD30 immunohistochemical staining of L1236 and L428 cell lines. Representative immunohistochemical staining of the cell lines.

7.5.2 Expression of CAIX is induced by hypoxia

As a first step, we examined the effects of hypoxia in the L1236 and L428 cHL cell lines. Different incubation times were used during our experiments (24-48-72 hours), but the most reproducible results were achieved with the 24-hour incubation period.

7.5.2.1 Quantitative determination of CA9 gene expression

The mRNA expression of CA9 was induced under hypoxia as compared to normoxia, however, the extent of induction was different (Figure 28). There was a 10-fold increase in the L1236 upon hypoxia, while there was a similar trend in the expression of the CA9 in L428 cells, but that did not reach statistical significance.

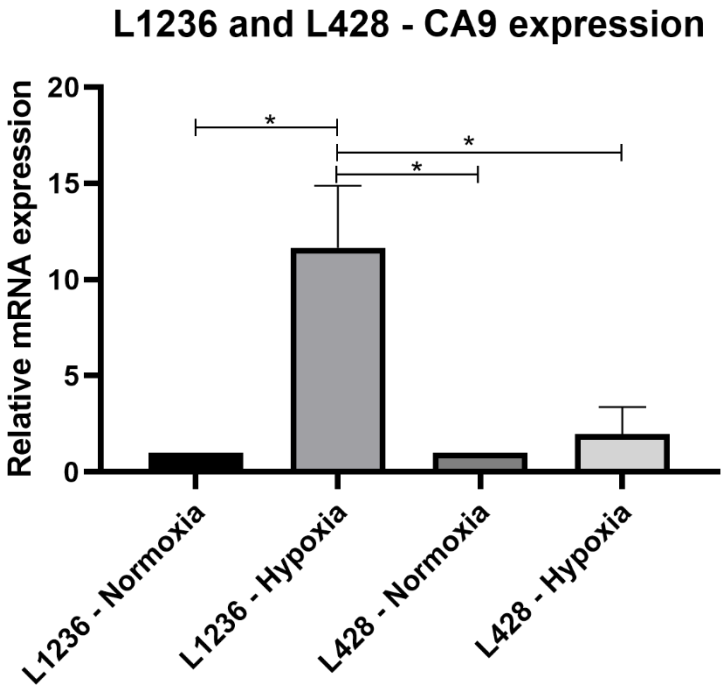

Figure 28 CA9 mRNA levels were measured in L1236 and L428 cell lines by RT-qPCR. Cells were harvested after 24h hypoxia/normoxia treatment (60.000 cells/dish). Statistical significance was calculated using one-way ANOVA statistical analysis (not significant). According to Tukey's multiple analysis, there was a significant difference between the L1236 Normoxia-Hypoxia and L428 Hypoxia – L1236 Hypoxia pairs. Paired t-test showed a significant difference between the L1236 normoxia and L1236 Hypoxia pair, furthermore, unpaired t-tests showed a significant difference between L1236 Hypoxia – L428 normoxia and hypoxia pairs (, p<0,05). Bars represent mean and SEM (n=4, independent experiments).*

7.5.2.2 Hypoxia induced changes of CAIX expression at the cellular level

Histological examination of the formalin-fixed cell lines specimens revealed that they have distinct expression patterns for the CAIX enzyme (Figure 29.), which was in line with the RT-qPCR results.

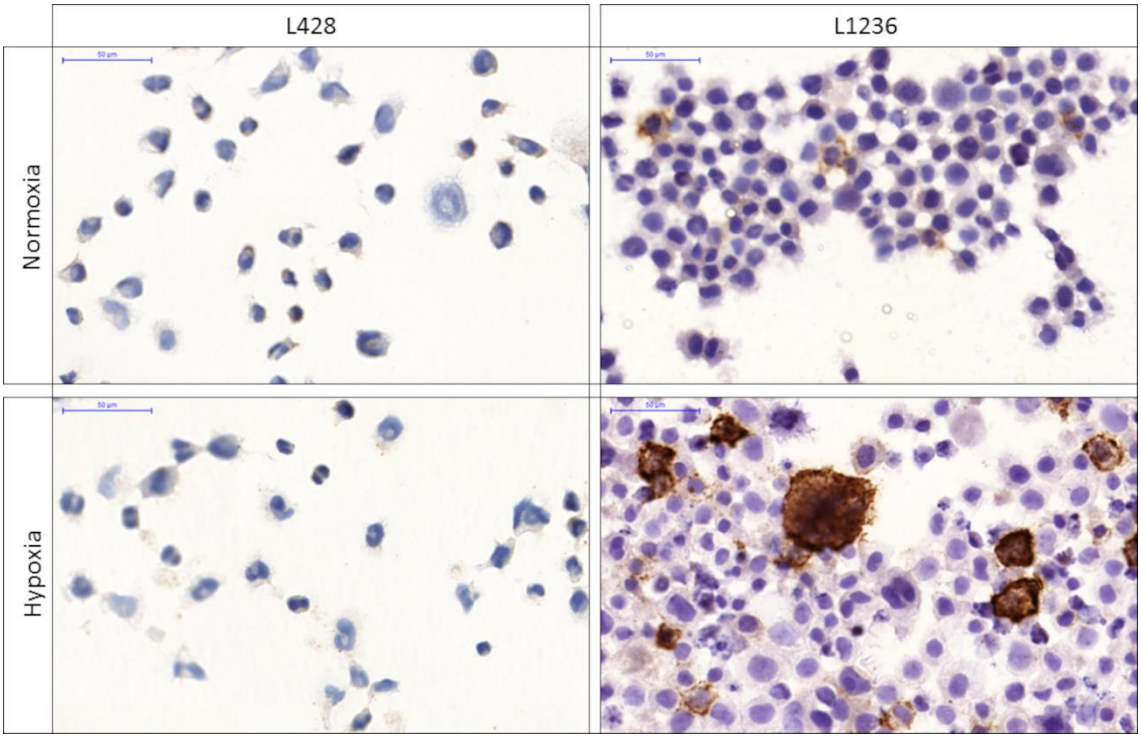

Figure 29 Examination of CAIX expression in two cells lines. Magnification 40x Representative immunohistochemical stainings of the cell lines. Note the increased number of positive cells in the L1236 cell line (DAB – diaminobenzidine – brown color indicates the positive cells).

L428 showed only a minimal upregulation of the enzyme, while in the L1236 cell line the expression of CAIX proved to be highly inducible upon hypoxia.

To semi-quantitatively analyze the samples, digital image analysis was applied. Slides were scanned with Pannoramic MIDI Scanner, and the DensitoQuant algorithm was carried out to quantify the positive and negative pixels in the specimens (Figure 30.), similar to the previously mentioned retrospective clinical study.

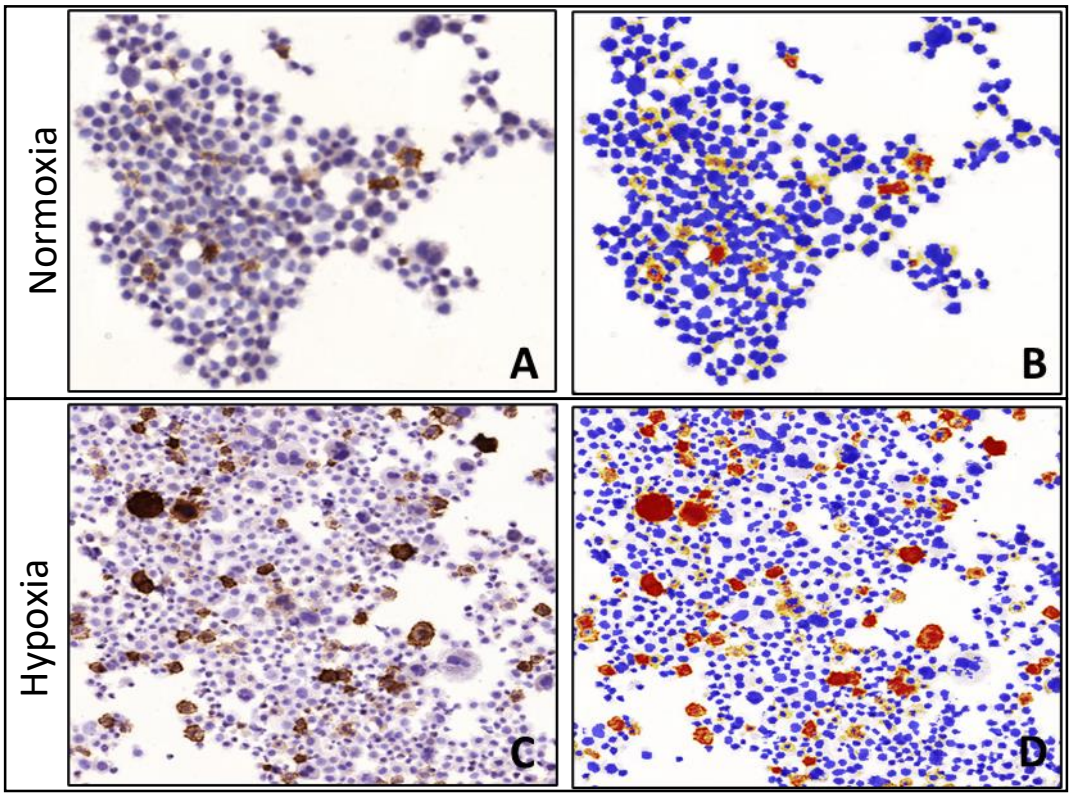

Figure 30 Representative digital image areas of the formalin-fixed L1236 cell line specimen. Digital image analysis was carried out with the DensitoQuant algorithm after segmentation of objects with positive labeling (A and C – before, B and D following segmentation). Note the increased number of positive cells in the hypoxic specimen (C and D) in comparison with the normoxic samples (A and B), with an increased number of positive pixels.

In normoxia, a little fraction of the pixels were positive for CAIX (Figure 31.). In contrast, under hypoxia, almost 80% of the nuclei stained positive for CAIX (Figure 31.).

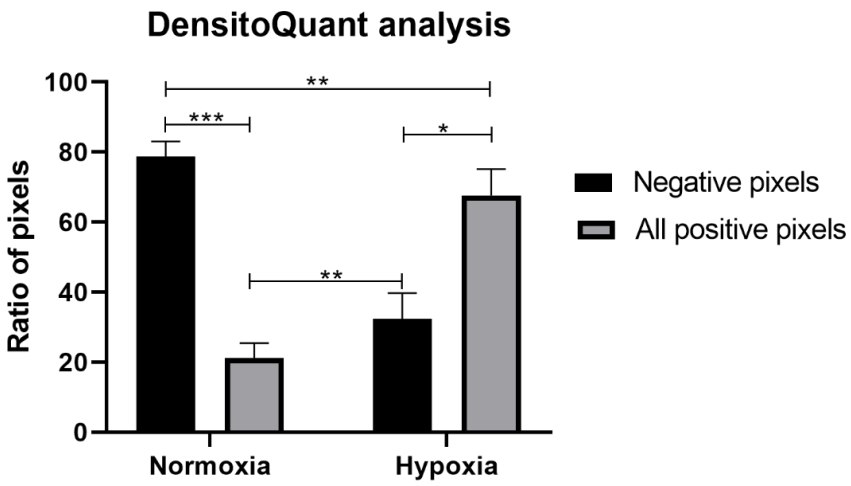

*Figure 31 Digital image analysis was carried out on the in vitro samples, showing the increased expression of CAIX in hypoxia. Formalin-fixed specimen were stained against CAIX antibody, then digitalized with Pannoramic MIDI Scanner, which was followed by the DensitoQuant analysis. Statistical significance was determined using one-way ANOVA analysis followed by Tukey's multiple comparison test. *; **, and *** indicate statistically significant differences at $p < 0.05$, $p < 0.01$, and $p < 0.001$.*

Other markers, such as the expression of CAXII, GLUT1, and MIB1 were also examined in the cell lines. CAXII staining was non-specific as dominant staining was in the cytosol and the nucleus, while CAXII is a membrane protein, thus we excluded this enzyme from the further analysis (Figure 32.).

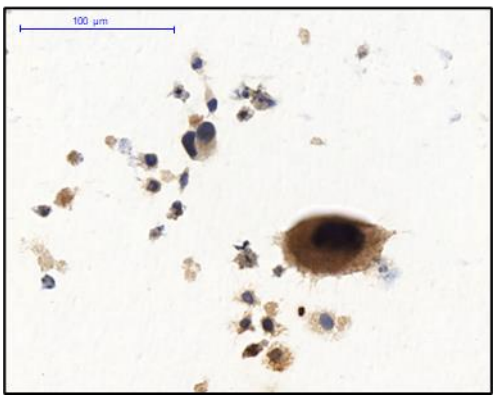

Figure 32 CAXII expression in L1236, a representative picture is provided. There was no specific reaction to the CAXII antibody in the cell lines, we excluded the examination of this isoform.

Expression of glucose transporter GLUT1 appeared to be independent of *in vitro* hypoxia treatment in the otherwise hypoxia sensitive L1236 cells, as compared to the normoxic control cultures there was no significant change in the membrane-bound staining in the samples hold under hypoxic circumstances for up to 72h (Figure 33.)

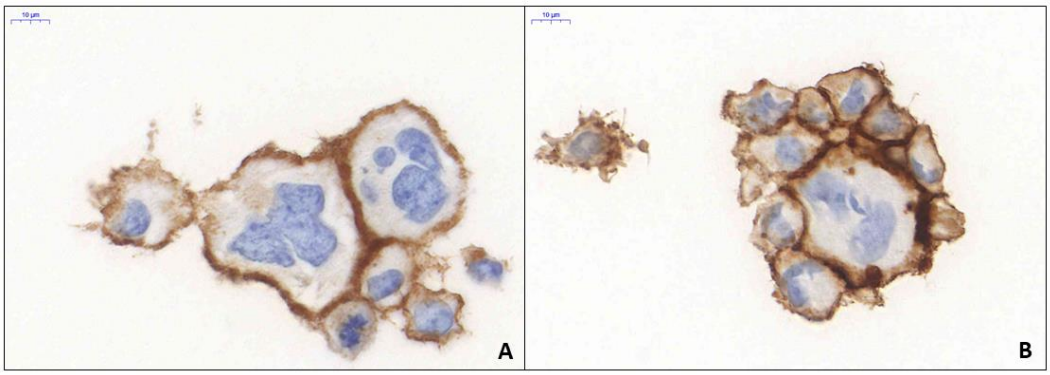

Figure 33 Expression of GLUT1 in the L1236 cell line. Representative pictures. There was no significant difference in expression of GLUT1 between the normoxic control (A) and hypoxic samples (B) (Maginification 85x)

7.5.2.3 Investigation of cell proliferation (MIB1) activity and CAIX expression

We also examined the MIB1 expression in the case of the L1236 cell line to investigate the potential relationship between the proliferation index and CAIX expression (Figure 34.) similar to the retrospective clinical study. Double immunohistochemical staining was carried out to visualize the relation between MIB1 and CAIX.

Interestingly, we found that MIB1 and CAIX positivity may have an inverse relation, because the cells presenting with strong nuclear MIB1 positivity missed, or only minimally showed cell membrane CAIX expression. In contrast, large CAIX positive cells remained negative for the MIB1 immunostaining. The loss of proliferation potential may indicate that CAIX+ cells are about to enter a resting cellular state or cellular arrest as a response to hypoxia.

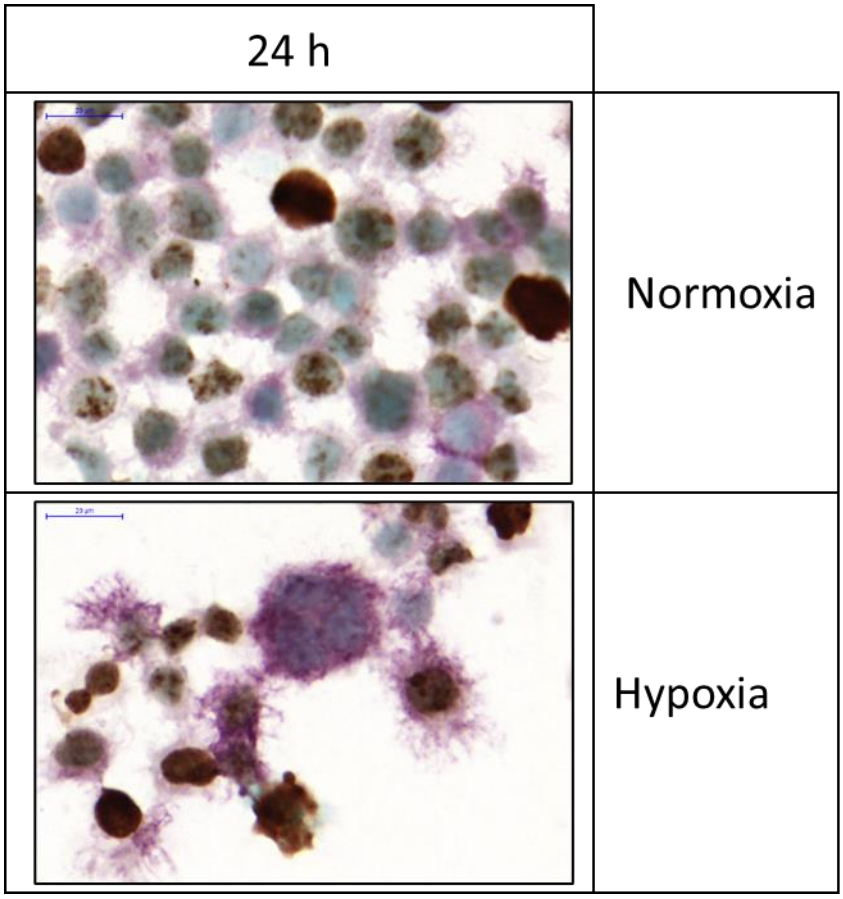

Figure 34 Representative in vitro L1236 culture samples showing expression of CAIX and MIB1 in HRS cells. (Mib1 – diaminobenzidine, DAB brown chromogen, CAIX – VIP-chromogen(violet.) Magnification 20x.

The evaluation of CAIX and MIB1 double-stained slides included the relative quantification of the positive cells by counting. We classified the staging groups into 4 categories: double negative (CAIX- and MIB1-), double-positive (CAIX+ and MIB1+), CAIX positive (CAIX+ and MIB1-), and MIB1 (CAIX- and MIB1+) cells (Figure 35.).

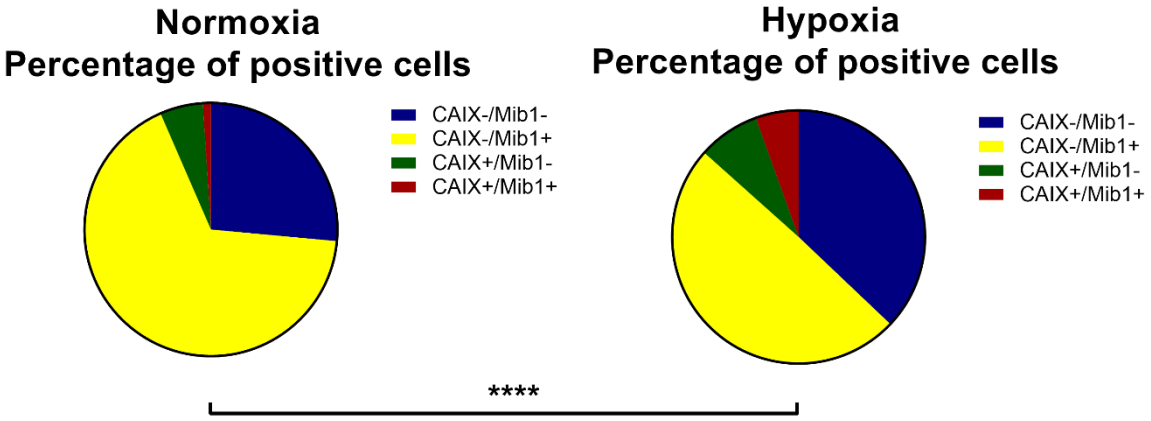

*Figure 35 Distribution of the positive cells following CAIX and Mib1 immunocytochemistry in L1236 cultures. Note that the MIB1+ population decreases in hypoxia, unlike the CAIX+ group, in which there was a visible increase in the expression of the enzyme. Also, there was a slight increase in the double-positive subpopulation. Statistical significance was determined using the Chi-square test, **** indicates statistically significant $p < 0.0001$. A Chi-square test was applied to each observed value, but for better visualization, we used the percentage of the cells.*

We observed a significant decrease in the MIB1 staining consisted of CAIX-/MIB1+ and CAIX+/MIB1+ population in the samples treated in the hypoxia chamber compared to the normoxic control. As expected, the expression of CAIX was increased as CAIX+/MIB1- and CAIX+/MIB1+ fraction. The double-positive subpopulation might represent the cell compartment just finalizing cell cycle, or cells with strongly reduced cell cycle duration.

Figure 36. shows the percentage of MIB1+ and CAIX+ cells in normoxic and in hypoxic conditions.

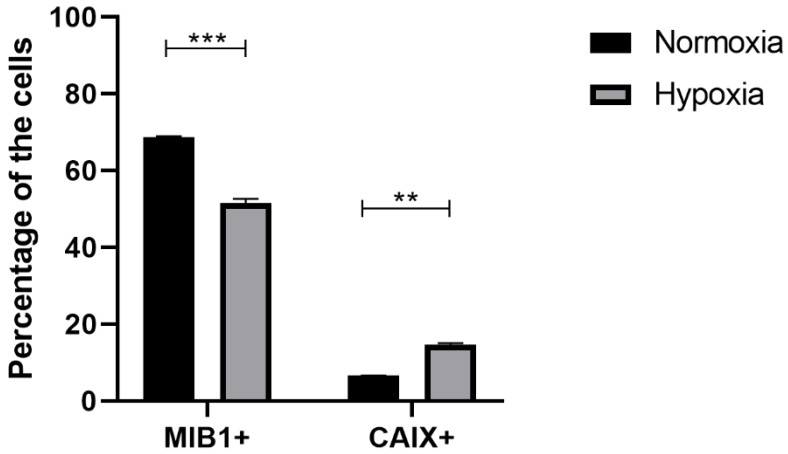

*Figure 36 Percentage of CAIX+ and MIB1+ cells in normoxia and in hypoxia (24h). Statistical significance was determined using two-way ANOVA analysis followed by Tukey's multiple comparison test. **, and *** indicate statistically significant differences at $p < 0.01$, and $p < 0.001$. Bars represent mean plus SEM.*

7.5.2.4 Examination of the CAIX expression dynamics by flow cytometry

We assessed CAIX expression using flow cytometry which allowed the easy distinction of CAIX+ and CAIX- cell populations.

As a characteristic feature, the proportion of CAIX+ cells significantly increased upon hypoxia in L1236 cells (Figure 37.).

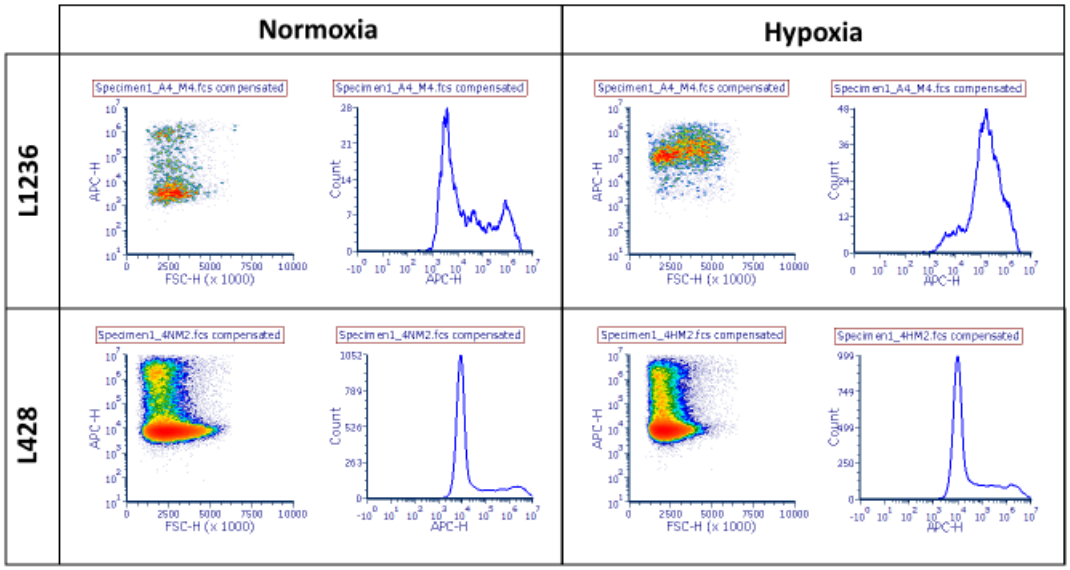

Figure 37 Representative dot plot and histogram of Novocyte measurements. Fluorescence intensities under normoxia (left) and hypoxia (right) clearly show a differential intensity distribution of L1236 (upper row) and L428 cells (lower row) following incubation with the CAIX-specific antibody. 10^6 cells were treated with normoxia and hypoxia for 48h, then the cells were harvested. CAIX expression was determined by flow cytometry with the use of an APC Conjugation Lightning-link kit. 10.000 cells were counted during the measurement.

As the dot plots show, in normoxia, there was a massive CAIX- cell population and only the minority of cells expressed CAIX. In L1236 39.44% (1273/3228) of cells showed high CAIX positivity and 59.88% (2175/3228) of cells proved to be negative. However, in hypoxia, there was a drastic change in the distribution of the cells. A shift into a CAIX positive range was observed and this result could indicate that the cells underwent a phenotypic change to adapt to the hypoxic stress. According to our measurements 87.37% (4606/5272) of cells showed high CAIX positivity, the main cell population gaining 100x intensity compared to the negative cells, while only 12.22% (644/5272) of cells remained in the negative range.

In contrast to L126 cells in L428 cells there was only a slight change in the proportions of CAIX+ cells. In L428 14.59% (1599/10961) of cells showed high CAIX positivity and 80.21% (8792/10961) of cells showed to be CAIX negative under normoxic conditions. The distribution of was grossly

unchangedunder hypoxic condition after 48 hours: 19.62% (1996/10174) of the cells showed high CAIX positivity and 79.88% (8127/10174) of cells was CAIX negative.

7.5.2.5 Effect of cytotoxic treatment in L1236 cell line

Acetazolamide (AA) is a pharmacological inhibitor of CAIX. To evaluate the potential effect of CAIX inhibition in our experimental model, we assessed whether AA treatment can modulate the response of *in vitro* cultivated cHL cells to the ABVD regimen.

ABVD treatment induced cell death in L1236 cells under normoxia (Figure 38.). Hypoxia-induced the proportions of propidium iodide-positive cells that did not further increase upon ABVD treatment (Figure 38.).

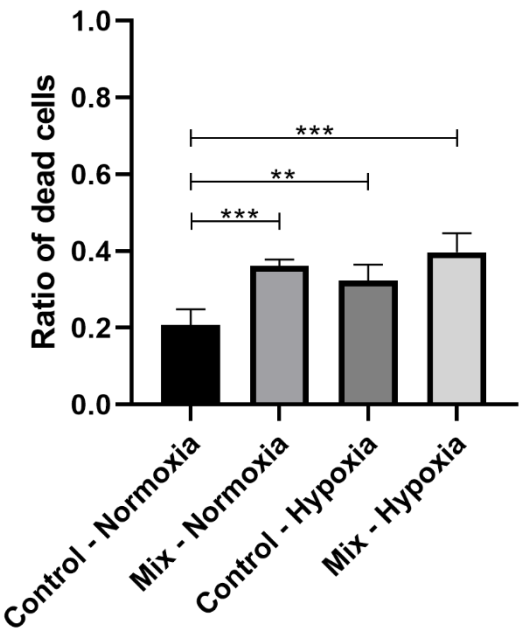

*Figure 38 Results of the ABVD-treatment on L1236 cells in normoxia and hypoxia. Ratio of dead cells as stained with propidium iodide (PI) and analyzed by flow cytometry. 60.000 cells/well were seeded conditioned in hypoxia/normoxia for 24h and then treated with ABVD-mix for 24h in hypoxia/normoxia. After the treatment, the cells were harvested. Cells were stained with PI Apoptosis Kit and analyzed by flow cytometry (n = 4). Data are plotted as mean ± SEM. Significance was calculated using a one-way ANOVA test (***, p<0,001). According to Tukey's multiple comparison test, there was a significant difference between the analyzed groups (**, and *** indicate statistically significant differences at p < 0.01, and p < 0.001). Mix refers to the used drug mixture (ABVD).*

As we could not exclude the fact that the high cellular death could be due to the hypoxic microenvironment, we examined the effect of drugs in normoxic conditions and shorter incubation

times. In the next experiment, we plated the cells a day before we treated them with ABVD mix and acetazolamide.

Next, we co-treated cultivated L1236 cells with ABVD and AA. In normoxia, AA did not induce cell death, while in combination with AVBD we observed increases in the proportions of propidium-iodide positive cells (Figure 39.).

Figure 37. shows the increase of cell death when AA was also applied to the treatment protocol, however, there was no significant difference between the MIX (ABVD) and MIX+AA groups.

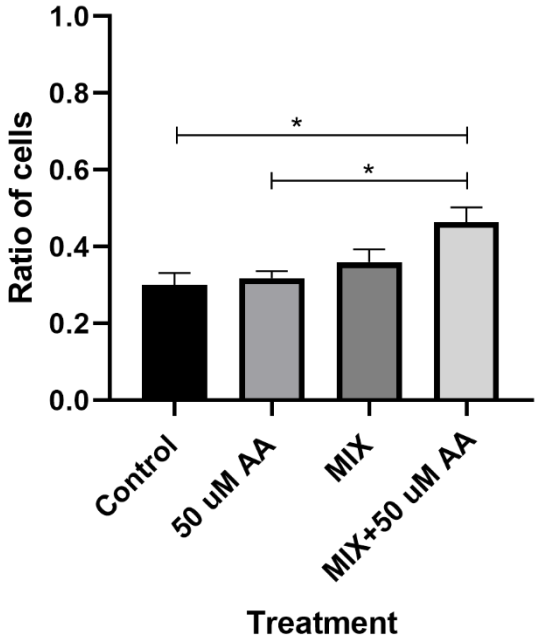

Figure 39 The effect of adjuvant acetazolamide (AA) on the response of ABVD mix in L1236 cell cultures. 60.000 cells/well were seeded and treated with ABVD-mix in normoxic conditions for 2h. After the treatment, the cells were harvested. Cells were stained with Annexin-FITC-PI Apoptosis Kit and analyzed by flow cytometry (n = 4). Dead cells were stained with propidium iodide (PI) and analyzed by flow cytometry. Data are plotted as mean ± SEM. Significance was calculated using a one-way ANOVA test (, p<0,05). According to Tukey's multiple comparison test, there was a significant difference between the analyzed groups (*, p<0,05). Mix refers to the used drug mixture (ABVD).*

Taken together, we propose that modulation of CAIX to cease enzyme activation may be a promising therapeutic approach to increase the efficacy and efficiency of chemotherapeutic drugs.

8. DISCUSSION

There is a need for biomarkers that can determine the prognosis and treatment response in cHL. In our retrospective and tissue-based study, we aimed to identify a possible biomarker, which can predict the possible outcome in this hematological malignancy. A better understanding of the characteristics of solid tumors – e.g. tumor hypoxia, acidosis – and also in metabolic rewiring can contribute to the development of effective diagnostic and therapeutic approaches [114,115].

CAIX is a member of a large zink-metalloenzyme family. The expression of this membrane-associated enzyme is strongly associated with malignant transformation and its expression is highly HIF1α-dependent. The role of the enzyme is to eliminate protons from the intracellular space to create a near-physiological pH, while the extracellular pH becomes acidic. This contributes to the survival of neoplastic cells within the hostile microenvironment. The importance of CAIX lies within the fact that CAIX levels are associated with poor prognosis and more aggressive tumor phenotype, thus correlating with therapy resistance [48,57,65,116,117].

This study aimed to examine the CAIX expression pattern and distribution in cHL to determine the quantity of CAIX positive neoplastic cells. Further, we aimed to assess a potential correlation between the expression of CAIX and the therapy response/clinical outcome. Finally, whole-slide digital analysis was carried out to quantitatively analyze the CAIX expression in the samples.

Our research group reported the aberrant expression of CAIX in HRS-cells in patients' samples for the first time. Interestingly, in the retrospective study, we found that the expression of CAIX is not limited to the perinecrotic foci, but it could also be expressed in those cells, that likely have undergone hypoxia-related metabolic adaptation elsewhere. These results suggest that a focal non-lethal hypoxic stress outside of the necrotic area and may be prior to massive HRS-cellular damage. In our study cohort, the LD subtype presented necrosis and all the LD cases were positive for CAIX. We assumed that CAIX expression in cHL cases is upregulated under hypoxic conditions via the HIF1α pathway, and thus influences the metabolic adaptation of neoplastic HRS cells, resulting in a more aggressive and resistant phenotype. The expression of CAIX was also high in NS variant. The expression of CAIX was less frequent in the MC and LR subtype, which may suggest that hypoxia-associated adaptation pathways are less relevant in these variants [113]. This observation may indicate that the unfavorable LD subtype tends to express the enzyme suggesting that high CAIX expression may be in relation to worse clinical outcomes. 75% (3/4) of the patients from the LD subtype died within 14 months of diagnosis, which may also strengthen the prognostic value of the enzyme.

We also collected data regarding our patient cohort. According to the patient records, EBV-serology and LMP1 staining were available in the majority of the cases. Results of the EBV serology showed that there was an infection in the past. Interestingly, those cells which showed LMP-1 positivity did not express CAIX, however, this observation of a negative correlation needs further examination (unpublished data).

Expression of CAXII was also examined, and according to our results, CAXII positivity was observed not only in the HRS-cell, but also in other bystander cells, such as histiocytes, stromal fibroblasts. Dual CAXII/MIB1 immunostaining failed because of the many CAXII+ non-neoplastic cells, thus the cellular composition could not be examined precisely[113].

One of the common characteristics of hypoxic cells and cancer stem cells is that they can acquire regressive features. MIB1, a proliferation index, is widely used to examine the proliferative activity of cancer cells. According to the literature, HRS cells tend to have high proliferative activity. However, in our study, those CAIX positive cells were in a suppressed cellular state, being blocked in the cell cycle, which was independent of the histological subtype. Moreover, CAIX positive cases had an unfavorable response to standard therapy [113]. In cultured cells, upon hypoxia, there was an inverse correlation between the expression of CAIX and MIB1 that is in good agreement with the observation that tumor hypoxia contributes to a cell cycle arrest [118]. To our best knowledge, nobody investigated the connection between CAIX expression and MIB1 activity in cHL, but our results indicate that the expression of CAIX – due to tumor hypoxia and acidosis – may contribute to a tumor cell phenotype change. Furthermore, it is also possible that CAIX positive cells may be in a cell cycle arrest-like state, or their metabolism slowed down due to the adaptation mechanisms. In L1236 cells CAIX was upregulated in a short period of time, and it seems that after reaching a steady-state point, the relative enzyme quantity did not increase further. Importantly, there was no increase in the MIB1+/CAIX- population in the hypoxic samples, thus it validates our results in the retrospective study. Böhme et al. [119] investigated the effect of tumor acidosis in malignant melanoma, and they found that low pH induces several cellular changes, among these, the upregulation of p21, SA-ß-galactosidase and the reduction of cellular proliferation through G1/G0 cell cycle arrest, which supports our results.

The upregulation of CAIX may refer to the neoplastic cells' versatile function which enables them to adapt to the metabolically challenging changes and also it could contribute to the alternation of many cellular signaling pathways, which provides survival to the malignant cells [60,120,121].

The occurrence and effect of CAIX has been widely studied in various kinds of solid tumors (including breast and colon carcinoma). In contrast to them it was barely studied in lymphatic malignancies [48,65]. Chen et al. examined the expression of CAIX in some NHL in vitro, and Raji, Ramos, and Granta 519 cell

lines were used. In their experiment, the Ramos tumor cell line had the highest area percentage, which was stained with CAIX, and Granta 519 had the most heterogenous percentage area staining pattern. Unfortunately, the *in vitro* results did not correlate with their *in vivo* results, as in their *in vitro* examination, the Granta19 cell line had higher CAIX expression, while according to the *in vivo* results, the Ramos cell line had greater CAIX expression and acidity score. This difference could be explained by the different oxygen levels, which induces both the expression of CAIX and the activation of pimonidazole, that was used to measure the level of hypoxia. The results are promising, but still, more research is required in this field [122].

We applied the digital analysis method to compensate for the variable number and/or uneven distribution of neoplastic cells in cHL because the conventional quantification of CAIX expression by light microscopy was not possible. Digitalized slides were analyzed by the whole slide digital analysis method (WSD), which provided a visual control over the neoplastic cells and their cellular background simultaneously [123,124]. Image analysis is a widely used method in tissue-based research, however, the number of this kind of study is still limited in relation to cHL, as the digital examination of this kind of lymphoma is challenging, because of the variable shape and size of HRS-cells [125–127].

With this method, we were able to quantify the expression level of CD30 and CAIX in human samples. Our data showed that the CAIX positive compartment is a subfraction of the CD30 positive cell mass. This result suggests that CAIX positivity is not an integral feature of the transformed cells and also, the CAIX expression was prominent in the perinecrotic foci, which indicates that the enzyme has a functional role in the adaptation mechanism to hypoxia. Moreover, higher CAIX scores have been associated with the most unfavorable clinical prognostic group, which was the LD subtype [112].

Hartman et al. [128] investigated the expression of GLUT1, which is not only a downstream factor of HIF1α but also has a significant role in glucose metabolism. They found that approximately 50% of their cases showed GLUT1 positivity, but there was a difference in the expression pattern in the different cHL subtypes. In their results, the NS variant has the highest expression rate. According to our results, GLUT1 expression seemed to be steady and did not show to be as inducible as CAIX in normoxia or hypoxia.

To our best knowledge, this is the first study that aimed to examine the expression of CAIX in cHL cell lines.

At the beginning of our *in vitro* experiments, we chose a chemical hypoxia mimetic agent – namely Cobalt-Chloride ($CoCl_2$). The compound is often used as a surrogate for generating hypoxia, because $CoCl_2$ directly inhibits the PHDs and therefore, HIF1α accumulates in the nucleus. Kewitz et al. [56] investigated the effect of $CoCl_2$ - a chemical inducer of hypoxia – and 1 % oxygen for 48h on HL cell

lines, and they found that it could significantly alter the gene expression profile of the cell lines. One of their target genes was XAF1 that is involved in the mechanism of cisplatin resistance and according to their results, the gene had a lower expression level in hypoxic cell cultures. However, $CoCl_2$ has been reported to have additional effects in a concentration and cell line-specific manner and can only mimic one aspect of hypoxic conditions, but we were more interested in the global effect of hypoxia, thus after a few experiments, we ceased the method and turned towards hypoxia chambers [129,130(p2),131].

One of the challenging aspects of our study was to find the right antibody to recognize relevant epitopes of the transmembrane CAIX enzyme protein for quantitative analyses. There are several commercially available antibodies, which recognizes different domains of the CAIX protein. In the end, we decided the use the EP161 clone for the *in vitro* samples (Figure 40.).

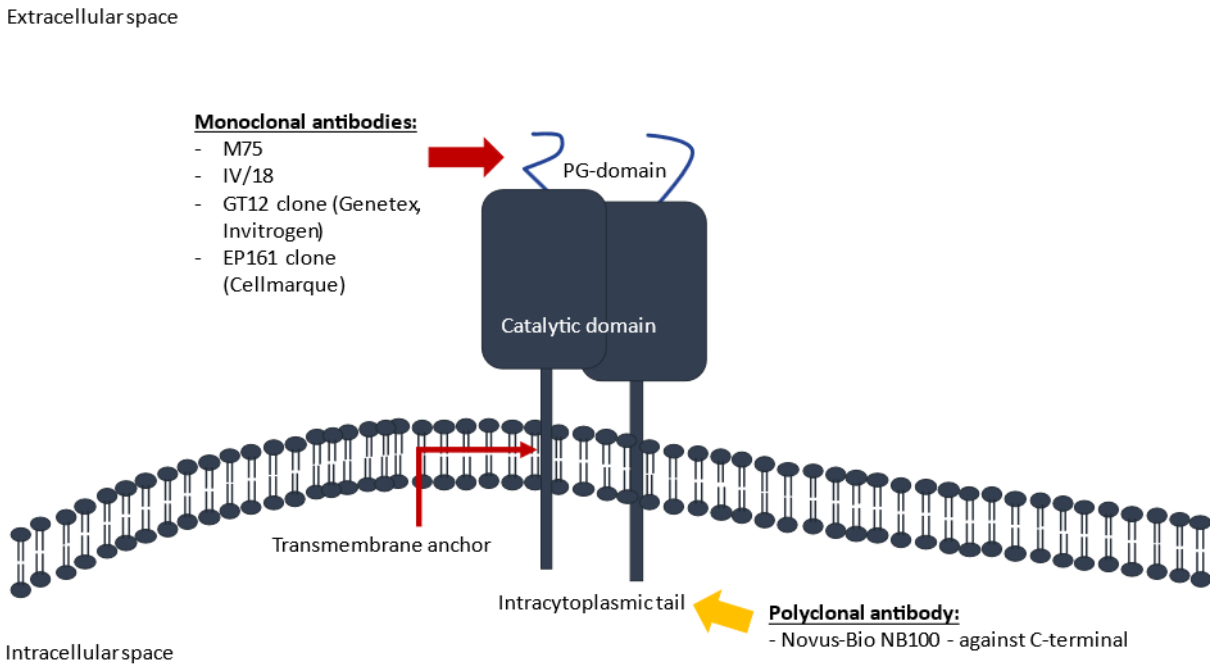

Figure 40 Schematic illustration of CAIX epitopes. There are several commercially available antibodies for the examination of CAIX. In in vitro study we used the EP161 clone.

We observed that the expression of CAIX was enriched to those cells which proved to be MIB1 negative especially when applying hypoxia. It is noteworthy, that the *in vitro* results are in line with previously published clinical data, as the reduced MIB1 activity was reported as a hallmark of the CAIX positive fraction in human malignancies. [113]. Interestingly, the two cHL cell lines have different CAIX expression patterns and distributions. While L428 expresses poorly CAIX under hypoxic conditions, on the other hand, in the case of L1236, CAIX seems to be highly inducible by hypoxia. The CAIX expression

was inducible in L1236 that validate our observations in the retrospective study that CAIX is induced in hypoxic regions in lymph nodes.

Importantly, we were able to show that the pharmacological manipulation of CAIX may influence the efficacy of conventional chemotherapy combinations. The fact that AA was able to enhance the efficacy of the ABVD treatment in vitro in terms of cell survival is highly promising and was not reported earlier. AA was chosen for CAIX inhibition because of the simple availability and the general acceptance in the literature as a CA-inhibitor, despite its known widespread effects. While the effect should be investigated in much more detail, this result point toward the applicability of AA and more selective CA-inhibitors as an adjuvant drug in a clinical setting. However, in vitro experiments do not fully represent issues related with the immediate microenvironment of the tumor cells. In our understanding hypoxia and related CAIX expression is a feature of specific sites (niches) and targeting these tumor areas might be a true challenge. Hypoxia related acidosis and cellular quiescence both interfere with the effect of most anti-cancer agents. The application of anti-CD30 antibody (Brentuximab Vedotin) or anti-PD-1 inhibitors in relapsed cHL cases has promising results. These inhibitors directly target surface structures of neoplastic cells, suggesting that complementation of these regimes with appropriate pH control (e.g. through the inhibition of CAIX) may have a beneficial clinical effect [12,84,132].

Based on our in vitro results, we concluded that CAIX has a dynamic expression pattern in cHL cell cultures, which is highly comparable with the observations we made in patients samples following histology. All available data support the hypothesis that the heterogenous expression of CAIX in neoplastic HRS cells could be a dynamically evolving feature of hypoxia-related adaptive changes. The presented early results further indicate that the enzyme facilitates the survival of neoplastic cells by altering the cell cycle (reduced MIB1 activity) and possibly by modulating the sensitivity to the chemotherapeutic drugs (Figure 41.).

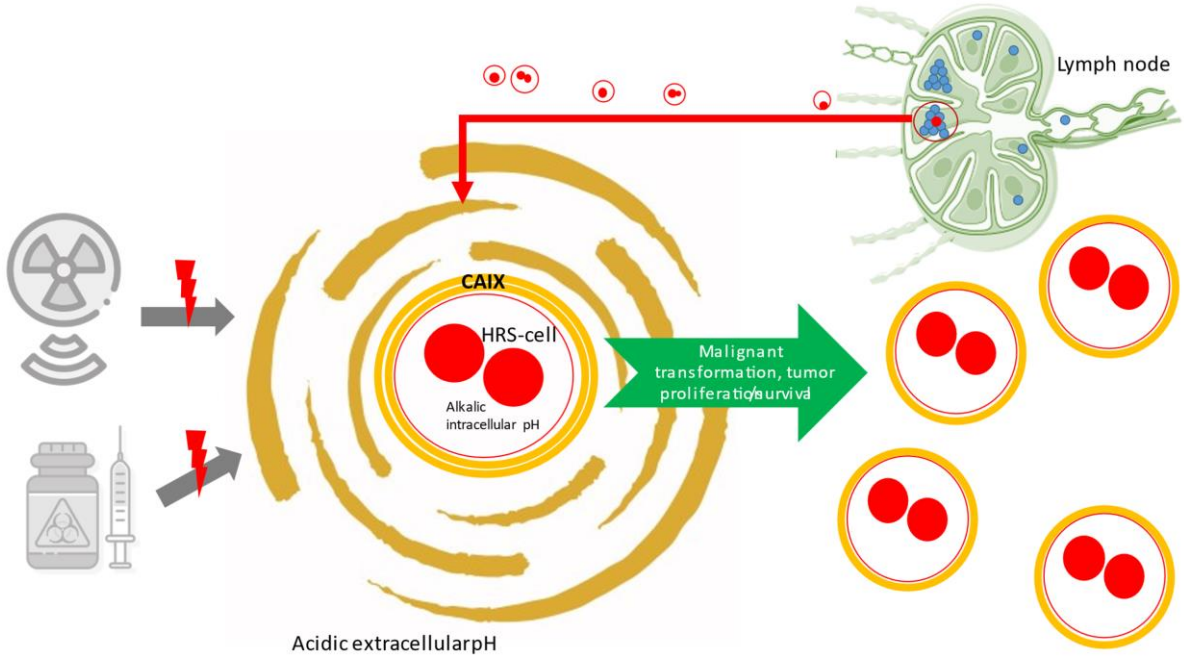

Figure 41 Schematic illustration of the intra- and extracellular changes in cHL potentially influencing treatment efficacy. The increased expression of CAIX contributes to the creation of a pro-tumor niche, supporting malignant transformation and survival of the neoplastic cells.

9. MAIN FINDINGS OF THE STUDY

In summary, the main statements of the Ph.D. work are the following:

- The pathognomic cells of cHL, namely HRS-cells express CAIX. The expression of CAIX was selectively predominant on the HRS-cells.
- The expression of the enzyme was characteristic in the perinecrotic areas.
- Detection of CAIX expression has a predictive value for cHL progression and could predict the possible treatment response and outcome, thus as a potential biomarker, the usage of CAIX should be considered.
- The whole-slide digital analysis-based examination can detect the CD30 and CAIX positive cells and quantify the manner of their expression. CAIX positive cells are a subfraction of CD30 positive cells.
- L1236 showed a significant increase in CAIX expression upon hypoxia.
- Increased CAIX expression is in an inverse correlation with MIB1 expression.
- It seems that CAIX expression may contribute to a cell cycle arrest, which could be a protective mechanism against hypoxia.

10. SUMMARY

Classic Hodgkin lymphoma is a lymphoid malignancy with an incidence of 83 087 persons in 2020 globally and has a bimodal disease distribution with peaks at the ages of 25-50 and over 50 years of age. It is characterized by a low number of neoplastic cells – so-called Hodgkin-Sternberg-Reed cells – which account only for 1% of cells and have an inflammatory cellular background.

CAIX is a member of a large enzyme family, which participates in cellular pH regulation and its expression is upregulated upon HIF1α activation. Increased enzyme activity leads to a near-physiological pH in neoplastic cells, while the extracellular pH becomes acidotic, and the rate of acidosis has a detrimental effect on cancer prognosis. In several solid tumors, expression of CAIX was studied and it was already suggested has already been linked to worse prognosis and outcome, however, it has never been examined in cHL. Thus, we aimed to examine the expression of CAIX and its effect on cellular metabolism and influence on the efficiency and efficacy of drugs.

Here we have shown that the expression of CAIX is limited to the HRS-cells in human samples, unlike CAXII, which did not show that specific manner in expression. Previous studies suggested that GLUT1 also has a special role in cHL, however, in our samples, GLUT1 expression was not specific for the pathognomonic cells.

Better detection of intratumor hypoxia might i) might provide a better insight into a reliable assessment of hypoxia-related metabolic alternations – intra- and extracellularly – ii) might contribute to better management and planning of anti-cancer therapy.

Nevertheless, a better understanding of the relationship between tumor hypoxia and hypoxia-related cellular adaptation mechanisms can create opportunities for increasing the efficiency and efficacy of chemoradiotherapy.

Our results show that CAIX could be a reliable marker of intratumor hypoxia and it could also show the current state of the cellular machinery. Based on our results, we suggest the exploitation of the CAIX activity in the management of cHL, especially in those cases which are shown to be CAIX positive. Our data, therefore, emphasize the development and application of CAIX-specific inhibitors.

11. ÖSSZEFOGLALÁS

A klasszikus Hodgkin lymphoma egy lymphoid daganattípus, ami 2020-ban világszinten 83,087 újonnan diagnosztizált beteget érintett. Incidenciáját tekintve bimodális eloszlású betegség, ami azt jelenti, hogy 25-50, valamint 50 év felettiek körében tapasztható magasabb előfordulás. A daganat jellegzetessége, hogy alacsony neoplasztikus sejtszámmal rendelkezik – amelyeket Hodgkin-Sternberg-Reed sejteknek nevezünk -, ami 1%-át teszik ki a sejteknek. A neoplasztikus sejteket jellegzetes módon gyulladásos sejtháttér veszi körül.

A CAIX egy nagy enzimcsalád tagja, ami a sejt pH-regulációjában vesz részt. Expressziója megemelkedik HIF1α aktivitás hatására. A megemelkedett enzimaktivitás egy közel fiziológiás pH kialakulásához vezet a daganatos sejtekben, míg az extracelluláris pH savassá válik és az acidózis mértéke jelentős mértékben befolyásolja a daganat prognózisát. Számos szolid tumorban tanulmányozták már a CAIX expresszióját és már összefüggésbe hozták a rosszabb prognózissal és kimenetellel, de eddig még nem vizsgálták cHL-ben.

Így célul tűztük ki a CAIX enzim expressziójának vizsgálatát, valamint a sejtszintű metabolizmusra és a gyógyszerhatékonyságra gyakorolt hatását.

A dolgozatban bemutattuk, hogy a CAIX expressziója a HRS-sejtekre korlátozódott a humán mintákban, a CAXII-el szemben, ami nem mutatott ilyen jellegű expressziót. Korábbi tanulmányok már jelezték, hogy a GLUT1-nek szintén szerepe lehet a cHL-ben, azonban mintáinkban a GLUT1 expresszió nem bizonyult a patognomikus sejtekre specifikusnak.

Az intratumoralis hypoxia jobb vizsgálhatósága lehetővé teszi i) a mélyebb betekintést a hypoxia-asszociálta metabolikus változások – intra- és extracellulárisan - megbízható vizsgálatára, ii) hozzájárulhat a sikeres daganatellenes terápia megtervezéséhez. Továbbá, a tumor hypoxia és a hypoxia-asszociálta celluláris adaptációs mechanizmusok megértése lehetőséget teremthet a kemoradioterápia hatékonyságának növeléséhez.

Eredményeink azt mutatják, hogy a CAIX megbízható markere lehet az intratumorális hypoxia jelzésére és megmutathatja az aktuális celluláris folyamat állapotát. Eredményeink alapján javasoljuk a CAIX aktivitásának vizsgálatát a cHL menedzselésében, főleg azon esetekben, amik CAIX pozitívnak bizonyultak. Eredményeink továbbá szorgalmazzák a szelektív CAIX inhibitorok kifejlesztését és azok használatát.

12. REFERENCES:

1. Piris MA, Medeiros LJ, Chang KC. Hodgkin lymphoma: a review of pathological features and recent advances in pathogenesis. *Pathology (Phila)*. 2020;52(1):154-165. doi:10.1016/j.pathol.2019.09.005

2. Ellis H. Sir Samuel Wilks (1824-1911): brilliant observer who "rediscovered" Hodgkin's disease. *Br J Hosp Med Lond Engl 2005*. 2011;72(11):654. doi:10.12968/hmed.2011.72.11.654

3. Montes-Moreno S. Hodgkin's Lymphomas: A Tumor Recognized by Its Microenvironment. *Adv Hematol*. 2011;2011:142395. doi:10.1155/2011/142395

4. *Hematológiai betegségek atlasza: morfologia, citokëmia, aramlascitometria, immunhis ztokëmia, citogenetika, molekularis genetika*. Medicina Könyvkiadá Zrt.; 2006.

5. Jaffe ES. The 2008 WHO classification of lymphomas: implications for clinical practice and translational research. *Hematol Am Soc Hematol Educ Program*. Published online 2009:523-531. doi:10.1182/asheducation-2009.1.523

6. Quintanilla-Martinez L. The 2016 updated WHO classification of lymphoid neoplasias. *Hematol Oncol*. 2017;35:37-45. doi:10.1002/hon.2399

7. Swerdlow SH, Campo E, Pileri SA, et al. The 2016 revision of the World Health Organization classification of lymphoid neoplasms. *Blood*. 2016;127(20):2375-2390. doi:10.1182/blood-2016-01-643569

8. Küppers R. Origin of Hodgkin Lymphoma. In: *Hematology*. Elsevier; 2018:1204-1211. doi:10.1016/B978-0-323-35762-3.00074-3

9. Wang HW, Balakrishna JP, Pittaluga S, Jaffe ES. Diagnosis of Hodgkin lymphoma in the modern era. *Br J Haematol*. 2019;184(1):45-59. doi:10.1111/bjh.15614

10. Eberle FC, Mani H, Jaffe ES. Histopathology of Hodgkin's Lymphoma. *Cancer J*. 2009;15(2):129-137. doi:10.1097/PPO.0b013e31819e31cf

11. Savage KJ, Mottok A, Fanale M. Nodular lymphocyte-predominant Hodgkin lymphoma. *Semin Hematol*. 2016;53(3):190-202. doi:10.1053/j.seminhematol.2016.05.009

12. Momotow J, Borchmann S, Eichenauer DA, Engert A, Sasse S. Hodgkin Lymphoma-Review on Pathogenesis, Diagnosis, Current and Future Treatment Approaches for Adult Patients. *J Clin Med*. 2021;10(5). doi:10.3390/jcm10051125

13. Hashmi AA, Hussain ZF, Hashmi KA, et al. Latent membrane protein 1 (LMP1) expression in Hodgkin lymphoma and its correlation with clinical and histologic parameters. *World J Surg Oncol*. 2017;15(1):89. doi:10.1186/s12957-017-1147-y

14. Kieser A, Sterz KR. The Latent Membrane Protein 1 (LMP1). *Curr Top Microbiol Immunol*. 2015;391:119-149. doi:10.1007/978-3-319-22834-1_4

15. Wang LW, Jiang S, Gewurz BE. Epstein-Barr Virus LMP1-Mediated Oncogenicity. *J Virol*. 2017;91(21):e01718-16. doi:10.1128/JVI.01718-16

16. Brune MM, Juskevicius D, Haslbauer J, Dirnhofer S, Tzankov A. Genomic Landscape of Hodgkin Lymphoma. *Cancers*. 2021;13(4):682. doi:10.3390/cancers13040682

17. Pileri SA, Ascani S, Leoncini L, et al. Hodgkin's lymphoma: the pathologist's viewpoint. *J Clin Pathol*. 2002;55(3):162-176. doi:10.1136/jcp.55.3.162

18. Thida AM, Tun AM. Lymphocyte Depleted Hodgkin Lymphoma. In: *StatPearls*. StatPearls Publishing; 2020. Accessed February 13, 2021. http://www.ncbi.nlm.nih.gov/books/NBK556042/

19. Eichenauer DA, Aleman BMP, André M, et al. Hodgkin lymphoma: ESMO Clinical Practice Guidelines for diagnosis, treatment and follow-up. *Ann Oncol*. 2018;29:iv19-iv29. doi:10.1093/annonc/mdy080

20. Jiang Y, Chen Y, Huang R, Chen G. Comparison of the efficiency of ABVD versus BEACOPP for Hodgkin lymphoma treatment: a meta-analysis. *Int J Hematol*. 2016;104(4):413-419. doi:10.1007/s12185-016-2080-5

21. Ansell SM. Hodgkin lymphoma: 2016 update on diagnosis, risk-stratification, and management: Hodgkin Lymphoma. *Am J Hematol*. 2016;91(4):434-442. doi:10.1002/ajh.24272

22. Ansell SM. Hodgkin lymphoma: 2018 update on diagnosis, risk-stratification, and management. *Am J Hematol*. 2018;93(5):704-715. doi:10.1002/ajh.25071

23. Engert A, Raemaekers J. Treatment of early-stage Hodgkin lymphoma. *Semin Hematol*. 2016;53(3):165-170. doi:10.1053/j.seminhematol.2016.05.004

24. PubChem. Doxorubicin. Accessed April 13, 2021. https://pubchem.ncbi.nlm.nih.gov/compound/31703

25. PubChem. Bleomycin. Accessed April 13, 2021. https://pubchem.ncbi.nlm.nih.gov/compound/5460769

26. PubChem. Vinblastine sulfate. Accessed April 13, 2021. https://pubchem.ncbi.nlm.nih.gov/compound/5388983

27. PubChem. Dacarbazine. Accessed April 13, 2021. https://pubchem.ncbi.nlm.nih.gov/compound/2942

28. Hodgkin Lymphoma - Cancer Stat Facts. SEER. Accessed April 13, 2021. https://seer.cancer.gov/statfacts/html/hodg.html

29. Parente P, Zanelli M, Sanguedolce F, Mastracci L, Graziano P. Hodgkin Reed–Sternberg-Like Cells in Non-Hodgkin Lymphoma. *Diagnostics*. 2020;10(12):1019. doi:10.3390/diagnostics10121019

30. Evens AM, Kanakry JA, Sehn LH, et al. Gray zone lymphoma with features intermediate between classical Hodgkin lymphoma and diffuse large B-cell lymphoma: Characteristics, outcomes, and prognostication among a large multicenter cohort: Gray Zone Lymphoma. *Am J Hematol*. 2015;90(9):778-783. doi:10.1002/ajh.24082

31. Goncharova O, Flinner N, Bein J, et al. Migration Properties Distinguish Tumor Cells of Classical Hodgkin Lymphoma from Anaplastic Large Cell Lymphoma Cells. *Cancers*. 2019;11(10). doi:10.3390/cancers11101484

32. Matsuki E, Younes A. Lymphomagenesis in Hodgkin lymphoma. *Semin Cancer Biol*. 2015;34:14-21. doi:10.1016/j.semcancer.2015.02.002

33. Küppers R, Engert A, Hansmann ML. Hodgkin lymphoma. *J Clin Invest*. 2012;122(10):3439-3447. doi:10.1172/JCI61245

34. Xavier de Carvalho A, Maiato H, Maia AF, et al. Reed-Sternberg Cells Form by Abscission Failure in the Presence of Functional Aurora B Kinase. Zhang L, ed. *PLOS ONE*. 2015;10(5):e0124629. doi:10.1371/journal.pone.0124629

35. Weniger MA, Küppers R. Molecular biology of Hodgkin lymphoma. *Leukemia*. 2021;35(4):968-981. doi:10.1038/s41375-021-01204-6

36. Ashton-Key M, Wright P, Wright D. *Diagnostic Lymph Node Pathology*. 0 ed. CRC Press; 2018. doi:10.1201/9781315382654

37. Müschen M, Rajewsky K, Bräuninger A, et al. Rare occurrence of classical Hodgkin's disease as a T cell lymphoma. *J Exp Med*. 2000;191(2):387-394. doi:10.1084/jem.191.2.387

38. Rengstl B, Newrzela S, Heinrich T, et al. Incomplete cytokinesis and re-fusion of small mononucleated Hodgkin cells lead to giant multinucleated Reed-Sternberg cells. *Proc Natl Acad Sci*. 2013;110(51):20729-20734. doi:10.1073/pnas.1312509110

39. Rengstl B, Rieger MA, Newrzela S. On the origin of giant cells in Hodgkin lymphoma. *Commun Integr Biol*. 2014;7(3):e28602. doi:10.4161/cib.28602

40. Nakashima M, Watanabe M, Nakano K, Uchimaru K, Horie R. Differentiation of Hodgkin lymphoma cells by reactive oxygen species and regulation by heme oxygenase-1 through HIF-1α. *Cancer Sci*. 2021;112(6):2542-2555. doi:10.1111/cas.14890

41. Jing X, Yang F, Shao C, et al. Role of hypoxia in cancer therapy by regulating the tumor microenvironment. *Mol Cancer*. 2019;18(1):157. doi:10.1186/s12943-019-1089-9

42. Vaupel P. The Role of Hypoxia-Induced Factors in Tumor Progression. *The Oncologist*. 2004;9(S5):10-17. doi:10.1634/theoncologist.9-90005-10

43. Schito L, Semenza GL. Hypoxia-Inducible Factors: Master Regulators of Cancer Progression. *Trends Cancer*. 2016;2(12):758-770. doi:10.1016/j.trecan.2016.10.016

44. Huang Y, Lin D, Taniguchi CM. Hypoxia inducible factor (HIF) in the tumor microenvironment: friend or foe? *Sci China Life Sci*. 2017;60(10):1114-1124. doi:10.1007/s11427-017-9178-y

45. Masoud GN, Li W. HIF-1α pathway: role, regulation and intervention for cancer therapy. *Acta Pharm Sin B*. 2015;5(5):378-389. doi:10.1016/j.apsb.2015.05.007

46. Suzuki N, Gradin K, Poellinger L, Yamamoto M. Regulation of hypoxia-inducible gene expression after HIF activation. *Exp Cell Res*. 2017;356(2):182-186. doi:10.1016/j.yexcr.2017.03.013

47. Vaupel P, Multhoff G. Fatal Alliance of Hypoxia-/HIF-1α-Driven Microenvironmental Traits Promoting Cancer Progression. In: Ryu PD, LaManna JC, Harrison DK, Lee SS, eds. *Oxygen Transport to Tissue XLI*. Vol 1232. Advances in Experimental Medicine and Biology. Springer International Publishing; 2020:169-176. doi:10.1007/978-3-030-34461-0_21

48. Matolay O, Méhes G. Sustain, Adapt, and Overcome—Hypoxia Associated Changes in the Progression of Lymphatic Neoplasia. *Front Oncol*. 2019;9:1277. doi:10.3389/fonc.2019.01277

49. Shannon AM, Bouchier-Hayes DJ, Condron CM, Toomey D. Tumour hypoxia, chemotherapeutic resistance and hypoxia-related therapies. *Cancer Treat Rev*. 2003;29(4):297-307. doi:10.1016/s0305-7372(03)00003-3

50. Moreno Roig E, Yaromina A, Houben R, Groot AJ, Dubois L, Vooijs M. Prognostic Role of Hypoxia-Inducible Factor-2α Tumor Cell Expression in Cancer Patients: A Meta-Analysis. *Front Oncol*. 2018;8:224. doi:10.3389/fonc.2018.00224

51. Giatromanolaki A, Harris AL. Tumour hypoxia, hypoxia signaling pathways and hypoxia inducible factor expression in human cancer. *Anticancer Res*. 2001;21(6B):4317-4324.

52. Ravenna L, Salvatori L, Russo MA. HIF3α: the little we know. *FEBS J*. 2016;283(6):993-1003. doi:10.1111/febs.13572

53. Pasanen A, Heikkilä M, Rautavuoma K, Hirsilä M, Kivirikko KI, Myllyharju J. Hypoxia-inducible factor (HIF)-3α is subject to extensive alternative splicing in human tissues and cancer cells and is regulated by HIF-1 but not HIF-2. *Int J Biochem Cell Biol*. 2010;42(7):1189-1200. doi:10.1016/j.biocel.2010.04.008

54. Duan C. Hypoxia-inducible factor 3 biology: complexities and emerging themes. *Am J Physiol-Cell Physiol*. 2016;310(4):C260-C269. doi:10.1152/ajpcell.00315.2015

55. Abou Khouzam R, Brodaczewska K, Filipiak A, et al. Tumor Hypoxia Regulates Immune Escape/Invasion: Influence on Angiogenesis and Potential Impact of Hypoxic Biomarkers on Cancer Therapies. *Front Immunol*. 2020;11:613114. doi:10.3389/fimmu.2020.613114

56. Kewitz S, Kurch L, Volkmer I, Staege MS. Stimulation of the hypoxia pathway modulates chemotherapy resistance in Hodgkin's lymphoma cells. *Tumor Biol*. 2016;37(6):8229-8237. doi:10.1007/s13277-015-4705-3

57. Pastorekova S, Gillies RJ. The role of carbonic anhydrase IX in cancer development: links to hypoxia, acidosis, and beyond. *Cancer Metastasis Rev*. 2019;38(1-2):65-77. doi:10.1007/s10555-019-09799-0

58. Ward C, Meehan J, Gray ME, et al. The impact of tumour pH on cancer progression: strategies for clinical intervention. *Explor Target Anti-Tumor Ther*. 2020;1(2):71-100. doi:10.37349/etat.2020.00005

59. Pethő Z, Najder K, Carvalho T, et al. pH-Channeling in Cancer: How pH-Dependence of Cation Channels Shapes Cancer Pathophysiology. *Cancers*. 2020;12(9):2484. doi:10.3390/cancers12092484

60. Lee SH, Griffiths JR. How and Why Are Cancers Acidic? Carbonic Anhydrase IX and the Homeostatic Control of Tumour Extracellular pH. *Cancers*. 2020;12(6). doi:10.3390/cancers12061616

61. Asgharzadeh MR, Barar J, Pourseif MM, et al. Molecular machineries of pH dysregulation in tumor microenvironment: potential targets for cancer therapy. *BioImpacts BI*. 2017;7(2):115-133. doi:10.15171/bi.2017.15

62. Mboge M, Mahon B, McKenna R, Frost S. Carbonic Anhydrases: Role in pH Control and Cancer. *Metabolites*. 2018;8(1):19. doi:10.3390/metabo8010019

63. Choschzick M, Oosterwijk E, Müller V, et al. Overexpression of carbonic anhydrase IX (CAIX) is an independent unfavorable prognostic marker in endometrioid ovarian cancer. *Virchows Arch*. 2011;459(2):193-200. doi:10.1007/s00428-011-1105-y

64. Ward C, Meehan J, Gray M, Kunkler IH, Langdon SP, Argyle DJ. Carbonic Anhydrase IX (CAIX), Cancer, and Radiation Responsiveness. *Metabolites*. 2018;8(1). doi:10.3390/metabo8010013

65. Matolay O, Bádon SE, Balázs L, Juhász P, Csonka T, Méhes G. [The role of carbonic anhydrase IX in the progression of malignant tumors - a potential therapeutic target?]. *Magy Onkol*. 2021;65(2):157-166.

66. Drenckhan A, Freytag M, Supuran CT, Sauter G, Izbicki JR, Gros SJ. CAIX furthers tumour progression in the hypoxic tumour microenvironment of esophageal carcinoma and is a possible therapeutic target. *J Enzyme Inhib Med Chem*. 2018;33(1):1024-1033. doi:10.1080/14756366.2018.1475369

67. Claudiu T. Supuran. Carbonic Anhydrase Inhibition and the Management of Hypoxic Tumors. *Metabolites*. 2017;7(3):48. doi:10.3390/metabo7030048

68. Sedlakova O. Carbonic anhydrase IX, a hypoxia-induced catalytic component of the pH regulating machinery in tumors. *Front Physiol*. 2014;4. doi:10.3389/fphys.2013.00400

69. Andreucci E, Peppicelli S, Carta F, et al. Carbonic anhydrase IX inhibition affects viability of cancer cells adapted to extracellular acidosis. *J Mol Med*. 2017;95(12):1341-1353. doi:10.1007/s00109-017-1590-9

70. D'Ignazio L, Bandarra D, Rocha S. NF-κB and HIF crosstalk in immune responses. *FEBS J*. 2016;283(3):413-424. doi:10.1111/febs.13578

71. Kajanova I, Zatovicova M, Jelenska L, et al. Impairment of carbonic anhydrase IX ectodomain cleavage reinforces tumorigenic and metastatic phenotype of cancer cells. *Br J Cancer*. 2020;122(11):1590-1603. doi:10.1038/s41416-020-0804-z

72. Hektoen HH, Ree AH, Redalen KR, Flatmark K. Sulfamate inhibitor S4 influences carbonic anhydrase IX ectodomain shedding in colorectal carcinoma cells. *J Enzyme Inhib Med Chem*. 2016;31(5):779-786. doi:10.3109/14756366.2015.1069286

73. Meijer TWH, Bussink J, Zatovicova M, et al. Tumor microenvironmental changes induced by the sulfamate carbonic anhydrase IX inhibitor S4 in a laryngeal tumor model. *PloS One*. 2014;9(9):e108068. doi:10.1371/journal.pone.0108068

74. McDonald PC, Winum JY, Supuran CT, Dedhar S. Recent developments in targeting carbonic anhydrase IX for cancer therapeutics. *Oncotarget*. 2012;3(1):84-97. doi:10.18632/oncotarget.422

75. Supuran CT, Alterio V, Di Fiore A, et al. Inhibition of carbonic anhydrase IX targets primary tumors, metastases, and cancer stem cells: Three for the price of one. *Med Res Rev*. 2018;38(6):1799-1836. doi:10.1002/med.21497

76. Siebels M, Rohrmann K, Oberneder R, et al. A clinical phase I/II trial with the monoclonal antibody cG250 (RENCAREX®) and interferon-alpha-2a in metastatic renal cell carcinoma patients. *World J Urol*. 2011;29(1):121-126. doi:10.1007/s00345-010-0570-2

77. Courcier J, de la Taille A, Nourieh M, Leguerney I, Lassau N, Ingels A. Carbonic Anhydrase IX in Renal Cell Carcinoma, Implications for Disease Management. *Int J Mol Sci*. 2020;21(19). doi:10.3390/ijms21197146

78. Ibrahim HS, Abou-Seri SM, Tanc M, Elaasser MM, Abdel-Aziz HA, Supuran CT. Isatin-pyrazole benzenesulfonamide hybrids potently inhibit tumor-associated carbonic anhydrase isoforms IX and XII. *Eur J Med Chem*. 2015;103:583-593. doi:10.1016/j.ejmech.2015.09.021

79. Nocentini A, Moi D, Balboni G, Salvadori S, Onnis V, Supuran CT. Synthesis and biological evaluation of novel pyrazoline-based aromatic sulfamates with potent carbonic anhydrase isoforms II, IV and IX inhibitory efficacy. *Bioorganic Chem*. 2018;77:633-639. doi:10.1016/j.bioorg.2018.02.021

80. Williams KJ, Gieling RG. Preclinical Evaluation of Ureidosulfamate Carbonic Anhydrase IX/XII Inhibitors in the Treatment of Cancers. *Int J Mol Sci*. 2019;20(23):6080. doi:10.3390/ijms20236080

81. Singh S, Lomelino CL, Mboge MY, Frost SC, McKenna R. Cancer Drug Development of Carbonic Anhydrase Inhibitors beyond the Active Site. *Mol Basel Switz*. 2018;23(5). doi:10.3390/molecules23051045

82. McKenna R, Supuran CT. Carbonic Anhydrase Inhibitors Drug Design. In: Frost SC, McKenna R, eds. *Carbonic Anhydrase: Mechanism, Regulation, Links to Disease, and Industrial Applications*. Vol 75. Subcellular Biochemistry. Springer Netherlands; 2014:291-323. doi:10.1007/978-94-007-7359-2_15

83. Supuran CT. Drug interaction considerations in the therapeutic use of carbonic anhydrase inhibitors. *Expert Opin Drug Metab Toxicol*. 2016;12(4):423-431. doi:10.1517/17425255.2016.1154534

84. Méhes G, Matolay O, Beke L, et al. Carbonic Anhydrase Inhibitor Acetazolamide Enhances CHOP Treatment Response and Stimulates Effector T-Cell Infiltration in A20/BalbC Murine B-Cell Lymphoma. *Int J Mol Sci*. 2020;21(14):5001. doi:10.3390/ijms21145001

85. Waheed A, Sly WS. Carbonic anhydrase XII functions in health and disease. *Gene*. 2017;623:33-40. doi:10.1016/j.gene.2017.04.027

86. Lounnas N, Rosilio C, Nebout M, et al. Pharmacological inhibition of carbonic anhydrase XII interferes with cell proliferation and induces cell apoptosis in T-cell lymphomas. *Cancer Lett*. 2013;333(1):76-88. doi:10.1016/j.canlet.2013.01.020

87. Abbott RK, Thayer M, Labuda J, et al. Germinal Center Hypoxia Potentiates Immunoglobulin Class Switch Recombination. *J Immunol Baltim Md 1950*. 2016;197(10):4014-4020. doi:10.4049/jimmunol.1601401

88. Spencer JA, Ferraro F, Roussakis E, et al. Direct measurement of local oxygen concentration in the bone marrow of live animals. *Nature*. 2014;508(7495):269-273. doi:10.1038/nature13034

89. Cho SH, Raybuck AL, Stengel K, et al. Germinal centre hypoxia and regulation of antibody qualities by a hypoxia response system. *Nature*. 2016;537(7619):234-238. doi:10.1038/nature19334

90. Kojima H, Sitkovsky M, Cascalho M. HIF-1α Deficiency Perturbs T and B Cell Functions. *Curr Pharm Des*. 2003;9(23):1827-1832. doi:10.2174/1381612033454388

91. Kojima H, Kobayashi A, Sakurai D, et al. Differentiation Stage-Specific Requirement in Hypoxia-Inducible Factor-1α–Regulated Glycolytic Pathway during Murine B Cell Development in Bone Marrow. *J Immunol*. 2010;184(1):154-163. doi:10.4049/jimmunol.0800167

92. Burrows N, Maxwell PH. Hypoxia and B cells. *Exp Cell Res*. 2017;356(2):197-203. doi:10.1016/j.yexcr.2017.03.019

93. Franchina DG, Grusdat M, Brenner D. B-Cell Metabolic Remodeling and Cancer. *Trends Cancer*. 2018;4(2):138-150. doi:10.1016/j.trecan.2017.12.006

94. Stewart M, Talks K, Leek R, et al. Expression of angiogenic factors and hypoxia inducible factors HIF 1, HIF 2 and CA IX in non-Hodgkin's lymphoma: Angiogenesis in non-Hodgkin's lymphoma. *Histopathology*. 2002;40(3):253-260. doi:10.1046/j.1365-2559.2002.01357.x

95. Doerr JR, Malone CS, Fike FM, et al. Patterned CpG Methylation of Silenced B Cell Gene Promoters in Classical Hodgkin Lymphoma-derived and Primary Effusion Lymphoma Cell Lines. *J Mol Biol*. 2005;350(4):631-640. doi:10.1016/j.jmb.2005.05.032

96. Tiacci E, Döring C, Brune V, et al. Analyzing primary Hodgkin and Reed-Sternberg cells to capture the molecular and cellular pathogenesis of classical Hodgkin lymphoma. *Blood*. 2012;120(23):4609-4620. doi:10.1182/blood-2012-05-428896

97. Ushmorov A, Leithäuser F, Sakk O, et al. Epigenetic processes play a major role in B-cell-specific gene silencing in classical Hodgkin lymphoma. *Blood*. 2006;107(6):2493-2500. doi:10.1182/blood-2005-09-3765

98. Wein F, Otto T, Lambertz P, Fandrey J, Hansmann ML, Kuppers R. Potential role of hypoxia in early stages of Hodgkin lymphoma pathogenesis. *Haematologica*. 2015;100(10):1320-1326. doi:10.3324/haematol.2015.127498

99. Mayer A, Schmidt M, Seeger A, Serras AF, Vaupel P, Schmidberger H. GLUT-1 expression is largely unrelated to both hypoxia and the Warburg phenotype in squamous cell carcinomas of the vulva. *BMC Cancer*. 2014;14(1):760. doi:10.1186/1471-2407-14-760

100. Sasaki H. Overexpression of GLUT1 correlates with Kras mutations in lung carcinomas. *Mol Med Rep*. Published online December 22, 2011. doi:10.3892/mmr.2011.736

101. Tirpe AA, Gulei D, Ciortea SM, Crivii C, Berindan-Neagoe I. Hypoxia: Overview on Hypoxia-Mediated Mechanisms with a Focus on the Role of HIF Genes. *Int J Mol Sci*. 2019;20(24):6140. doi:10.3390/ijms20246140

102. Koh YW, Han JH, Park SY, Yoon DH, Suh C, Huh J. GLUT1 as a Prognostic Factor for Classical Hodgkin's Lymphoma: Correlation with PD-L1 and PD-L2 Expression. *J Pathol Transl Med*. 2017;51(2):152-158. doi:10.4132/jptm.2016.11.03

103. Passam FH, Alexandrakis MG, Kafousi M, et al. Histological expression of angiogenic factors: VEGF, PDGFRα, and HIF-1α in Hodgkin lymphoma. *Pathol - Res Pract*. 2009;205(1):11-20. doi:10.1016/j.prp.2008.07.007

104. Korkolopoulou P, Thymara I, Kavantzas N, et al. Angiogenesis in Hodgkin's lymphoma: a morphometric approach in 286 patients with prognostic implications. *Leukemia*. 2005;19(6):894-900. doi:10.1038/sj.leu.2403690

105. Marinaccio C, Nico B, Maiorano E, Specchia G, Ribatti D. Insights in Hodgkin Lymphoma angiogenesis. *Leuk Res*. 2014;38(8):857-861. doi:10.1016/j.leukres.2014.05.023

106. Doussis-Anagnostopoulou IA, Talks KL, Turley H, et al. Vascular endothelial growth factor (VEGF) is expressed by neoplastic Hodgkin-Reed-Sternberg cells in Hodgkin's disease. *J Pathol*. 2002;197(5):677-683. doi:10.1002/path.1151

107. Rueda A, Olmos D, Vicioso L, et al. Role of vascular endothelial growth factor C in classical Hodgkin lymphoma. *Leuk Lymphoma*. 2015;56(5):1286-1294. doi:10.3109/10428194.2014.952227

108. Drexler HG, Pommerenke C, Eberth S, Nagel S. Hodgkin lymphoma cell lines: to separate the wheat from the chaff. *Biol Chem*. 2018;399(6):511-523. doi:10.1515/hsz-2017-0321

109. Diehl V, Kirchner HH, Schaadt M, et al. Hodgkin's disease: Establishment and characterization of four in vitro cell lines. *J Cancer Res Clin Oncol*. 1981;101(1):111-124. doi:10.1007/BF00405072

110. Kanzler H, Hansmann ML, Kapp U, et al. Molecular Single Cell Analysis Demonstrates the Derivation of a Peripheral Blood-Derived Cell Line (L1236) From the HodgkWReed-Sternberg Cells of a Hodgkin's Lymphoma Patient. :9.

111. Sári Z, Mikó E, Kovács T, et al. Indoxylsulfate, a Metabolite of the Microbiome, Has Cytostatic Effects in Breast Cancer via Activation of AHR and PXR Receptors and Induction of Oxidative Stress. *Cancers*. 2020;12(10):2915. doi:10.3390/cancers12102915

112. Matolay O, Beke L, Gyurkovics A, et al. Quantitative Analysis of Carbonic Anhydrase IX Uncovers Hypoxia-Related Functional Differences in Classical Hodgkin Lymphoma Subtypes. *Int J Mol Sci*. 2019;20(14). doi:10.3390/ijms20143463

113. Méhes G, Matolay O, Beke L, et al. Hypoxia-related carbonic anhydrase IX expression is associated with unfavourable response to first-line therapy in classical Hodgkin's lymphoma. *Histopathology*. 2019;74(5):699-708. doi:10.1111/his.13808

114. Chen D, Bobko AA, Gross AC, et al. Involvement of Tumor Macrophage HIFs in Chemotherapy Effectiveness: Mathematical Modeling of Oxygen, pH, and Glutathione. Tang D, ed. *PLoS ONE*. 2014;9(10):e107511. doi:10.1371/journal.pone.0107511

115. Belisario DC, Kopecka J, Pasino M, et al. Hypoxia Dictates Metabolic Rewiring of Tumors: Implications for Chemoresistance. *Cells*. 2020;9(12):2598. doi:10.3390/cells9122598

116. Wykoff CC, Beasley NJ, Watson PH, et al. Hypoxia-inducible expression of tumor-associated carbonic anhydrases. *Cancer Res*. 2000;60(24):7075-7083.

117. Zamanova S, Shabana AM, Mondal UK, Ilies MA. Carbonic anhydrases as disease markers. *Expert Opin Ther Pat*. 2019;29(7):509-533. doi:10.1080/13543776.2019.1629419

118. Rohwer N, Cramer T. Hypoxia-mediated drug resistance: Novel insights on the functional interaction of HIFs and cell death pathways. *Drug Resist Updat*. 2011;14(3):191-201. doi:10.1016/j.drup.2011.03.001

119. Böhme I, Bosserhoff A. Extracellular acidosis triggers a senescence-like phenotype in human melanoma cells. *Pigment Cell Melanoma Res*. 2020;33(1):41-51. doi:10.1111/pcmr.12811

120. Chafe SC, Vizeacoumar FS, Venkateswaran G, et al. Genome-wide synthetic lethal screen unveils novel CAIX-NFS1/xCT axis as a targetable vulnerability in hypoxic solid tumors. *Sci Adv*. 2021;7(35):eabj0364. doi:10.1126/sciadv.abj0364

121. Pillai SR, Damaghi M, Marunaka Y, Spugnini EP, Fais S, Gillies RJ. Causes, consequences, and therapy of tumors acidosis. *Cancer Metastasis Rev*. 2019;38(1-2):205-222. doi:10.1007/s10555-019-09792-7

122. Chen LQ, Howison CM, Spier C, et al. Assessment of carbonic anhydrase IX expression and extracellular pH in B-cell lymphoma cell line models. *Leuk Lymphoma*. 2015;56(5):1432-1439. doi:10.3109/10428194.2014.933218

123. Pantanowitz L, Farahani N, Parwani A. Whole slide imaging in pathology: advantages, limitations, and emerging perspectives. *Pathol Lab Med Int*. Published online June 2015:23. doi:10.2147/PLMI.S59826

124. Pantanowitz L, Sinard JH, Henricks WH, et al. Validating whole slide imaging for diagnostic purposes in pathology: guideline from the College of American Pathologists Pathology and Laboratory Quality Center. *Arch Pathol Lab Med*. 2013;137(12):1710-1722. doi:10.5858/arpa.2013-0093-CP

125. Schäfer T, Schäfer H, Schmitz A, et al. Image database analysis of Hodgkin lymphoma. *Comput Biol Chem*. 2013;46:1-7. doi:10.1016/j.compbiolchem.2013.04.003

126. Schäfer H, Schäfer T, Ackermann J, et al. CD30 cell graphs of Hodgkin lymphoma are not scale-free—an image analysis approach. *Bioinformatics*. Published online September 11, 2015:btv542. doi:10.1093/bioinformatics/btv542

127. Hannig J, Schäfer H, Ackermann J, et al. Bioinformatics analysis of whole slide images reveals significant neighborhood preferences of tumor cells in Hodgkin lymphoma. Papin JA, ed. *PLOS Comput Biol*. 2020;16(1):e1007516. doi:10.1371/journal.pcbi.1007516

128. Hartmann S, Agostinelli C, Diener J, et al. GLUT1 expression patterns in different Hodgkin lymphoma subtypes and progressively transformed germinal centers. *BMC Cancer*. 2012;12(1):586. doi:10.1186/1471-2407-12-586

129. Fuchs Q, Pierrevelcin M, Messe M, et al. Hypoxia Inducible Factors' Signaling in Pediatric High-Grade Gliomas: Role, Modelization and Innovative Targeted Approaches. *Cancers*. 2020;12(4):979. doi:10.3390/cancers12040979

130. Rana NK, Singh P, Koch B. CoCl2 simulated hypoxia induce cell proliferation and alter the expression pattern of hypoxia associated genes involved in angiogenesis and apoptosis. *Biol Res*. 2019;52(1):12. doi:10.1186/s40659-019-0221-z

131. Wu D, Yotnda P. Induction and Testing of Hypoxia in Cell Culture. *J Vis Exp*. 2011;(54):2899. doi:10.3791/2899

132. Vassilakopoulos TP, Asimakopoulos JV, Konstantopoulos K, Angelopoulou MK. Optimizing outcomes in relapsed/refractory Hodgkin lymphoma: a review of current and forthcoming

therapeutic strategies. *Ther Adv Hematol*. 2020;11:2040620720902911. doi:10.1177/2040620720902911

13. PUBLICATION LIST (APPROVED BY THE KENÉZY LIFE SCIENCE LIBRARY)

UNIVERSITY AND NATIONAL LIBRARY
UNIVERSITY OF DEBRECEN
H-4002 Egyetem tér 1, Debrecen
Phone: +3652/410-443, email: publikaciok@lib.unideb.hu

Registry number: DEENK/481/2021.PL
Subject: PhD Publication List

Candidate: Orsolya Matolay
Doctoral School: Doctoral School of Clinical Medicine

List of publications related to the dissertation

1. Méhes, G., **Matolay, O.**, Beke, L., Czenke, M., Jóna, Á., Miltényi, Z., Illés, Á., Bedekovics, J.: Hypoxia related carbonic anhydrase IX expression is associated with unfavourable response to first-line therapy in classical Hodgkin's lymphoma.
Histopathology. 74 (5), 699-708, 2019.
DOI: http://dx.doi.org/10.1111/his.13808
IF: 3.626

2. **Matolay, O.**, Beke, L., Gyurkovics, A., Francz, M., Varjasi, G., Rejtő, L., Illés, Á., Bedekovics, J., Méhes, G.: Quantitative Analysis of Carbonic Anhydrase IX Uncovers Hypoxia-Related Functional Differences in Classical Hodgkin Lymphoma Subtypes.
Int. J. Mol. Sci. 20 (14), 1-12, 2019.
DOI: http://dx.doi.org/10.3390/ijms20143463
IF: 4.556

List of other publications

3. **Matolay, O.**, Bádon, E. S., Balázs, L., Juhász, P., Csonka, T., Méhes, G.: A szénsavanhidráz IX szerepe a malignus daganatok progressziójában - lehetséges terápiás célpont?
Magyar Onkol. 65, 157-166, 2021.

4. Kis, A., Dénes, N., Péli-Szabó, J., Arató, V. Z., Beke, L., **Matolay, O.**, Enyedi, K. N., Méhes, G., Mező, G., Bai, P., Kertész, I., Trencsényi, G.: In Vivo Molecular Imaging of the Efficacy of Aminopeptidase N (APN/CD13) Receptor Inhibitor Treatment on Experimental Tumors Using 68Ga-NODAGA-c(NGR) Peptide.
BioMed Res. Inter. 2021, 1-11, 2021.
IF: 3.411 (2020)

UNIVERSITY AND NATIONAL LIBRARY
UNIVERSITY OF DEBRECEN
H-4002 Egyetem tér 1, Debrecen
Phone: +3652/410-443, email: publikaciok@lib.unideb.hu

5. Méhes, G., **Matolay, O.**, Beke, L., Czenke, M., Pórszász, R., Mikó, E., Bai, P., Berényi, E., Trencsényi, G.: Carbonic Anhydrase Inhibitor Acetazolamide Enhances CHOP Treatment Response and Stimulates Effector T-Cell Infiltration in A20/BalbC Murine B-Cell Lymphoma.
Int. J. Mol. Sci. 21 (14), 1-14, 2020.
DOI: http://dx.doi.org/10.3390/ijms21145001
IF: 5.923

6. Kis, A., Péli-Szabó, J., Dénes, N., Vágner, A., Nagy, G., Garai, I., Fekete, A., Szikra, D. P., Hajdu, I., **Matolay, O.**, Méhes, G., Mező, G., Kertész, I., Trencsényi, G.: In vivo Imaging of Hypoxia and Neoangiogenesis in Experimental Syngeneic Hepatocellular Carcinoma Tumor Model Using Positron Emission Tomography.
Biomed Res. Int. 2020, 1-10, 2020.
DOI: http://dx.doi.org/10.1155/2020/4952372
IF: 3.411

7. Varga, G., Ghanem, S., Szabó, B., Nagy, K., Pál, N., Tánczos, B., Somogyi, V., Baráth, B., Deák, Á., **Matolay, O.**, Bidiga, L., Pető, K., Németh, N.: Which remote ischemic preconditioning protocol is favorable in renal ischemia-reperfusion injury in the rat?
Clin. Hemorheol. Microcirc. 76 (3), 439-451, 2020.
DOI: http://dx.doi.org/10.3233/CH-200916
IF: 2.375

8. **Matolay, O.**, Méhes, G.: Sustain, Adapt, and Overcome: hypoxia Associated Changes in the Progression of Lymphatic Neoplasia.
Front Oncol. 9, 1-7, 2019.
DOI: http://dx.doi.org/10.3389/fonc.2019.01277
IF: 4.848

Total IF of journals (all publications): 28,15
Total IF of journals (publications related to the dissertation): 8,182

The Candidate's publication data submitted to the iDEa Tudóstér have been validated by DEENK on the basis of the Journal Citation Report (Impact Factor) database.

29 October, 2021

14. KEYWORDS

hypoxia, HIF1α, CAIX, CAXII, GLUT1, Hodgkin, lymphoma, metabolic adaptation, cellular adaptation

Tárgyszavak

hypoxia, HIF1α, CAIX, CAXII, GLUT1, Hodgkin, lymphoma, metabolikus adaptáció, sejtszintű adaptáció

15. ACKNOWLEDGEMENT

First of all, I would like to thank my supervisor, Gábor Méhes M.D., Ph.D., D.Sc, head of the Department of Pathology, University of Debrecen, Clinical Centre, for the patient guidance, encouragement, continuous support, and motivation during my Ph.D. study.

I would also like to thank Péter Bay, Ph.D., D.Sc. for allowing me to work at the Department. I am grateful that he gave me the opportunity to learn and work in his research group.

Many thanks to Edit Mikó Kapitányné Ph.D, Judit Szabó Péliné, M.Sc. for the valuable discussions and helpful advices. I am very grateful for Tünde Kovács, Ph.D., Gyula Újlaki, Zsanett Mercédesz Sárközi Ph.D., Laura Jankó Ph.D. for their help in carrying out the experiments.

I am very thankful to Lívia Beke Mrs. for the immunohistological stainings.

My sincere thanks also go to György Vereb M.D., Ph.D., D.Sc, and István Rebenku, M.Sc., who provided me an opportunity to join their team, and who gave me access to the laboratory and research facilities. Without their precious support, it would not be possible to conduct this research.

I would like to thank all of my former scientific students/TDK-students for joining me on this marvelous journey and for not only learning from me but teaching me: Áron Vajda, M.D, Nóra Tárkányi, M.D., Viktória Edina, Kiss M.D, Szabolcs Viola, and Péter Dobi, M.Sc, Ádám Fülöp.

Last but not least, I would like to show my gratitude towards my loving and supporting family and to all my dear friends for their continuous encouragement, support, and tolerance during my Ph.D. studies.

Our research was supported by the following grants: the EFOP-3.6.1-16-2016-00022 VENTURE CATAPULT, EFOP-3.6.3-VEKOP-16-2017-00009, and the ÚNKP-20-3-II-DE-488, ÚNKP-21-4-I-DE-253 NEW NATIONAL EXCELLENCE PROGRAM OF THE MINISTRY FOR INNOVATION AND TECHNOLOGY FROM THE SOURCE OF THE NATIONAL RESEARCH, DEVELOPMENT AND INNOVATION FUND (OM).

16. APPENDIX

The thesis is based on the following publications: